A GROUNDWATER FLOW MODEL FOR THE EAST FLATHEAD VALLEY, FLATHEAD COUNTY, MONTANA

James Berglund,[1] Andrew Bobst, and Ali Gebril

Montana Bureau of Mines and Geology
Ground Water Investigation Program

[1]Current affiliation: University of Wisconsin at Platteville

MBMG
Montana Bureau of Mines and Geology

Front photo: The Swan Range north of Lake Blaine. Photo by James Berglund.

A GROUNDWATER FLOW MODEL FOR THE EAST FLATHEAD VALLEY, FLATHEAD COUNTY, MONTANA

James Berglund,[1] Andrew Bobst, and Ali Gebril

Montana Bureau of Mines and Geology
Ground Water Investigation Program

[1]Current affiliation: University of Wisconsin at Platteville

TABLE OF CONTENTS

FIGURES

TABLES

PREFACE

The Ground Water Investigation Program (GWIP) at the Montana Bureau of Mines and Geology (MBMG) investigates areas prioritized by the Ground-Water Assessment Steering Committee (2-15-1523 MCA). Prioritization is based on such factors as current and anticipated growth of industry, housing and commercial activity, or changing irrigation practices. Additional program information and project-ranking details are available at http://www.mbmg.mtech.edu/, Ground Water Investigation Program.

Anticipated products of the East Flathead Groundwater Investigation include the following:

- This Groundwater Modeling Report, which combines water-budget information with observed groundwater and surface-water behavior to advance calibrated steady-state and transient MODFLOW numerical groundwater flow models for the East Flathead study area. These models are used to test various development and drought scenarios to understand the types of hydrologic effects that might be expected.

- An Aquifer Test Report (Myse and others, 2023), summarizing the results of three aquifer tests conducted in the East Flathead study area.

- An Interpretive Report (Bobst and others, in prep.), that presents interpretations of the data and summarizes the project results.

Data collected from this study are permanently archived in the MBMG GWIC database. GWIC is accessible at: http://mbmggwic.mtech.edu/. Within GWIC, data are grouped into project areas to allow easy access to project-specific information. The East Flathead project data are found by going to GWIC's "Projects" page, then "Groundwater Investigation Program" Project Group, and then "East Flathead." Groundwater and surface-water monitoring sites are identified in appendices A and B.

ABSTRACT

Ongoing development in the Flathead Valley, Montana has raised concerns about the impact of increased groundwater use on both surface-water and groundwater availability. We developed groundwater flow models to investigate and interpret the hydrogeology of the East Flathead area.

The regional aquifer system generally consists of shallow and deep aquifer systems separated by discontinuous confining layers. A three-dimensional (3D), four-layer transient numerical flow model was developed using new and existing hydrologic data along with geologic interpretations of aquifer and confining layer thicknesses from both previous studies and well logs. A preliminary groundwater budget was developed based on field observations, climatic information, and remote sensing data. This water budget was used to define boundary conditions and provide flux targets for calibration. Observed groundwater elevations were also used as calibration targets.

The calibrated transient model was used to test two scenarios involving increased groundwater pumping. Scenario 1 doubled residential pumping, and Scenario 2 doubled irrigation pumping. Doubling residential pumping (Scenario 1) showed an average groundwater level decrease of 0.4–0.7 ft, and decreased groundwater outflow to surface waters by about 0.7 cubic feet per second (cfs). Doubling irrigation pumping (Scenario 2) showed an average groundwater level decrease of 1.1–1.5 ft and a decrease in groundwater flow to surface waters by about 2.1 cfs. Doubling irrigation pumping had about a three times greater effect.

Two additional scenarios (Scenario 3 and Scenario 4) were investigated to evaluate the effects of natural variability in the system. In each case mountain front recharge was decreased by 25% to approximate a 20-yr drought. For Scenario 3 this reduction was for 1 yr, and for Scenario 4 the reduction was for 5 yr. These drought scenarios showed short-term decreases in groundwater levels and surface-water flows that were greater than for

the pumping scenarios. The simulated 1-yr drought (Scenario 3) showed an average drawdown of up to 2.7 ft, and groundwater outflow to surface waters decreased by up to 2.2 cfs. The simulated 5-yr drought (Scenario 4) caused simulated groundwater levels to decrease by up to 3.7 ft, and groundwater outflow to surface waters decreased by up to 4.6 cfs. In both cases the maximum effects occurred during the last year of the drought. By the end of the drought model scenarios (10–15 yr after the end of the droughts), groundwater levels and discharges had returned to near pre-drought values.

This study shows there are hydrogeologic connections between the shallow and deep aquifers in some parts of the study area. Due to these connections, groundwater pumping from either the shallow or deep aquifers causes groundwater drawdown in the area near pumping, decreased groundwater discharge to surface waters, and decreased groundwater outflow from the model domain. While these types of effects are expected, the degree to which the effects accrue to groundwater or surface waters, the timing of the effects, and the locations of those effects will depend on development details (e.g., location, aquifer properties, pumping schedule, etc.).

INTRODUCTION

Background

Ongoing commercial and residential development in the Flathead Valley, Montana has raised concerns that increased groundwater use may affect groundwater and surface-water availability. The East Flathead Groundwater Investigation focused on the east side of the valley (fig. 1) to provide an improved understanding of the interconnection between that area's aquifers and surface waters. Within this area there is a shallow unconfined aquifer system that is generally directly connected to surface waters, and the deep aquifer (also called the deep Kalispell aquifer or the deep alluvial aquifer) that is believed to be mostly confined (LaFave and others, 2004; Rose, 2018; Rose and others, 2022). Concerns that the deep aquifer may not be fully confined in some areas on the east side of the Flathead Valley caused the Montana Department of Natural Resources and Conservation (DNRC) to propose this project, and gave rise to its prioritization by the Ground Water Assessment Steering Committee.

Flathead County was the second fastest growing county in the State from 2010 to 2020, with a population increase of 16.5% (an increase of 14,988 residents; U.S. Census Bureau, 2021). Within the study area, groundwater is used for irrigated agriculture, individual homes, public water supply (PWS) systems, the Creston National Fish Hatchery, and industrial uses. There continue to be proposals for new large subdivisions on the east side of Flathead Valley, along with new irrigation wells and new commercial uses.

Scope and Objectives

Previous studies were conducted to define the complex geology (Smith, 2004a), monitor groundwater levels and water quality (LaFave and others, 2004), and develop a regional hydrostratigraphic model of the entire Flathead Valley (Rose, 2018). The purpose of the East Flathead project is to evaluate how increased groundwater pumping will affect groundwater levels in the unconsolidated shallow and deep aquifers, and surface-water availability. To address these issues, we developed a calibrated three-dimensional (3D) numerical groundwater model of the East Flathead Valley based on previous work and data collected specifically for this investigation.

Study Area Description

Physiography

The Flathead Valley is an intermontane basin in northwest Montana. The East Flathead Valley study area is bounded by the Swan Mountains on the east, and the Flathead River on the west (fig. 1). The Flathead River at Columbia Falls (USGS station 12363000; site 1 on fig. 2) had an average annual flow of 9,736 cfs from 1951 to 2022, with mean monthly discharges ranging from 5,230 (September) to 24,900 cfs (June). Other major surface-water features include Mooring Creek, Lake Blaine, Jessup Mill Pond, and Mill Creek (fig. 2).

Land surface elevations in the study area range from 2,889 feet above mean sea level (ft-amsl) along the Flathead River at the south end of the study area to 7,424 ft-amsl at the peak of Dorris Mountain in the Swan Range. In the model domain (fig. 1), which
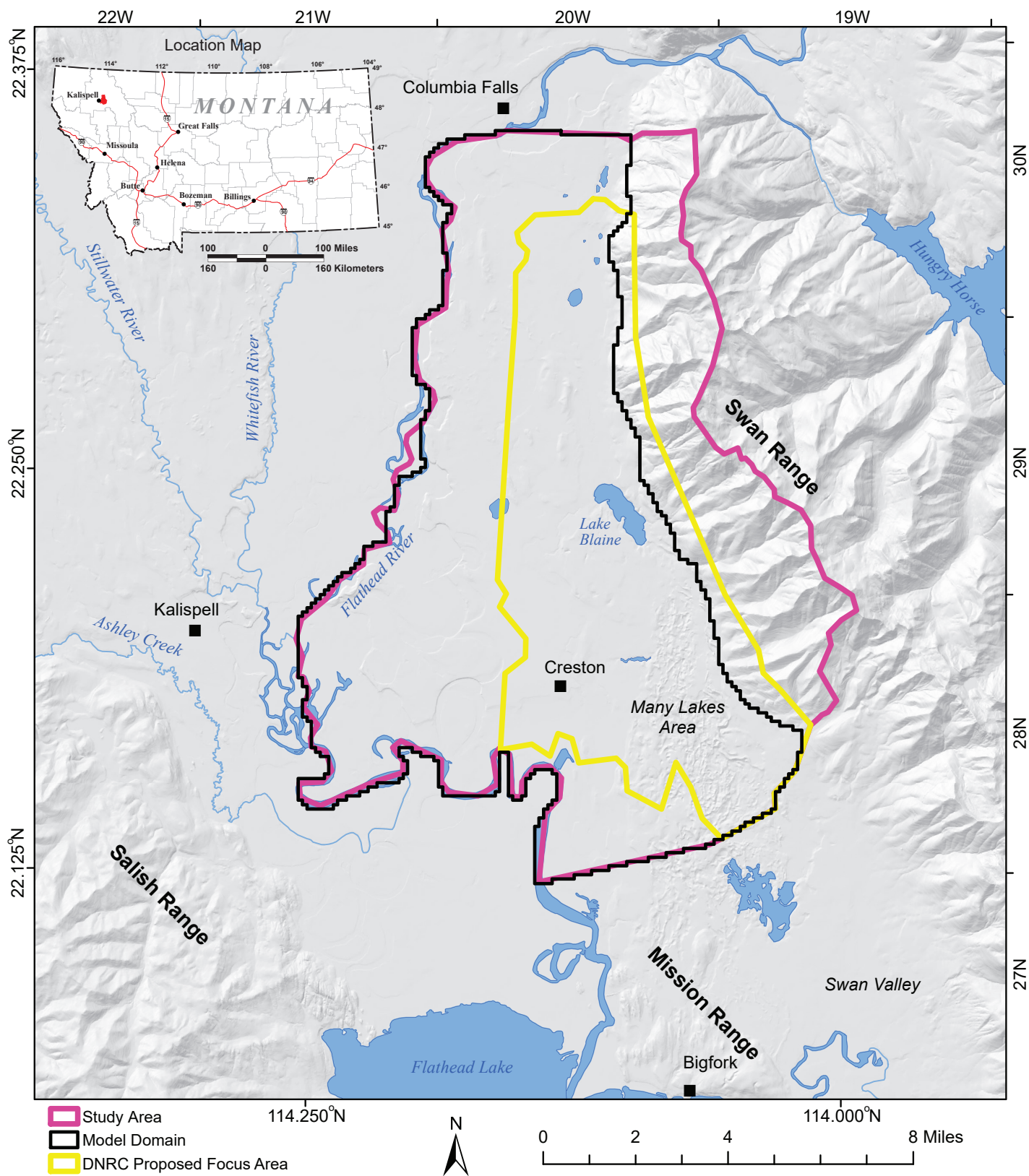
Figure 1. The East Flathead study area in Flathead County, extending along the east side of the Flathead Valley from south of Columbia Falls to the Many Lakes area. The project study area is larger than the DNRC proposed focus area so that natural boundaries (e.g., watershed divides and the Flathead River) can be used. The groundwater model domain is underlain by unconsolidated aquifers, but does not include the bedrock-dominated Swan Range where there are few wells.
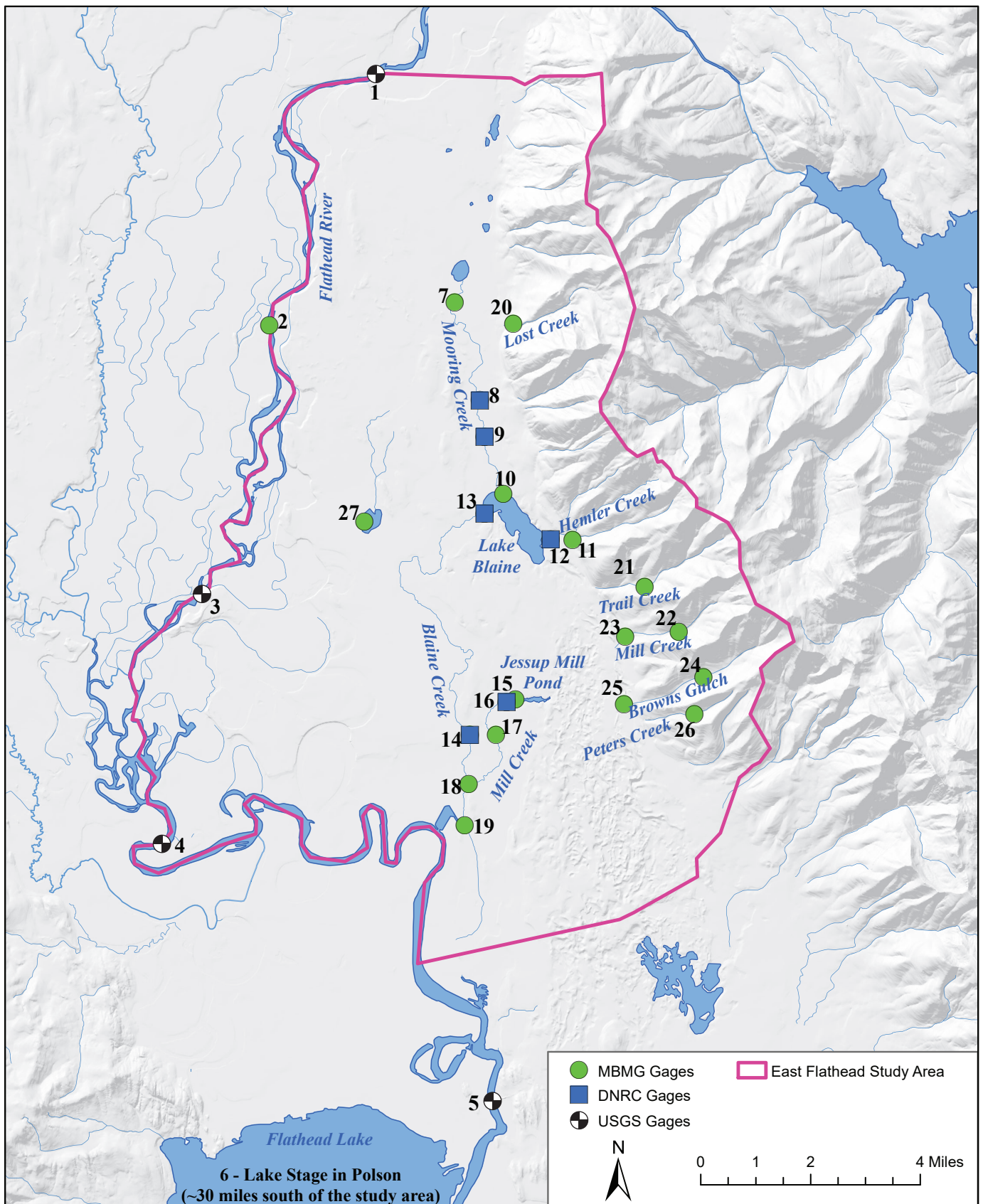
Figure 2. A network of 27 surface-water sites were used to measure stage, elevation, discharge, temperature, and water quality. Labels show site numbers that are cross referenced to GWIC ID numbers and data types in appendix B. These data were used to define boundary conditions, develop the water budget, and provide flux targets for model calibration.

covers that portion of the study area underlain by unconsolidated valley-fill sediments, the maximum elevation is 3,200 ft-amsl, within the foothills of the Swan Range.

Climate

Long-term average precipitation values from the PRISM (Parameter-Elevation Regressions on Independent Slopes Model; PRISM Climate Group, 2015) 1981–2010 normal precipitation values dataset indicate that normal precipitation ranged from about 15 in per year in the valley bottom to 70 in per year at the top of the Swan Range. During the monitoring period for this study from water year (WY) 2019 to WY2021, precipitation at the Creston Agrimet Station (fig. 1) was 94% of normal, with annual totals ranging from 89% (WY2020) to 101% (WY2021) of normal (US-BOR, 2022).

Temperature data from 1985 to 2021 at the Creston Agrimet Station (fig. 1) in the valley bottom shows that the mean annual temperature is 45°F. Mean monthly temperatures over the same time ranged from 26°F (January and December) to 66°F (July) (USBOR, 2022).

Land Use

Major land uses within the study area include irrigated and dryland agriculture and residential development. There is also a fish hatchery immediately downstream of Jessup Mill Pond. Over the last several decades irrigated agriculture has been shifting from flood irrigation with surface-water sources to sprinkler and pivot irrigation with groundwater sources (Kendy and Tresch, 1996; Rose and others, 2022). Residential development is increasing to accommodate the population growth. Much of the new development is in areas previously used for agriculture.

General Hydrogeologic Framework

The Flathead Valley is the southernmost expression of the Rocky Mountain Trench, which extends over 1,000 mi north into the Yukon Territory (Garland and others, 1961; Harrison and others, 1992). The Rocky Mountain Trench formed due to closely spaced normal faults and extension, which has caused crustal blocks to drop relative to the surrounding terrane. On the east edge of the Flathead Valley there is a sharp dropoff in bedrock elevation along the front of the Swan Range (fig. 3). A thick layer of valley-fill sedi-
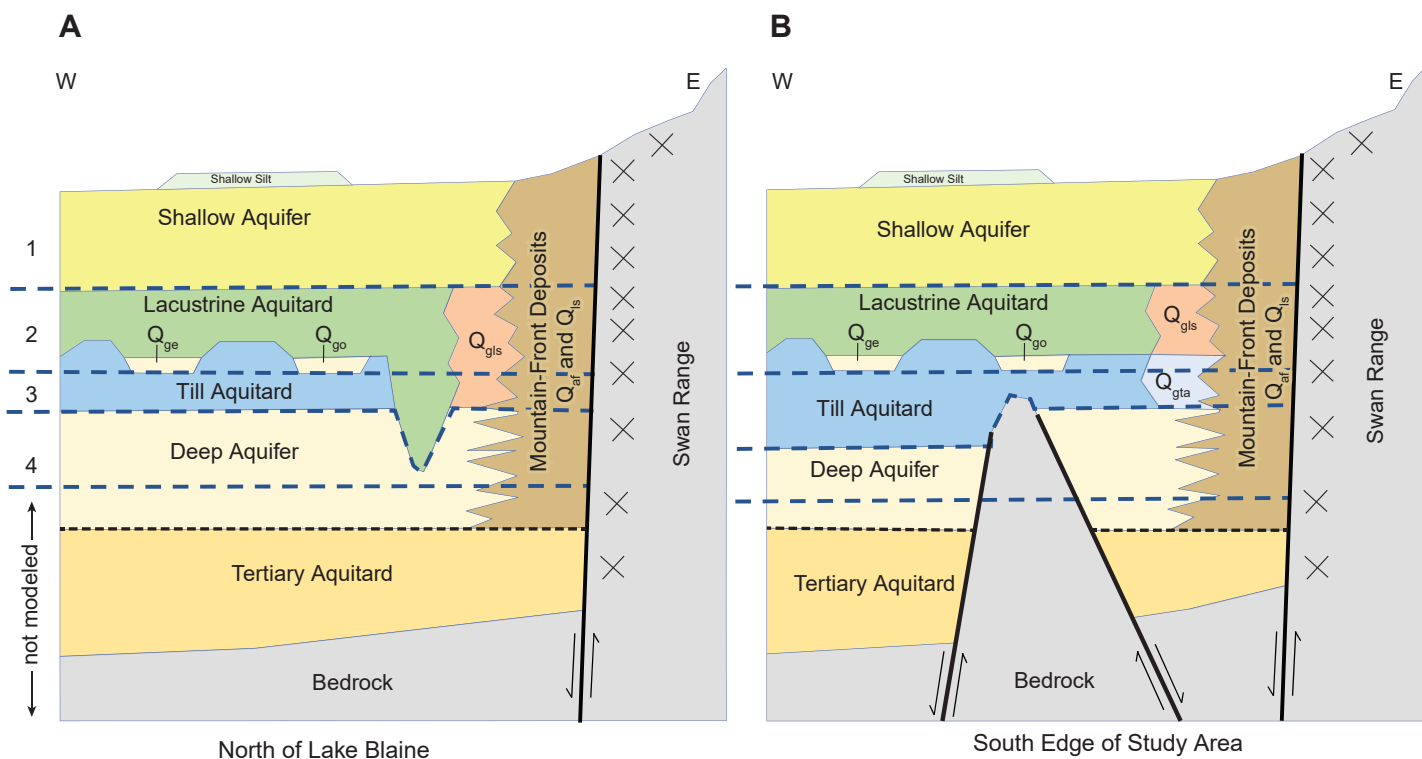
Figure 3. Schematic cross-sections using hydrogeologic units and corresponding model layers 1–4. In the northern portion of the study area (A) the shallow and deep aquifers are interconnected near the mountain front, but separated by fine lacustrine and basal till aquitards further into the basin. In the south (B) the shallow and deep aquifer are interconnected near the mountain front, and by the somewhat permeable deltaic (sandy lacustrine; Qgls) and ablation till (Qgta) deposits; a bedrock high bisects the deep aquifer. In both areas intermediate aquifers (Qge and Qgo) occur within the till, or near the contact between the till and lacustrine sediments.

ments lies on top of the bedrock west of the front. The sediments are up to 3,000 ft thick (Smith, 2004b). Different layers within the unconsolidated sediments constitute the main aquifers in the region (table 1). The base of the valley-fill package is composed of semi-lithified Tertiary valley-fill sediments. Quaternary sediments lie on top of the Tertiary, and are generally classified as the shallow, intermediate, and deep aquifer systems, based on depth and lithologic information.

Tertiary sediments are believed to overlie bedrock (Konizeski and others, 1968; LaFave and others, 2004; fig. 4). The deepest wells in the East Flathead area are ~800 ft deep, and they do not reach the Tertiary sediments. There is one known well in the Flathead Valley that intersects the Tertiary sediments (GWIC ID 317644; Bobst and others, 2022), and although it is outside of the East Flathead study area, it showed that the Tertiary sediments were encountered at about 1,200 ft below ground surface (bgs), with the deep aquifer being approximately 800 ft thick. The Tertiary sediments were interpreted to be the Kishenehn Formation, which functions as a basal aquitard in the valley.

The deep aquifer overlies the Tertiary sediments and is composed of sand, gravel, and cobbles of glacial outwash. This aquifer is a primary source of water in the Flathead Valley, and it is widely used for municipal water supplies, irrigation wells, and domestic wells. Wells in the deep aquifer may produce over 1,500 gpm (e.g., GWIC ID 81695).

In most of the area, the deep aquifer is overlain by low-permeability glacial till and glacial lake sediments. These low-permeability sediments are generally considered to be the confining layer (LaFave and others, 2004). Intermediate sand and gravel aquifers (likely lenses from proglacial and subglacial outwash channels) are present within the confining layer (fig. 3). Relatively thin confining layers (<100 ft) were mapped in some parts of the study area (Smith, 2004d). In some areas the deep and intermediate aquifers appear to be interconnected (Smith, 2004d). There are also areas where there are sandy glacial lake sediments (presumably near-shore deltaic deposits; Smith, 2004a). As such, there may be a hydrologic connection between the deep and shallow aquifers in portions of the study area.

A variety of sediments from the modern depositional environment typically cover the confining layer and form the shallow aquifers. These shallow aquifers are in direct communication with surface waters (Konizeski and others, 1968; Noble and Stanford, 1986; Smith, 2004a; LaFave and others, 2004).

Groundwater-level and water-quality data suggest that the deep aquifer receives substantial recharge along the east side of the Flathead Valley (LaFave and others, 2004). It is notable that while the Swan Range to the east receives high levels of precipitation, most of the mountain creeks draining off the mountain range cease to flow at the mountain front (fig. 2). This suggests that the mountain creeks infiltrate into the valley sediments shortly after crossing from the mountain front into the valley.

DATA COLLECTION

Field data were collected from June 2019 to December 2021. This included periodic (typically monthly) monitoring of groundwater levels in a network of 144 wells and piezometers (appendix A; fig. 4). The wells were monitored for different durations depending on land-owner permissions. Some wells were located outside the model domain and some wells completed in the same unit were close together. As such, water levels from 105 wells were used as calibration targets for this modeling effort (appendix A). We also measured stage, surface-water elevation, and discharge data from 27 surface-water sites (appendix B; fig. 2). These surface-water sites were monitored by the MBMG, the Montana Department of Natural Resources and Conservation (DNRC), and the United States Geological Survey (USGS).

The groundwater and surface-water monitoring data are publicly available, and are stored in MBMG's GWIC database, where the data are accessible by using each site's GWIC ID number (appendices A and B). A preliminary groundwater budget was developed for the East Flathead study area based on monitoring, remote sensing, and other sources of data (appendix C). Aquifer tests were conducted at 3 sites to evaluate the hydraulic properties of the aquifers (Myse and others, 2023; appendix D).

Montana Bureau of Mines and Geology Report of Investigation 36

Table 1. Hydrogeologic framework for the East Flathead Valley, with comparison to recent MBMG publications.

Geologic Age (Period)	Geologic Age (Epoch)	Geologic Units[1]	Geologic Interpretation[3]	Hydrogeologic Units — LaFave and others, 2004	Hydrogeologic Units — Rose, 2018	Hydrogeologic Units — This Study (EFV)	Groundwater Model — Modeled Thickness (ft)	Groundwater Model — Model Layers
Quaternary	Holocene	Lake deposits (Qlk)	Outwash, eolian sand sheets and dunes, fluvial, alluvial, lacustraine, and alluvial fan deposits.	Shallow aquifer	Shallow aquifer	Shallow silt / Shallow aquifers	5–276	1
Quaternary	Holocene	Eolian deposits (Qe)						
Quaternary	Holocene	Alluvial fan deposits (Qaf)						
Quaternary	Holocene	Landslide deposits (Qls)						
Quaternary	Holocene	Alluvium (Qal)						
Quaternary	Holocene	Older alluvium (Qao)						
Quaternary	Holocene	Glacial outwash deposit (Qgo)						
Quaternary	Holocene	Glacial esker deposits (Qge)						
Quaternary	Pleistocene	Glacial lake deposits (Qgl)	Most deposited from suspension in distal positions in lake that was initially pro-glacial; few gravels deposited from melting ice; subaqueous outwash fan deposits near recessional moraines; higher lacustrine deposits were abandoned successively as the lake receded.	Confining unit	Lacustrine–till aquitard	Fine lacustrine aquitard / Sandy lacustrine sediments	5–175	2
Quaternary	Pleistocene	Glacial lake deposits, sandy (Qgls)						
Quaternary	Pleistocene	Glacial outwash deposit (Qgo)	Intermediate alluvium; englacial or subglacial alluvial deposits that are encased in till.	Intermediate aquifers		Intermediate aquifers		
Quaternary	Pleistocene	Glacial esker deposits (Qge)						
Quaternary	Pleistocene	Glacial till, ablation deposits (Qgta)	Massive diamicton: Mostly till deposited subglacially by lodgement and melt-out processes; surface is marked by englacial or subglacial eskers, supraglacial ablation deposits, drumlins, and moraines.	Confining Unit		Ablation till / Till aquitard	5–513	3
Quaternary	Pleistocene	Glacial ice-contact deposits (Qgi)	Bedded diamicton: Flow till and debris flow deposits; typically reworked in ice contact environments.					
Quaternary	Pleistocene	Glacial till (Qgt)						
Quaternary	Pleistocene	Glacial outwash deposits, older (Qgoo)	Outwash deposited during glacial advance; may include some intraglacial alluvium.	Deep alluvial aquifer	Shallow deep aquifer / Deep aquifer	Deep aquifer	15–500	4
Tertiary	Oligocene / Eocene	Kishenehn (Tk)[2]	Tertiary sediments: Brown and orange medium- and coarse-grained pebbly sandstone; pebble and cobble conglomerate; carbonaceous shale and carbonized wood; gray, yellow, and orange mudstone; and orange clayey gravel (diamicton); gravel clasts of argillite, quartzite, and siltstone are mostly well rounded; sandstone and conglomerate beds have channelized, erosional bases. May include strata of the Kishenehn Formation and Paola gravel.	Tertiary sediments	Tertiary sediments	Tertiary sediments	Not modeled	
Middle Proterozoic		Belt Supergroup (Ybe)	Belt bedrock: Composed mostly of siltite, metacarbonates, and quartzite.	Bedrock	Bedrock	Bedrock	Not modeled	

[1] See figure 5 and Smith, 2004 for areal exposure of geologic units. All units are not present at all locations.
[2] Geologic age based on Dawson and Constenius, 2018.
[3] Modified from Smith, 2004.
Note. Not to scale.
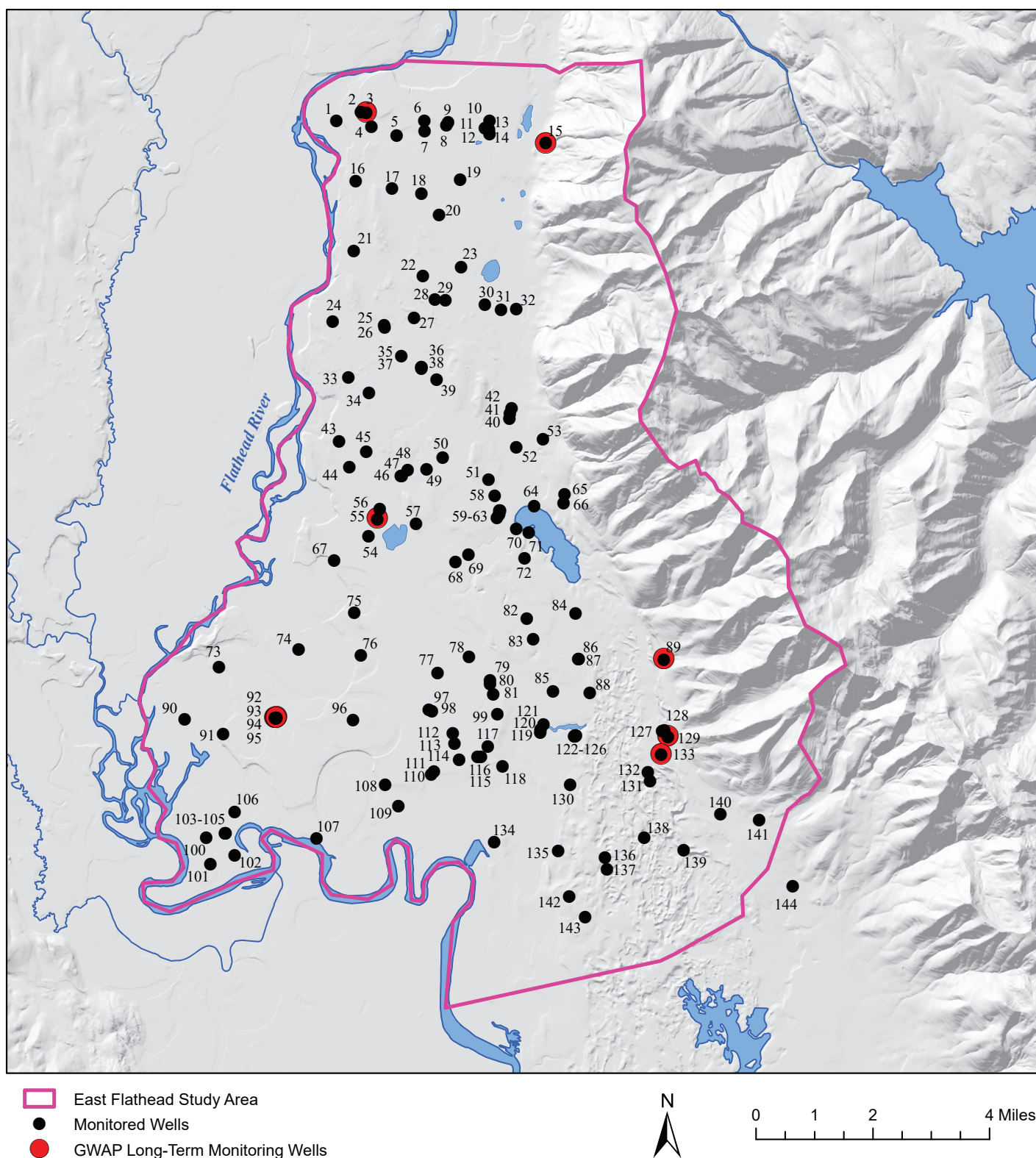
Figure 4. Water levels in 144 wells and piezometers were monitored generally monthly from July 2019 to November 2021. Labels show well numbers, which are cross referenced to GWIC ID numbers, hydrogeologic units, and model layers in appendix A. Measurements from 105 of these wells were used as head calibration targets (appendix A). Seven of the wells in the network are part of MBMG's long-term statewide Groundwater Assessment Program (GWAP) network.

DEVELOPING A STRATIGRAPHIC MODEL

A 3D model of the stratigraphy of the study area was developed to define the hydrogeologic units (HGUs). The HGUs are a simplification or combination of stratigraphic units and are used to define the layers for the numerical models (fig. 3).

Software Description (RockWorks)

Developing a 3D model of the distribution of HGUs within the study area was accomplished using RockWorks 17 software (Rockware, 2015). This software allows for wells and their corresponding lithologic data to be imported and converted into a 3D model.

Selecting Well Logs

Wells from the MBMG's GWIC database (https://mbmggwic.mtech.edu/) with lithologic information were used to construct a 3D geologic model of the study area. Well logs were selected based on the quality of location information, well depth, and the detail of the lithologic information. A total of 446 wells were used; 294 wells with GPS locations, 92 with PLSS location information, and 60 with locations determined from maps (appendix E). As drillers' descriptions can vary widely, the lithologic descriptions for each well log were reclassified into one of 24 simplified lithologic "keywords" (table 2).

Wells closest to the Swan Range mountain front may penetrate to bedrock, but most wells within the valley do not. Depth to bedrock in areas not intersected by wells was estimated from gravity survey information (Smith, 2004b; Stickney, 1980).

Table 2. Lithologic keywords for well log classification.

Bedrock	Gravel and silt
Bedrock fractured	Sand
Boulder	Sand and clay
Clay	Sand and gravel
Clay and gravel/sand	Sand and gravel and clay
Clay and gravel	Sand and silt
Clay and sand	Silt
Clay and silt	Silt and clay
Cobbles	Silt and gravel and sand
Gravel and clay	Silt and gravel
Gravel and sand	Silt and sand
Gravel and sand and clay	Soil

Developing and Exporting 3D Solids to Groundwater Vistas

Locations of the selected wells along with their simplified lithologies were imported into RockWorks to develop 3D solids of the geologic units. The ground surface was defined using LiDAR-derived elevation data (Watershed Sciences, 2010). The stratigraphic units were defined based on hand-drawn cross sections between wells. These cross sections were guided, in part, by previous detailed geologic mapping and hydrogeologic models of the area (Uthman and others, 2000; Smith, 2004a,b,c,d,e,f; Vuke and others, 2007; Rose, 2018; fig. 5). RockWorks produces 3D solids from the stratigraphic units, while interpolating the depth and thickness of each unit.

For groundwater flow modeling, the many lithologic units identified using RockWorks were simplified into eight HGUs based on their similar aquifer properties. The identified HGUs are: shallow aquifer, lacustrine aquitard, sandy lacustrine sediments, intermediate aquifers, till aquitard, deep aquifer, mountain front deposits, and bedrock. Once defined, these solids were used to define the aquifer properties for four MODFLOW model layers in Groundwater Vistas (fig. 3, table 1).

NUMERICAL MODEL CONSTRUCTION

Development of the East Flathead numerical groundwater model included both steady-state and transient groundwater models. The steady-state model was based on midwinter conditions (calibrated to January 2020). We selected these data because they represent a relatively static, quasi-steady condition for the East Flathead model domain. This is consistent with literature guidance for calibration of a steady-state model (Anderson and others, 2015). The steady-state model is useful for calibrating non-dynamic aquifer properties, such as hydraulic conductivity, streambed conductance, and drain conductance.

The transient model is based on monitoring data collected from 2019 to 2021, and time-dependent water budget parameters (table 3, appendix C). The transient model was used to evaluate the time-dependent effects of stresses on the system and evaluate effects at key times (e.g. late-summer stream flows).
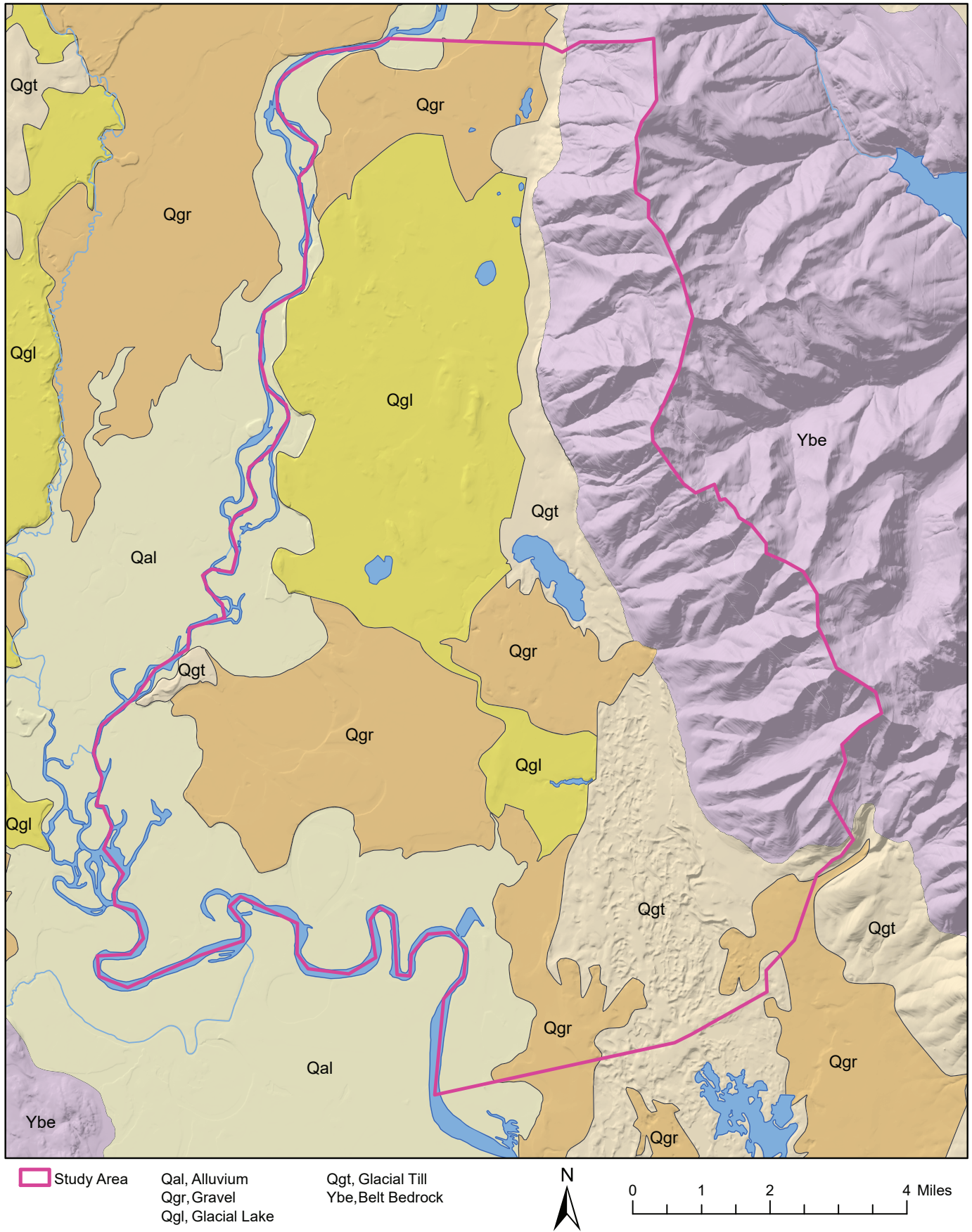
Figure 5. The surficial geology of the East Flathead area (modified from Vuke and others, 2007) informed the geologic model. This was supplemented with more detailed information from Smith, 2004.

Table 3. Water budget comparison (acre-ft).

Preliminary Water Budget (Appendix C)

	Oct	Nov	Dec	Jan	Feb	Mar	Apr	May	Jun	Jul	Aug	Sep	Annual Total
Mountain front recharge	1,777	1,659	1,594	1,395	1,216	1,409	2,296	5,587	7,020	4,043	2,202	1,704	31,902
Groundwater inflow	878	850	878	878	800	878	850	878	850	878	878	850	10,346
Areal recharge	728	705	728	728	663	728	705	728	705	728	728	705	8,578
Lake Blaine infiltration	536	518	536	536	488	536	518	536	518	536	536	518	6,311
Irrigation recharge	0	0	0	0	0	0	0	0	917	1,334	896	548	3,695
Septic returns	59	57	59	59	54	59	57	59	57	59	59	57	693
TOTAL inflows	3,978	3,788	3,795	3,595	3,222	3,610	4,425	7,787	10,065	7,578	5,299	4,381	61,524
Well pumping	228	181	180	182	166	185	183	398	2,129	3,829	2,773	470	10,903
Discharge to surface waters	2,354	2,279	2,354	2,354	2,146	2,354	2,279	2,354	2,279	2,354	2,354	2,279	27,741
Lake evaporation	91	29	14	14	30	75	141	293	326	421	345	199	1,977
Riparian evapotranspiration	34	0	0	0	0	45	46	77	78	109	109	73	572
Net residual outflow*	1,726	1,670	1,726	1,726	1,572	1,726	1,670	1,726	1,670	1,726	1,726	1,670	20,330
TOTAL outflows	4,433	4,158	4,274	4,276	3,915	4,384	4,318	4,849	6,482	8,438	7,307	4,690	61,524
Change in storage	-455	-370	-478	-681	-693	-774	107	2,938	3,583	-860	-2,008	-309	0

Simulated Water Budget (Last Model Year; 2036)

	Oct	Nov	Dec	Jan	Feb	Mar	Apr	May	Jun	Jul	Aug	Sep	Annual Total
Mountain front recharge	1,751	1,626	1,561	1,376	1,199	1,376	2,251	5,472	6,879	3,971	2,157	1,657	31,276
Groundwater inflow	939	908	939	939	863	939	908	939	908	939	939	908	11,066
Areal recharge	664	643	664	664	611	664	643	976	944	976	664	643	8,758
Lake Blaine infiltration	671	650	671	671	617	671	650	671	650	671	671	650	7,916
Irrigation recharge	0	0	0	0	0	0	0	0	876	1,262	841	526	3,504
Septic returns	54	53	54	54	50	54	53	54	53	54	54	53	641
TOTAL inflows	4,080	3,880	3,890	3,705	3,340	3,705	4,505	8,112	10,310	7,873	5,327	4,437	63,162
Well pumping	224	179	179	181	167	183	181	384	2,064	3,710	2,682	451	10,586
Discharge to surface waters	2,350	2,250	2,302	2,280	2,075	2,234	2,142	2,231	2,215	2,362	2,382	2,294	27,118
Lake evaporation	91	29	14	14	31	75	141	293	326	421	345	199	1,978
Riparian evapotranspiration	34	0	0	0	0	45	45	77	78	107	107	72	564
Net residual outflow*	3,271	3,169	3,277	3,279	3,015	3,280	3,067	2,773	2,647	3,113	3,250	3,158	37,298
TOTAL outflows	5,969	5,627	5,772	5,754	5,288	5,817	5,577	5,758	7,329	9,712	8,767	6,174	77,543
Change in storage	-1,889	-1,748	-1,882	-2,049	-1,948	-2,112	-1,072	2,354	2,981	-1,839	-3,440	-1,737	-14,381

*Includes outflow to Flathead River and groundwater.

Software Description

We used the U.S. Geological Survey (USGS) MODFLOW-2005 code, version 1.12.00 (Harbaugh, 2005) with Groundwater Vistas (GWV, version 8.15) as a graphical user interface (Environmental Simulations Incorporated, 2020). GWV facilitates the use of geographic information system (GIS) products, such as ESRI shapefiles. Parameter Estimation software (PEST) was used for automated model calibration (Doherty and Hunt, 2010).

Model Domain

The model domain covers the valley fill sediments above the Tertiary basal aquitard on the east side of the Flathead Valley (fig. 1; appendix F). The full study area extends up to the drainage divide of the Swan Range to account for snowfall and snowmelt; however, since there are few wells in the Swan Range, the area of exposed bedrock was not explicitly included in the numerical model. The areal extent of the model domain is 94.7 mi^2.

The model domain is bounded on most of its perimeter by hydrogeologic flow boundaries (figs. 6, 7). The Flathead River is on the western edge, and the Swan Range is to the east. For all four model layers the northern boundary follows a groundwater flow line (hydraulic no-flow boundaries) as defined by previous studies (LaFave and others, 2004; Rose and others, 2022; figs. 6, 7), and supported by monitoring during this study. In the upper three layers (layers 1–3), the southern boundary follows a surface divide, which is also a groundwater divide. In the deep aquifer (layer 4), groundwater inflow is across the southern boundary due to a low-permeability bedrock high (northern extension of the Mission Range) forming a flow barrier on the west side of this boundary (figs. 3, 7). This bedrock flow barrier forces groundwater from the Swan Valley to flow further north before turning west into the main Flathead Valley.

Spatial Discretization

A four-layer model (fig. 3) was constructed using 174 rows and 117 columns, with uniform cells 500 x 500 ft horizontally. Excluding cells outside the model domain, and no-flow cells in layers 3 and 4 due to bedrock topography (fig. 7), the grid contains 41,460 active model cells.

Elevations and thicknesses of the four model layers were determined from the 3D solids imported into GWV from RockWorks (appendix F, figs. F1–F6). It should be noted that the deep aquifer was modeled as having a maximum thickness of 500 ft, since the total thickness of the deep aquifer is poorly defined, and the upper portion of the aquifer is where most wells are completed.

Initial Hydraulic Parameters

Initial hydraulic parameters [hydraulic conductivity (K), specific yield (S_y), and specific storage (S_s), drain conductance, and streambed conductance] were assigned based on aquifer tests conducted in the area (appendix D) and literature values based on sediment types (Freeze and Cherry, 1979; Heath, 1983; Fetter, 2018). These parameters were adjusted during the calibration process (see steady-state calibration section below).

Initial Heads

Heads were set to 3,400 ft-amsl for the first model run, which is about 200 ft higher than the highest point in the model, to ensure that there were no dry cells. For subsequent model runs the final heads from the previous iteration of the model were used as starting heads.

Boundary Conditions and Water Budget

Boundary conditions are either sources or sinks of water in the groundwater model. Initial model inflows and outflows were parameterized based on values obtained from the preliminary water budget (appendix C, table 3) and are summarized below. The total amount of water moving through the groundwater model domain was estimated to be about 60,000 acre-ft/yr. These sources and sinks were implemented using several MODFLOW packages, as discussed below.

Inflows

Mountain Front Recharge (MFR) along the Swan Mountain front was the largest source of groundwater inflow (52% of inflows; fig. 6). MFR was assigned to layer 1 at the mountain front using the well package (specified flux) to represent the infiltration of stream flow and shallow groundwater inflow from bedrock to the unconsolidated aquifers. About a third of the MFR applied was groundwater inflow (MBR in appendix
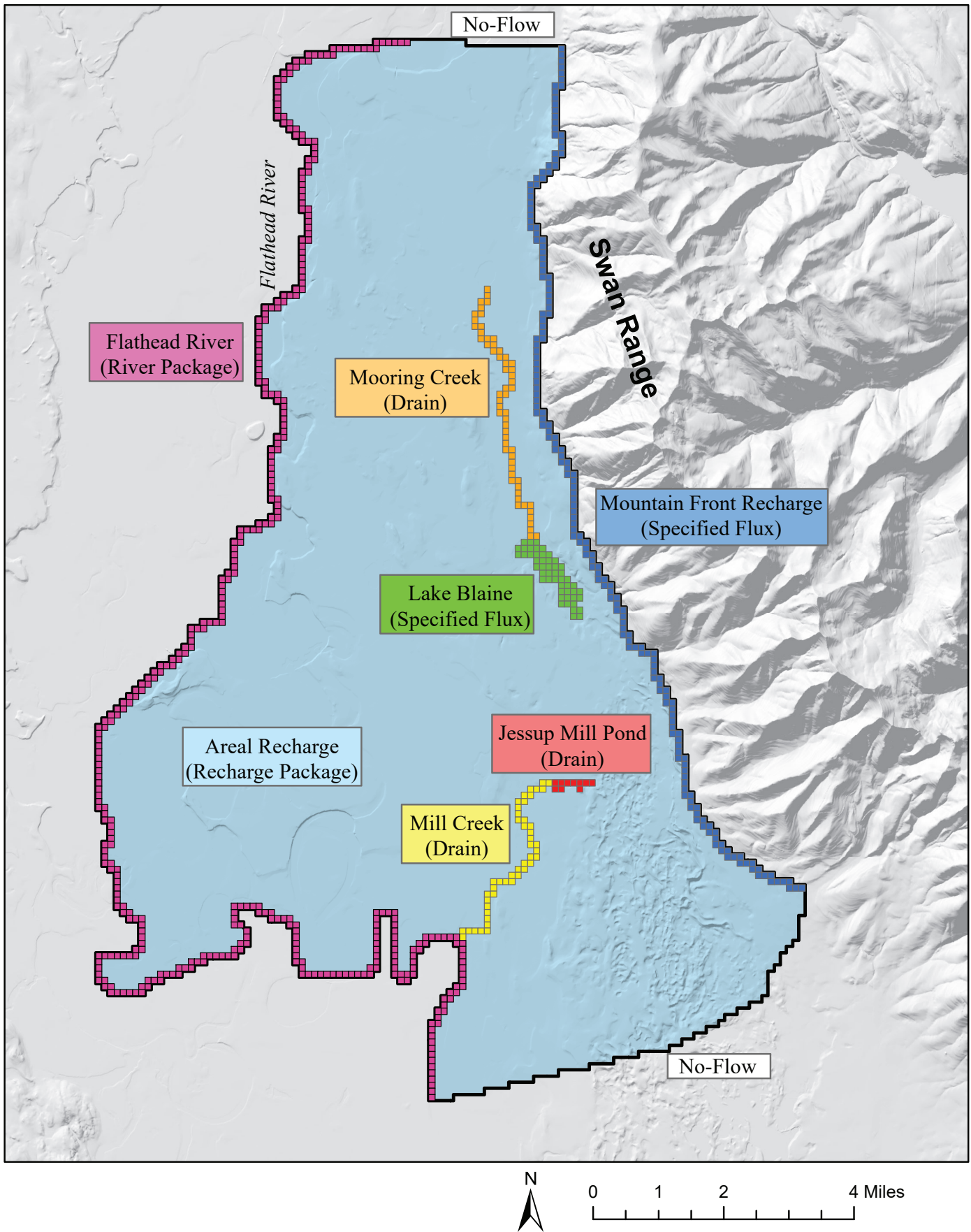
Figure 6. Boundaries and model features in layer 1. For clarity, wells, septic returns, irrigation recharge, lake evaporation, and riparian ET are not shown.
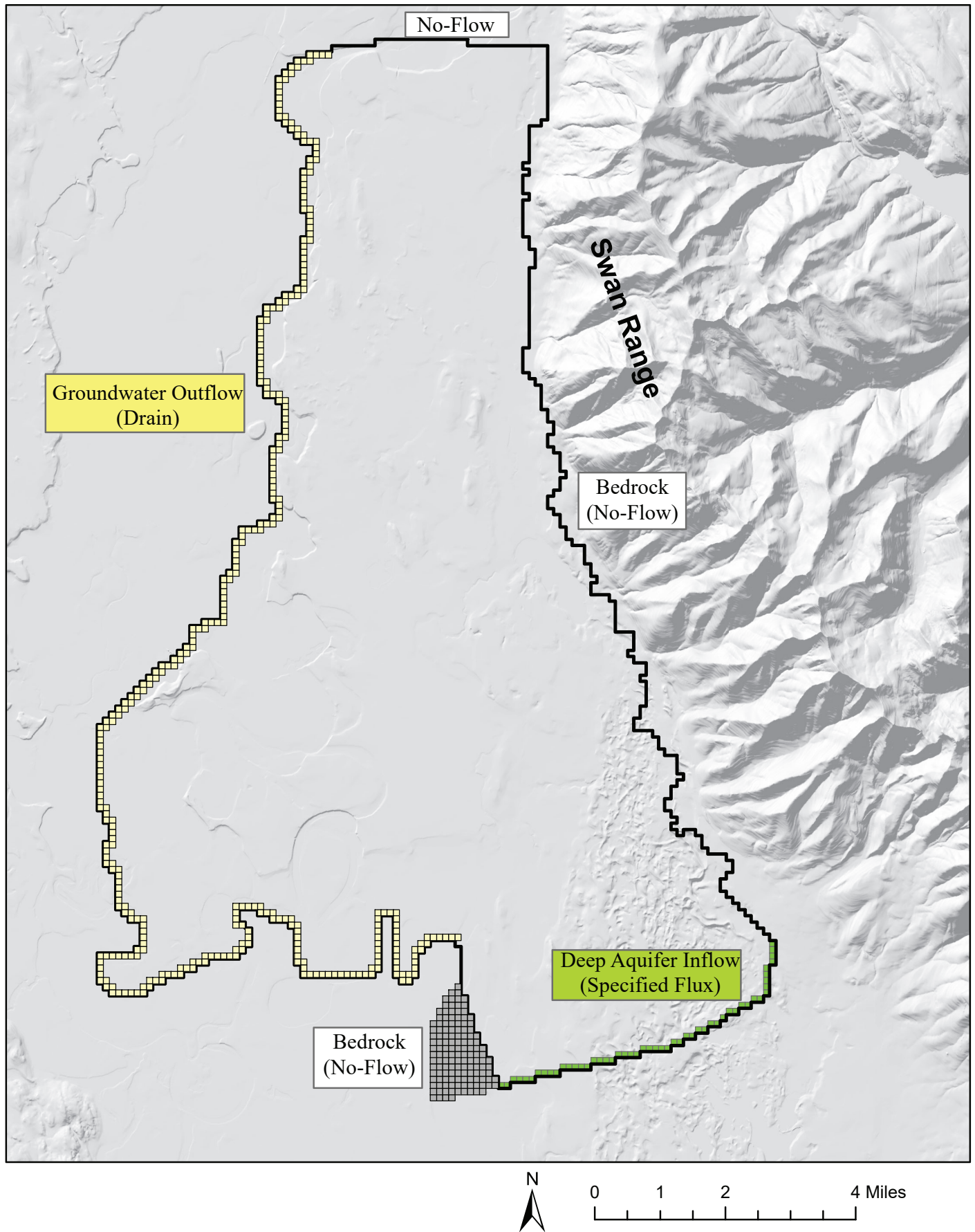
Figure 7. Boundaries and model features in layer 4. Note that while the east side of layer 4 is a no-flow boundary (reflecting the bedrock contact), there is substantial inflow from the overlaying layers on the east site (reflecting the mountain front deposits; fig. 4). For clarity, wells are not shown.

C), and the other two-thirds was from stream infiltration at the mountain front (MFRs in appendix C).

Based on observations of the deep aquifer potentiometric surface developed from our monitoring data, along with layer thicknesses and bedrock elevations, groundwater inflow into the model area occurs into the deep aquifer (Layer 4) along the southeastern edge of the model from the Swan Valley (17% of inflows; fig. 7). This deep Swan Valley groundwater inflow was also modeled as a specified flux using the well package.

Areal recharge from infiltration of precipitation (14% of inflow; fig. 6) occurs throughout the study area, and was modeled using the recharge package. Recharge also occurred as infiltration at Lake Blaine (10%; fig. 6) and septic returns (1%), both of which were modeled using the well package. For the transient model, irrigation recharge was also included (6%) and was modeled using the well package. Irrigation recharge was not included for the steady-state model since it was calibrated to January 2020 conditions, when there was no irrigation occurring.

Outflows

Model outflows include outflows to streams, groundwater outflow, pumping wells, evaporation from groundwater-fed lakes, and evapotranspiration. Notable surface-water outflow features include Jessup Mill Pond (27% of outflow; fig. 6), Mill Creek (14%; fig. 6), and Mooring Creek (4%; fig. 6), which were all modeled using the drain package, and were calibration targets. Evaporation from groundwater-fed lakes throughout the study area was modeled using the well package (3%), and riparian evapotranspiration along the Flathead River and other water bodies was modeled using the evapotranspiration segments package (1%). Pumping wells, including domestic wells (3%) and commercial/industrial wells (3%), were modeled using the well package. For the transient model, irrigation wells were also included (11%). While they are nearly impossible to measure directly, or to separate based on monitoring data, the water budget indicated that the combined outflows to the Flathead River (river package; fig. 6) and beneath the river as underflow (drain package; fig. 7) were also important (33%, combined).

STEADY-STATE NUMERICAL MODEL

Steady-State Calibration

To aid in model calibration, each of the layers was divided into zones (appendix F, figs. F7–F10); 84 zones were used. Within each zone, aquifer parameters are assumed to be homogeneous. In layer 1 we used 22 zones based on the distribution of geologic units mapped at the surface (Smith, 2004a; fig. 5). Layer 2 used the same geographic distribution of zones as layer 1. In layer 3, due to having no wells completed in this layer and apparently laterally similar lithologies, 13 zones were initially used, using combined hexagonal polygons and narrow zones along the east side to account for mountain front deposits. Layer 4 was divided into 26 zones based on hexagonal polygons. During model calibration an additional zone (zone 84) composed of 3 polygons was added to layer 3 to allow for more permeable "windows" through the confining layer, which connect the shallow and deep aquifers in the southern portion of the study area. These more permeable zones were needed because we were unable to satisfactorily calibrate the model with a continuous low-K confining layer separating the shallow and deep aquifers. These windows allowed simulated groundwater to discharge to Jessup Mill Pond and Mill Creek at rates similar to monitoring results, while maintaining simulated groundwater elevations similar to observed.

Static water levels measured in 105 wells during January 2020 were used as targets for the steady-state calibration (appendix A). Twenty-six wells were associated with layer 1, 25 wells for layer 2, and 54 wells for layer 4. There were no monitored wells in layer 3, which is dominated by low productivity till and lacustrine deposits. Three flux targets representing the flow of groundwater to Mooring Creek, Jessup Mill Pond, and Mill Creek (appendix B) were also used as calibration targets.

Following manual calibration, automated calibration was conducted using PEST. The same 105 wells and 3 flux targets were used. Due to the much higher magnitude of values for the flux targets (because of different units; e.g., ft³/d vs. ft) relative to head targets, the flux targets were weighted at 0.0002, so that their influence on the objective function would be similar to the heads. During the steady-state PEST calibration,

the adjusted parameters were the K values in the 84 zones, along with conductance values for the drain and river reaches.

Root mean squared error (RMSE) is a calibration criterion for groundwater heads that is usually considered to be the best measure of normally distributed errors (Anderson and others, 2015). Prior to model calibration we established that the RMSE should be less than 10 ft, which is approximately 5% of the observed head range in the model area. After calibration the steady-state model had an RMSE of 8.16 ft.

The potentiometric surfaces produced by the calibrated steady-state model were generally similar to potentiometric surfaces developed from monitoring data (appendix G, figs. G1–G4; Bobst and others, in prep.). Eighty-four of the wells (76%) had a residual less than 10 ft (fig. 8). The distribution of residuals by elevation and by geographic location was non-patterned (fig. 8, appendix G, fig. G5). Simulated groundwater levels for the four model layers followed the same overall pattern (appendix G, figs. G1–G4). Groundwater flow is generally from the east (Swan Range) to the west and southwest (toward the Flathead River and Flathead Lake). In layer 4 the no-flow boundary representing the bedrock high associated with the northern end of the Mission Range (figs. 3, 7) causes groundwater flow in the southeast portion of the model to be to the north, and then to the west as groundwater flows around the bedrock high (appendix G, fig. G4).

The simulated flux values of the drains were also similar to the targets. Discharge to Mooring Creek estimated from monitoring data was at an average annual rate of 3.2 cfs, while the calibrated steady-state model simulated a flux of 3.9 cfs. Similarly, the monitoring-based fluxes to Jessup Mill Pond and Mill Creek were 23.4 and 13.1 cfs, while the simulated fluxes were 23.2 and 12.5 cfs, respectively. Overall the simulated total flux to drains (39.72 cfs) was nearly identical to observed (39.70 cfs). Conductance values are shown in appendix G (figs. G6–G7, table G1).

Calibrated horizontal K for the model zones were heterogeneous, with modeled values from 0.003 to 419 ft/d (appendix G; figs. G8–G11). Model layer 1 ranged from 1.2 ft/d to 300 ft/d. Model layer 2 was somewhat lower, with values ranging from 0.4 ft/d to 100 ft/d. Model layer 3 has the lowest hydraulic conductivity, ranging from 0.003 ft/d to 20 ft/d. Higher conductivity zones in layer 3 are limited to zone 47 (20 ft/d), on the western boundary of the model, and zone 84 (7.3 ft/d), composed of three polygons in the southern region of the model (appendix F, fig. F9; appendix G, fig. G10). Model layer 4 had a hydraulic conductivity range from 1.6 ft/d to 419 ft/d, and is dominantly values greater than 10 ft/d (fig. G11).
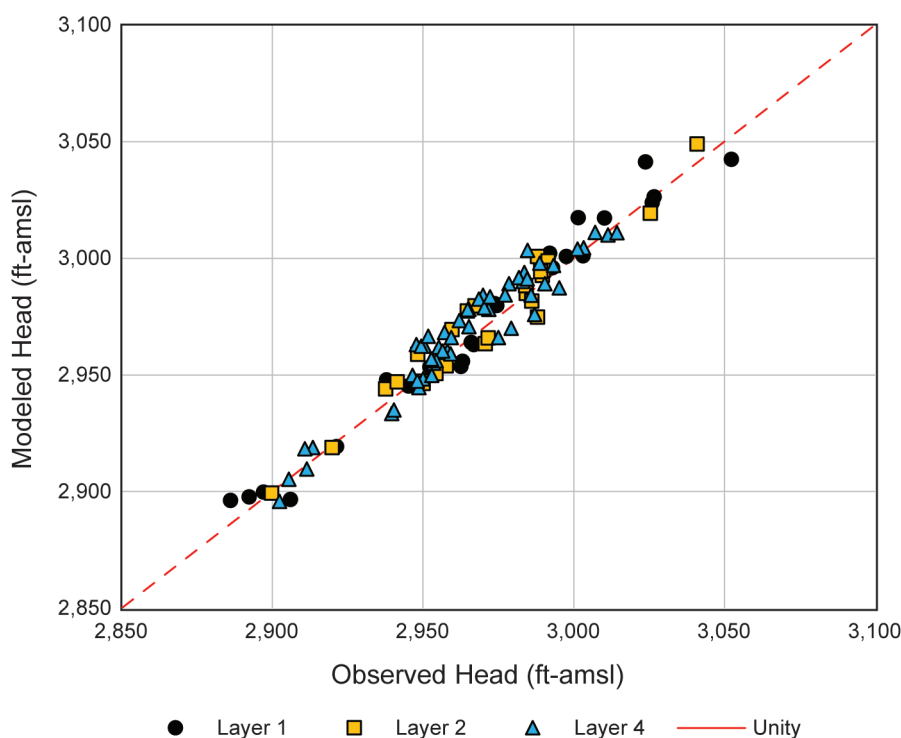
Figure 8. Observed vs. modeled groundwater elevations for the calibrated steady-state model. There were no monitoring wells in layer 3.

Sensitivity Analysis

Sensitivity analysis of parameters within the steady-state model was performed during PEST runs. That is, when PEST runs, a Jacobian matrix is created that guides automated parameter adjustments, and also provides information on which parameters are most sensitive (Anderson and others, 2015; Doherty and Hunt, 2010). The sensitivity coefficients are unitless, and indicate how much the model output at the targets (i.e., the objective function) changes as a result of adjusting each parameter. The tested parameters included K of all zones (with vertical K defined as 10% of horizontal K; i.e., $K_z/K_x = 0.1$) and the drain and river conductance values. Sensitivity values were averaged for K-values within each of the four layers. Sensitivity values were also averaged for the drain conductance associated with Mooring Slough, Jessup Mill Pond, and Mill Creek, the river conductance of the Flathead River, and the drain conductance of the layer 4 outflow drain (figs. 6, 7, 9). The most sensitive parameters were the drain conductance of Jessup Mill Pond and the hydraulic conductivity of layer 3 (the confining layer), while the least sensitive parameters included Mooring Slough drain conductance and the Flathead River conductance (fig. 9). Hydraulic conductivity val-ues of layers 1, 2, and 4, and the drain conductance for layer 4 groundwater outflow, had similar and relatively low sensitivities.

TRANSIENT NUMERICAL MODEL

Groundwater levels showed distinct transient patterns that reflect seasonal recharge from spring snowmelt and irrigation pumping in the summer (figs. 10, 11; Bobst and others, in prep.). The transient groundwater model was developed and calibrated to simulate these observed seasonal patterns. Spring recharge results in an asymmetric hydrograph, with peak water levels occurring from June to August, followed by a gradual decline until the pattern repeats a year later. This pattern is attributed to short duration, intense recharge from snowmelt along the mountain front, resulting in a sharp rise in water levels. Water levels then gradually decline until the onset of the following annual snowmelt event. Irrigation pumping results in a "plateau" pattern in the hydrograph, where water levels are generally constant from September to June, punctuated by a sharp water-level drop in July and August due to pumping. This plateau-response hydrograph is particularly clear in wells that are geographically removed from snowmelt recharge, or
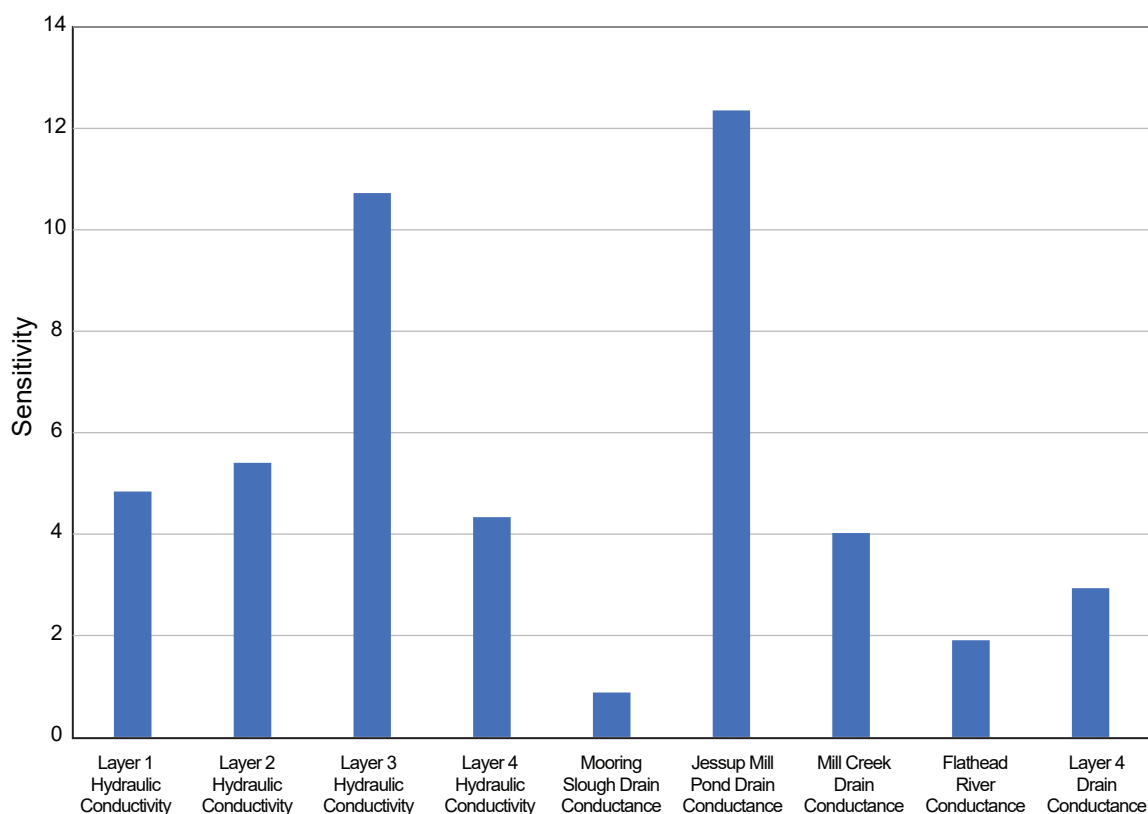
Figure 9. Modeled sensitivities of varying the hydraulic conductivity and drain conductance parameters (higher sensitivity value equates to greater sensitivity; sensitivity is unitless; Anderson and others, 2015; Doherty and Hunt, 2010).
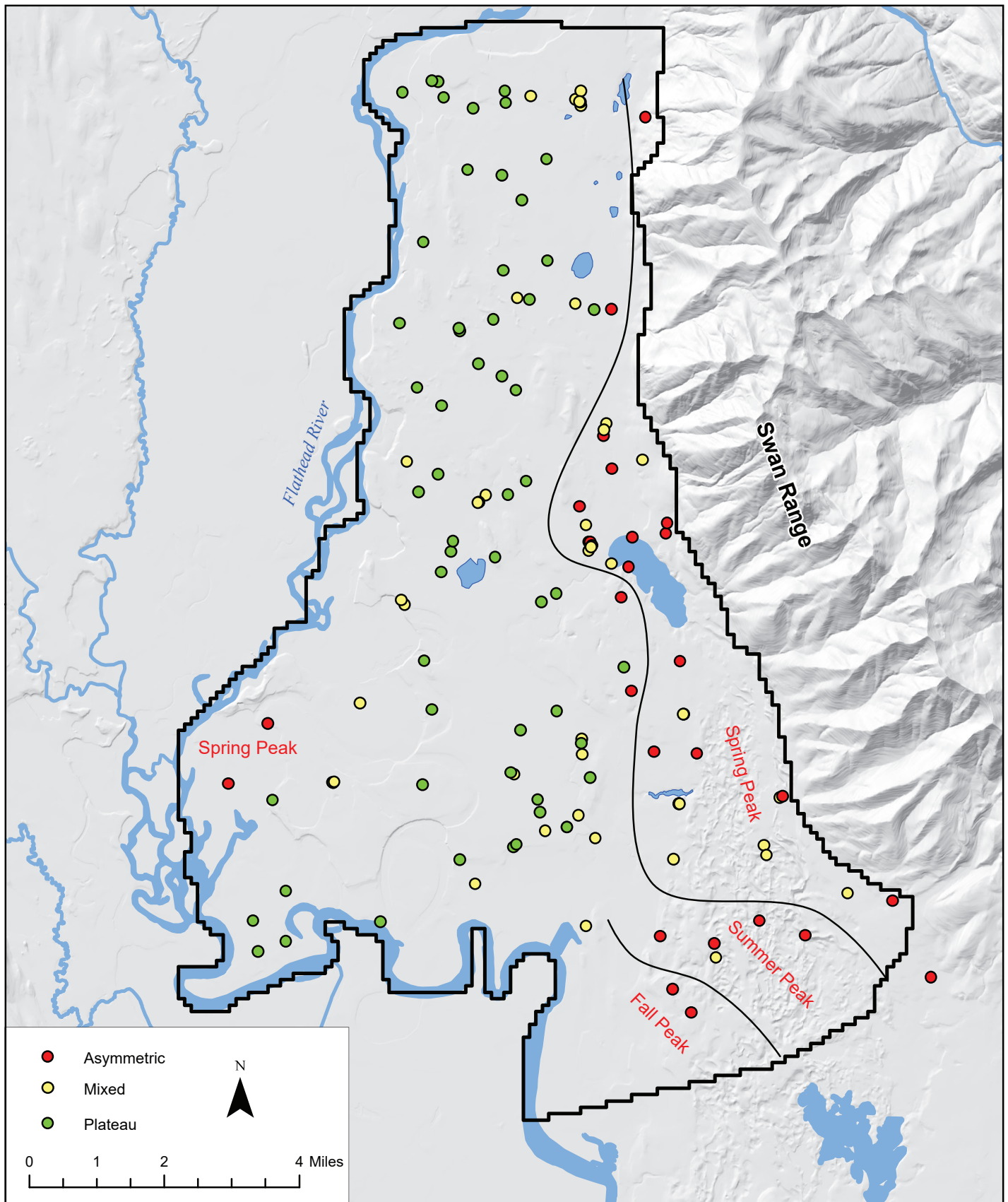
Figure 10. Distribution of wells with asymmetric, plateau, or mixed hydrograph types, and timing of peaks for asymmetric hydrographs. Wells near the Swan Mountain front peaked in the spring, while wells further from the front peaked in the summer or fall. Some wells near the Flathead River also peaked in the spring, likely due to high river stage.
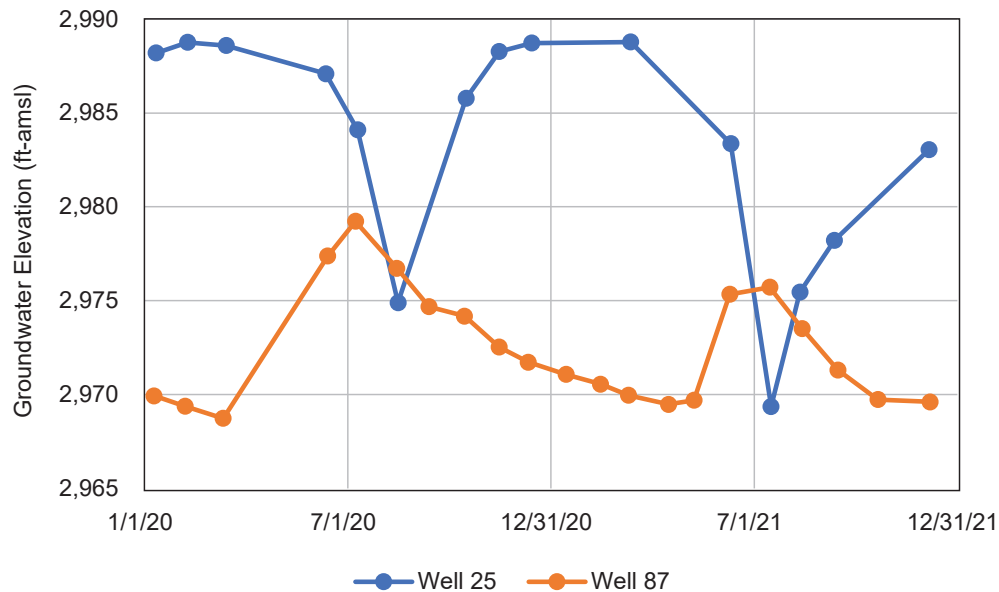
Figure 11. Example hydrographs for wells showing seasonal signals dominated by summer pumping (well 25; plateau hydrograph) and spring recharge (well 87; asymmetric hydrograph).

geologically separated from it. In particular, the wells in the northwest portion of the study area appear to be separated from snowmelt recharge at the Swan Range mountain front due to the presence of a previously documented "trench" in the top of the deep aquifer trending parallel with the mountain front, where lacustrine sediments have filled in an eroded channel (appendix F, fig. F5; Smith, 2004c,d; Rose, 2018). This lack of a snowmelt recharge signal results in generally stable water levels throughout the non-irrigation season. Other wells display mixed patterns, where both the spring recharge and summer pumping signals are apparent. These hydrographs have two water-level maxima occurring around June and November with declines in between.

Temporal Discretization

Monthly stress periods, with five time steps in each stress period, were used for the transient models. A 5-yr model was used for transient model calibration, running from January 1, 2017 to December 31, 2021. Each model year used the same transient boundary conditions for each monthly stress period, which precluded incorporating the effects of particularly wet or dry years. Heads from the steady-state model were used as initial heads for the first transient run, then the final heads from each subsequent run were used as initial heads for the next run. Calibration was relative to field observations (2019–2021).

Transient Calibration

Transient boundary conditions defined by the preliminary groundwater budget (appendix C) and storage parameters (S_y and S_s) were adjusted during the transient calibration. We used the Nash–Sutcliffe (NS) coefficient of efficiency (Nash and Sutcliffe, 1970; Anderson and others, 2015) to quantify the fit between simulated and measured drawdowns (appendix H). NS values range from negative infinity to 1, with values greater than 0 and closer to 1 indicating a good fit. The modeled change in heads was used to measure the model's performance. NS provided an objective summary statistic to guide the calibration of the storage parameters. Drawdown was used rather than absolute head since the absolute head values are largely determined by the K and conductance parameters set during the steady-state calibration. Using drawdown "will often facilitate better estimation of storage and/or recharge parameters than would result if head values alone were employed in the calibration process" (Doherty and Hunt, 2010).

The transient calibration used the same 84 zones as the steady-state calibration. Of the 105 wells used for the steady-state model, 98 wells had sufficient observations to use for the transient calibration. The objective was to maximize the median NS coefficient for the transient observation wells. The final calibrated model had a median NS coefficient of 0.27, and 88% of the wells had NS coefficients between -0.5 and 1 (appendix H). The transient model reasonably simu-

lated the variations in water levels observed from 2019 to 2021. For wells where fits were poor (NS coefficients <-1) there were nearby wells with good fits (NS coefficients >0.5; fig. H1). This prevented improving the poor fits since it would degrade the good fits. This suggests that the zones used (appendix F; figs. F7–F10) were unable to fully represent the heterogeneity of the hydrogeologic units, or that some local factors were not fully simulated.

Following calibration, the transient model was extended to run for 20 years (1/1/2017–12/31/2036). This 20-yr model was used to compare the simulated groundwater budget to the preliminary groundwater budget (appendix C), and was used to conduct scenario testing. As with the 5-yr model, each model year used the same transient boundary conditions for each monthly stress period.

Water-Budget Evaluation

The water budget (mass balance) for the final year of the transient model (appendix H) was evaluated relative to the preliminary groundwater budget (fig. 12, table 3, appendix C). Inflows and outflows for the transient model averaged about 70,000 acre-ft/yr, which is somewhat greater than the preliminary budget estimate of about 62,000 acre-ft/yr (appendix C). The inflows matched well between the preliminary and modeled values (61,500 vs. 63,200 acre-ft/yr, respectively), which is expected since many of them were model inputs using specified flux boundaries. Over the last model year, the outflows were about 120% of inflows (77,500 vs 63,900 acre-ft/yr, respectively), showing that the model had not completely reached dynamic equilibrium. However, the average difference in head over the last year of the model run was less than 0.02 ft, indicating that the model is near dynamic equilibrium, and suitable for evaluation of the likely changes due to different scenarios relative to the baseline run. The individual components of modeled outputs were similar to preliminary estimates (since they were often used as calibration targets), except for residual outflow (groundwater outflow and discharge to the Flathead River), which was not unexpected since it was estimated as the residual of the other water budget components, and was neither specified nor used as a target.

SCENARIO TESTING

Four model scenarios were tested to evaluate the potential effects from increased well pumping and drought. For each scenario, the model was run for 5 yr (2017–2021) using the baseline values, then a change was applied to either well pumping or recharge (table 4). The calibrated 20-yr transient model was used as baseline for scenario testing. Effects to groundwater availability were evaluated by examining changes in head (dh) in the shallow and deep aquifers (layers 1 and 4; table 5), and changes in groundwater outflow from the model domain (fig. 13, table 6). Effects to surface-water availability were evaluated by examining the changes in groundwater outflow to the surface-water features receiving the most groundwater outflow (Jessup Mill Pond, Mill Creek, and the Flathead River; fig. 13, table 6). As all scenarios involve increased pumping or reduced recharge, the reported changes in head (dh) for these scenarios indicates lower groundwater levels (drawdown).

The tested scenarios provide an understanding of the overall system response to increased groundwater development and drought conditions. The results provide examples of the types of effects that should be expected from different stresses on the system. These development scenarios are hypothetical, and do not represent any particular proposed development. Many other scenarios could be tested using the model, and the authors invite others to perform additional testing.

Scenario 1: Double Residential Well Pumping

Model Modifications

Rather than hypothesize about future areas of development and well completions, we simply doubled the rates from the existing residential supply wells (domestic and public water supply wells) in model layers 1, 2, and 4 for this scenario. This was an increase from 2,153 to 4,306 acre-ft/yr. Septic return inflows to layer 1 were also doubled from 693 to 1,386 acre-ft/yr.

Results

Increased pumping for residential uses reduced groundwater levels and reduced groundwater outflow to surface waters and the groundwater outflow from the model domain. This is consistent with many years of hydrogeologic research (e.g., Theis, 1940; Jenkins,

Preliminary Inflows

Mountain Front Recharge — 52%
Lake Blaine Infiltration — 10%
Groundwater Inflow — 17%
Areal Recharge — 14%
Irrigation Recharge — 6%
Septic Returns — 1%

Legend:
- Mountain Front Recharge
- Lake Blaine Infiltration
- Groundwater Inflow
- Areal Recharge
- Irrigation Recharge
- Septic Returns

Modeled Inflows

Mountain Front Recharge — 50%
Lake Blaine Infiltration — 10%
Groundwater Inflow — 18%
Areal Recharge — 14%
Irrigation Recharge — 6%
Septic Returns — 1%

Legend:
- Mountain Front Recharge
- Lake Blaine Infiltration
- Groundwater Inflow
- Areal Recharge
- Irrigation Recharge
- Septic Returns

Preliminary Outflows

Well Pumping — 18%
Discharge to Surface Waters — 45%
Lake Evaporation — 3%
Riparian Evapotranspiration — 1%
Groundwater Outflow and Discharge to Flathead River — 33%

Legend:
- Well Pumping
- Discharge to Surface Waters
- Lake Evaporation
- Riparian Evapotranspiration
- Groundwater Outflow and Discharge to Flathead River

Modeled Outflows

Well Pumping — 12%
Discharge to Surface Waters — 36%
Lake Evaporation — 3%
Riparian Evapotranspiration — 1%
Groundwater Outflow and Discharge to Flathead River — 49%

Legend:
- Well Pumping
- Discharge to Surface Waters
- Lake Evaporation
- Riparian Evapotranspiration
- Groundwater Outflow and Discharge to Flathead River

Figure 12. Comparison of the annual total modeled water budget components to the preliminary water budget (appendix C). Annual total and monthly values are presented in table 3.

Table 4. Tested model scenarios.

Scenario	Calendar Year																			
	2017	2018	2019	2020	2021	2022	2023	2024	2025	2026	2027	2028	2029	2030	2031	2032	2033	2034	2035	2036
(1) Double residential				Baseline																x
(2) Double irrigation																				x
(3) 1-yr Drought						x	x				x					x				
(4) 5-yr Drought										x	x				x					x

Note. Blue, baseline conditions; x, tabulated results (tables 5 and 6); orange, changed pumping or recharge.

Table 5. Summary of change in head for the tested scenarios.

Scenario	Evaluation Time	Average dh Layer 1	Max dh Layer 1	Average dh Layer 4	Max dh Layer 4	1 ft dh area Layer 1	10 ft dh area Layer 1	1 ft dh area Layer 4	10 ft dh area Layer 4
		(ft)				(mi²)			
(1) Double residential	August 2036	0.43	4.06	0.66	2.84	14	0.00	13	0.00
(2) Double irrigation	August 2036	1.12	8.08	1.46	3.80	46	0.00	55	0.00
(3) 1-yr Drought	August 2022	1.50	34.64	2.74	26.87	43	0.07	51	0.46
	August 2023	0.82	34.69	2.47	26.89	40	0.06	49	0.46
	August 2027	0.47	33.99	2.07	26.38	36	0.06	46	0.31
	August 2032	0.52	33.97	2.11	26.41	37	0.05	47	0.32
(4) 5-yr Drought	August 2026	2.30	36.19	3.65	27.83	53	0.94	69	3.24
	August 2027	1.21	35.48	2.93	27.28	46	0.12	60	0.71
	August 2031	0.61	34.19	2.22	26.47	39	0.06	48	0.34
	August 2036	0.64	34.10	2.24	26.49	40	0.07	48	0.35

Note. Total area of layer 1 is 95 mi² and layer 4 is 89 mi². dh, change in head (drawdown).

1968; Winter and others, 1998). Extraction of water from an aquifer will result in less groundwater storage (groundwater head is reduced, resulting in areas of drawdown). Storage losses from the aquifer must be balanced by changes in the amount of water entering or leaving the system to maintain long-term dynamic equilibrium. Since the pumping rates were increased and then held constant at the new level, subsequent drawdown and stream depletion occurred immediately after the change and then leveled off as a new dynamic equilibrium was approached (fig. 13). At the end of the model run (2036), the simulated average change in groundwater levels for layers 1 and 4 was 0.43 and 0.66 ft, respectively (table 5). Groundwater dis-

charge to Jessup Mill Pond (which receives the most groundwater discharge) was reduced by 0.6 cfs (a 3% reduction; fig. 13A, table 6). Simulated groundwater outflow from the model domain was reduced by 15.1 acre-ft/mo (a 1% reduction; fig. 13D, table 6).

Scenario 2: Double Irrigation Well Pumping

Model Modifications

The 20-yr model was modified by doubling the pumping rates for the simulated irrigation wells (table 4). This was a total increase in irrigation pumping from 6,679 to 13,358 acre-ft/yr. Rather than hypothesize about future areas of development and well
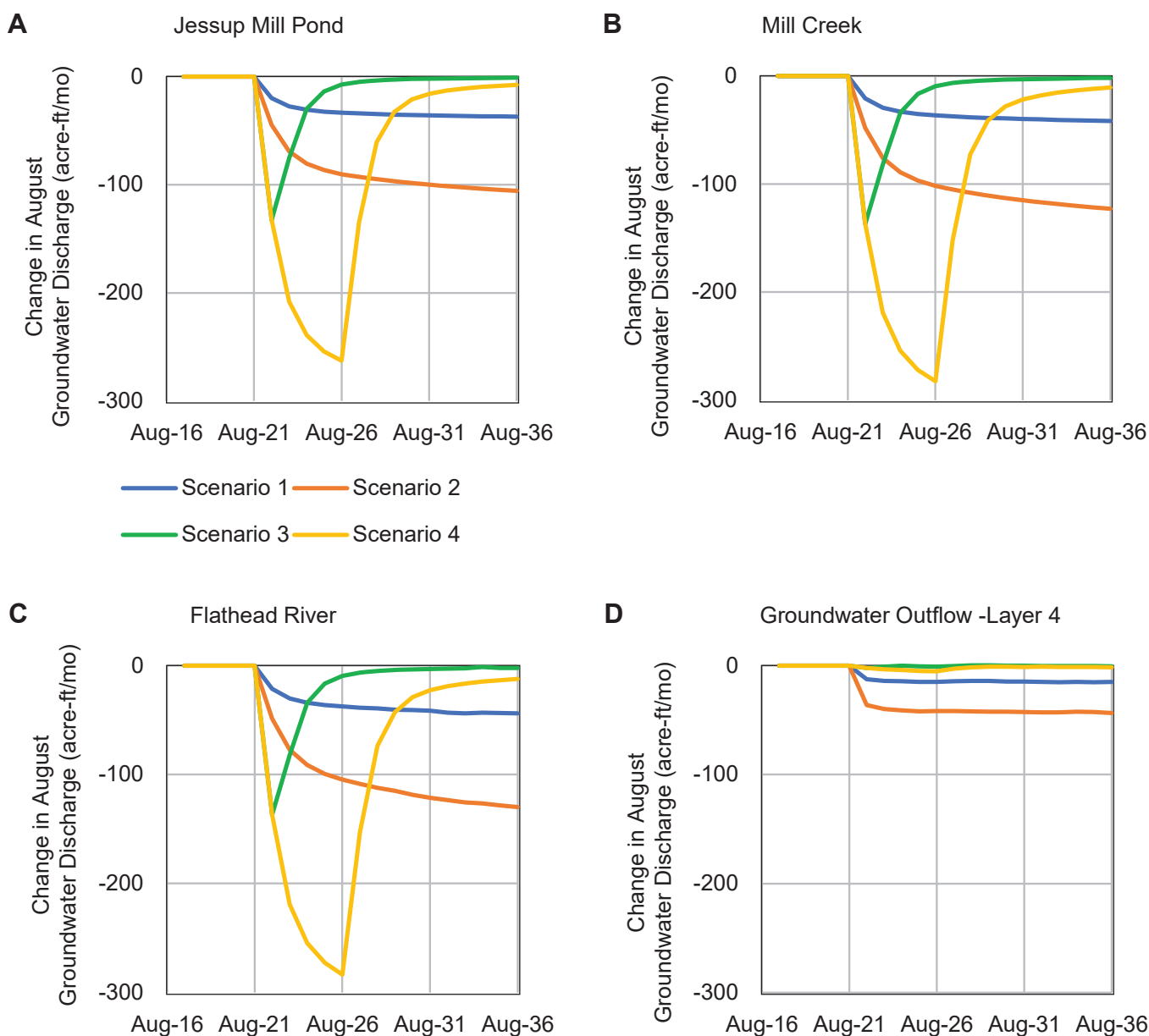
Figure 13. Changes in groundwater fluxes for different receptors for the tested scenarios. Note that the changes for Mill Creek include the change in flux to Jessup Mill Pond, since it is a tributary to Mill Creek. Similarly the changes for the Flathead River include changes for both Jessup Mill Pond and Mill Creek.

Table 6. Summary of changes from baseline in selected outflows for the tested scenarios.

Scenario	Evaluation Time	Jessup Mill Pond	Mill Creek	Flathead River	Groundwater Outflow	Jessup Mill Pond	Mill Creek	Flathead River	Groundwater Outflow
		Change in Discharge (acre-ft/mo)				Change in Discharge (cfs)			
(1) Double Residential	August 2036	-37.2	-41.5	-43.9	-15.1	-0.60	-0.67	-0.71	-0.24
(2) Double Irrigation	August 2036	-105.6	-122.8	-130.0	-43.4	-1.72	-2.00	-2.11	-0.71
(3) 1-yr Drought	August 2022	-132.8	-136.9	-136.9	-2.1	-2.16	-2.23	-2.23	-0.03
	August 2023	-75.3	-81.9	-82.1	-1.2	-1.22	-1.33	-1.33	-0.02
	August 2027	-4.9	-6.4	-6.6	-0.3	-0.08	-0.10	-0.11	0.00
	August 2032	-1.8	-2.5	-2.8	-0.3	-0.03	-0.04	-0.05	0.00
(4) 5-yr Drought	August 2026	-262.6	-282.6	-283.4	-5.3	-4.27	-4.60	-4.61	-0.09
	August 2027	-134.4	-151.8	-152.8	-2.8	-2.19	-2.47	-2.49	-0.05
	August 2031	-16.0	-21.6	-22.7	-1.4	-0.26	-0.35	-0.37	-0.02
	August 2036	-7.6	-10.8	-12.2	-1.7	-0.12	-0.18	-0.20	-0.03

Note. Mill Creek includes reduced flux from Jessup Mill Pond in addition to reduced flux to Mill Creek itself. Flathead River includes reduced flux to Jessup Mill Pond and Mill Creek, in addition to reduced flux to Flathead River itself.

completions, we simply doubled the rates from the existing irrigation wells.

Results

Increased irrigation well pumping decreased groundwater heads and decreased groundwater discharge to surface waters and groundwater outflow from the model domain. Since irrigation wells pump more water than the domestic wells, doubling their rates resulted in greater effects. At the end of the model run (2036), the average groundwater drawdown for layer 1 and layer 4 was 1.12 and 1.46 ft, respectively (table 5). The reduction in outflow to Jessup Mill Pond was 1.7 cfs (a 7% reduction; fig. 13A, table 6). Groundwater outflow from the model domain was reduced by 43.4 acre-ft/mo (a 2% reduction; fig. 13D, table 6).

Scenario 3: 1-yr Drought

Model Modifications

Multi-year and decadal scale droughts are a natural feature of Montana's climate (e.g. 2001 and 2002), and assessment of climate change in Montana suggests that droughts may increase in frequency, severity, and duration (Whitlock and others, 2017). To assess the effects of a 1-yr drought, the 20-yr model was modified by reducing the specified flux representing MFR

(MBR + MFRs from appendix C) and areal recharge during simulated year 2022 (table 4).

Simulating a drought with MFR in this way assumes that changes in precipitation in the Swan Range are quickly reflected in changes in MFR. For the stream infiltration portion of MFR (MRFs, ~2/3 of MFR), this is likely strictly true. The timing of changes in mountain block groundwater inflow (MBR, ~1/3 of MFR) due to changes in precipitation and infiltration will depend on the bedrock aquifer properties, and was not explicitly modeled. Low storativity values, as are common in fractured bedrock, would cause changes in groundwater recharge to be more quickly reflected in changes to groundwater discharge, but we recognize that there will be some buffering of this signal.

Based on precipitation data from the Creston Agrimet station (USBOR, 2022; data from 1989–2021; $n = 33$), the median annual precipitation in the East Flathead Valley is 16.4 in. The fifth percentile is 11.6 in, which is 29% less than the median. Therefore, to represent a severe drought, we reduced MFR and areal recharge by 25% to reflect an approximate 20-yr drought event (an event that would be expected, on average, to occur once every 20 yr, or 5% of the time). This represents a 1-yr reduction in overall MFR from 31,902 acre-ft/yr to 23,927 acre-ft/yr. Areal recharge

was reduced from 8,578 to 6,434 acre-ft/yr. Note that the model was calibrated to data collected from 2019 to 2021, during which precipitation ranged from 89 to 101% of the median (averaging 94%).

Results

Decreasing recharge to the aquifer causes a decrease in groundwater levels, groundwater discharge to surface waters, and groundwater outflow from the model domain. Since the change in MFR was applied for only 1 yr, we can evaluate both the maximum effects and the time it takes for the system to recover. During August of the simulated drought year the average groundwater drawdown was 1.50 ft in layer 1 and 2.74 ft in layer 4 (table 5). The reduction in groundwater discharge to Jessup Mill Pond was 2.2 cfs (an 11% reduction; fig. 13A, table 6). Groundwater outflow from the model domain was reduced by 2.1 acre-ft/mo (a 0.1% reduction; fig. 13D, table 6). The effects of the drought year generally became less over time; however, the groundwater system was slow to recover, and 10 yr after the drought (in August 2032) average drawdown was 0.52 ft in layer 1 and 2.11 ft in layer 4 (table 5). Groundwater outflow from the model domain was reduced by less than 1 acre-ft/mo after 10 yr. Groundwater discharge to surface waters recovered more quickly, with the change in discharge to Jessup Mill Pond being near 0 cfs after 10 years (fig. 13A, table 6).

Scenario 4: 5-yr Drought

Model Modifications

To evaluate the effects of a more prolonged drought, the 20-yr model was modified by reducing the specified flux representing MFR and areal recharge during simulated years 2022 to 2026 (table 4). The annual reduction in recharge was the same as in scenario 3, but it was held at the reduced values for 5 consecutive years.

Results

The effects from a 5-yr drought were similar to those from the 1-yr drought, but maximum effects were larger and the influence was more prolonged (fig. 13). During August of the last drought year (simulated year 2026), the average groundwater drawdown was 2.30 ft in layer 1 and 3.65 ft in layer 4 (table 5). The reduction in groundwater discharge to Jessup Mill Pond was 4.3 cfs (a 22% reduction; fig. 13A, table

6). Groundwater outflow from the model domain was reduced by 5.3 acre-ft/mo (a 0.2% reduction; fig. 13D, table 6). The effects of the drought year generally became less over time; however, as with the 1-yr drought, the groundwater system was slow to recover, and 10 yr after the drought (in August 2036), average drawdown was 0.64 ft in layer 1 and 2.24 ft in layer 4 (table 5). Groundwater outflow from the model domain after 10 yr was reduced by 1.7 acre-ft/mo (a 0.1% reduction; fig. 13D, table 6). Groundwater discharge to surface waters again recovered more quickly, with a decrease in discharge to Jessup Mill Pond of 0.1 cfs after 10 yr (a 1% reduction; fig. 13A, table 6).

Predictive Uncertainty

For any groundwater flow model predictions, there are two broad sources of uncertainty:

1. Uncertainty associated with the model itself where error results from field measurements, numerical approximations, and conceptual, spatial, and temporal simplifications.

2. Uncertainty associated with accurate specifications of future conditions, hydrological factors like the variation in recharge rates due to climate change, and non-hydrological factors such as political, economic, and sociological actions (such as changes in irrigation practices or development) that may affect future flow condition (Anderson and others, 2015).

This analysis addresses only the first source of uncertainty.

To evaluate the uncertainty associated with model predictions we used a one-at-a-time approach, where one parameter is changed per model run (realization) while all others are held at the calibrated values. This approach focuses on the set of model parameters that are expected to drive prediction uncertainty. While this approach provides an understanding of the range of estimates that would result from using model parameters different from the calibrated values, it does not allow for identification of interactions between parameters.

The target for the uncertainty analysis was the reduction in groundwater discharge (stream depletion) to Jessup Mill Pond caused by Scenario 2 in August 2036. Jessup Mill Pond was selected since it is the surface-water feature that receives the most groundwater discharge. Scenario 2 was selected since it caused

the greatest prolonged effect by the end of the model period (fig. 13A). August 2036 was selected since it is the peak of the dry season during the last year of the model run.

Three parameters were selected for variation in the uncertainty analysis. The steady-state sensitivity analysis showed that model results were most sensitive to the drain conductance for Jessup Mill Pond, and the hydraulic conductivity of layer 3 (fig. 9). As such, we included the Jessup Mill Pond drain conductance, and the hydraulic conductivities of zones 47 and 84, which represent the high-conductivity "windows" in layer 3. We also included the specific yield (S_y) for layer 1, which was not part of the steady-state model, but which we believed would be important to the transient model results. Model realizations for the baseline and Scenario 2 were developed where each parameter was multiplied by 0.5, 0.75, 1, 1.25, or 1.5 times its calibrated value (a total of 30 realizations; table 7).

The results of the uncertainty analysis showed that adjusting the selected parameters within the specified range resulted in the stream depletion caused by Scenario 2 (double irrigation pumping) to vary from 4.1% less than predicted by the calibrated model to 8.8% greater (a total difference of 12.9%). This is a range from 1.65 to 1.87 cfs, with the calibrated model showing 1.72 cfs of stream depletion (table 7). This suggests that the uncertainty associated with model predictions are on the order of ±10%.

DISCUSSION

Similar to previous work (e.g., LaFave and others, 2004; Rose, 2018; Rose and others, 2022), this study shows that the unconsolidated valley-fill aquifers in the East Flathead study area can generally be viewed as a system with shallow and deep aquifers that are often separated by a confining layer. While this general conceptual model is reasonable, it is important to note that none of these units are homogeneous across the entire study area. For the purposes of understanding hydrogeologic connections between the shallow and deep aquifers, it is particularly important to understand the continuity of the confining layer. The confining layer is often composed of fine-grained lacustrine deposits (silt and clay) and/or basal till (clay bound grav-

Table 7. Summary of predictive uncertainty analysis.

Uncertainty Parameter	Base Run Jessup Mill Pond Flux Aug 2036 (cfs)	Scenario2 Jessup Mill Pond Flux Aug 2036 (cfs)	Modeled Jessup Mill Depletion Aug 2036 (cfs)	% Difference
Layer 1 S_y *0.5	23.43	21.56	1.87	8.8%
Layer 1 S_y *0.75	23.17	21.43	1.74	1.1%
Layer 1 S_y *1.0	23.04	21.32	1.72	0.0%
Layer 1 S_y *1.25	22.91	21.21	1.70	-1.1%
Layer 1 S_y *1.5	22.78	21.08	1.70	-1.1%
Jessup Mill Pond Drain Conductance*0.5	22.40	20.76	1.65	-4.1%
Jessup Mill Pond Drain Conductance*0.75	22.82	21.13	1.69	-1.5%
Jessup Mill Pond Drain Conductance*1.00	23.04	21.32	1.72	0.0%
Jessup Mill Pond Drain Conductance*1.25	23.27	21.44	1.82	6.2%
Jessup Mill Pond Drain Conductance*1.5	23.17	21.52	1.65	-3.9%
Zones 47 & 84 K_h, K_v (Layer 3)*0.5	22.56	20.88	1.68	-2.1%
Zones 47 & 84 K_h, K_v (Layer 3)*0.75	22.86	21.15	1.70	-0.9%
Zones 47 & 84 K_h, K_v (Layer 3)*1.0	23.04	21.32	1.72	0.0%
Zones 47 & 84 K_h, K_v (Layer 3)*1.25	23.16	21.44	1.73	0.6%
Zones 47 & 84 K_h, K_v (Layer 3)*1.5	23.25	21.53	1.73	0.5%

Note. Shading indicates the calibrated values. K_h, horizontal hydraulic conductivity; S_y, specific yield; K_v, vertical hydraulic conductivity.

el), but in some areas the confining layer is composed of more permeable sandy lacustrine (deltaic) deposits and ablation till (Smith, 2004a; Myse and others, 2023; Bobst and others, in prep.). The deltaic deposits are interpreted to have been deposited in a glacial lake, but in the relatively high-energy near-shore environment that resulted in more coarse-grained sediments. Ablation till is reworked by melt waters, which preferentially removes the fine-grained sediments and leaves behind a relatively coarse-grained deposit. Sediments near the Swan Range front are also relatively permeable, as would be expected for alluvial fans, landslides, and associated mountain front deposits. Well logs, drilling, and model calibration also showed that in some areas further from the edge of the valley, fine-grained low-permeability deposits are either thin or not present. This is likely due to erosion of the fine-grained sediments by fluvial action (rivers), which would remove the fine-grained sediments and backfill with relatively coarse-grained deposits. In particular, flux to Jessup Mill Pond and groundwater heads near the Flathead River required hydrologic connection between the shallow and deep aquifers to achieve model calibration. As such, pumping from either the shallow or the deep aquifer in the East Flathead area likely results in surface-water depletion.

Simulated increases in groundwater pumping and drought reduced groundwater and surface-water availability. Therefore, the general types of effects are similar, but the magnitude, geographic distribution, and timing of those effects differ.

Since groundwater pumping for irrigation is currently about four times greater than residential use within the East Flathead area, modification of irrigation management practices such as changing from flood irrigation using surface-water sources to pivot irrigation using groundwater sources has relatively higher potential to affect groundwater and surface-water availability. Assuming the irrigated acreage remains the same, a shift from a surface-water diversion to a groundwater diversion would provide buffering of stream depletions because the effects from groundwater pumping on surface waters would be more spread out over time. The amount of buffering would depend on the distance the wells are from the surface waters and the aquifer properties (Jenkins, 1968).

Reducing both recharge along the mountain front and aerial recharge to simulate drought caused the greatest short-term declines in groundwater levels and groundwater discharge to surface waters. This demonstrates that shifting climatic conditions, such as reduced precipitation, reduced snowpack storage, or increased evapotranspiration in the mountain block have the potential to alter groundwater and surface-water availability in the East Flathead Valley. Thus, the unknown factor of climate change is something to be included with water-management planning.

Model Limitations

The East Flathead Valley study area is characterized by complex geologic settings. Bedrock, mountain front deposits, Tertiary sediments, till, lacustrine deposits, and fluvial deposits result in multiple hydrogeologic units that each have heterogeneous hydrogeologic properties. A model's limitation comes from the necessary simplification made during the construction of the model in order to have an efficient model to simulate the groundwater and surface water with reasonable accuracy. This includes simplifying the hydrogeologic units, the boundary conditions for the size of the model domain, and limiting the variability of the hydrogeologic parameters to zones. As is always the case, we were also limited by the number/distribution of observation wells, the frequency of monitoring, the duration of monitoring, and the degree to which the monitored period was representative of longer-term conditions.

RECOMMENDATIONS

This model can be used for other similar scenario tests for the size of the area, but if a more focused or detailed understanding is needed for smaller areas, new models may need to be created. In particular, for some more specific problems, the spatial and temporal discretization used for this model may not be appropriate; however, this model could still be used to define the boundary conditions for finer scale models. This model used long-term average annual and average monthly conditions to define the steady-state and transient boundary conditions; however, more detailed incorporation of climatic conditions may be needed for some uses. As with all groundwater models, scenarios tested near the model boundaries should be carefully assessed to ensure that the way the boundaries are simulated does not bias results. For example, if pumping was simulated near the northern no-flow boundary in this model (based on a flow line), simulated drawdown

would be unrealistically truncated at the boundary, and extend further into the model domain. It is also recommended that additional long-term field data be collected to provide an improved base for calibration.

ACKNOWLEDGMENTS

REFERENCES

Anderson, M.P., Woessner, W.W., and Hunt, R.J., 2015, Applied groundwater modeling: Simulation of flow and advective transport: Academic Press, San Diego, CA.

Bobst, A., Rose, J., and Berglund, J., 2022, An evaluation of the unconsolidated hydrogeologic units in the south-central Flathead Valley, Montana: Montana Bureau of Mines and Geology Open-File Report 752, 16 p., https://doi.org/10.59691/SRLK8303.

Bobst, A., Berglund, J., Smith, L., and Gebril, A., in preparation, Hydrogeologic investigation of the East Flathead valley, Flathead County, Montana: Montana Bureau of Mines and Geology Report of Investigation.

Doherty, J.E., and Hunt, R.J., 2010, Approaches to highly parameterized inversion—A guide to using PEST for groundwater-model calibration: U.S. Geological Survey Scientific Investigations Report 2010–5169, 59 p.

Environmental Simulations Incorporated, 2020, Guide to using Groundwater Vistas, Version 8, 515 p., available at https://www.groundwatermodels.com/Groundwater_Vistas.php [Accessed 6/15/23].

Freeze, R.A., and Cherry, J.A., 1979, Groundwater: Prentice-Hall, Englewood Cliffs, NJ.

Fetter, C., 2018, Applied hydrogeology: Waveland Press, Long Grove, IL.

Garland, G.D., Kanasewich, E.R., and Thompson, T.L., 1961, Gravity measurements over the southern Rocky Mountain Trench area of British Columbia: Journal of Geophysics Research, v. 66, no. 8, p. 2495–2505, https://doi.org/10.1029/JZ066i008p02495.

Harbaugh, A.W., 2005, MODFLOW-2005, The U.S. Geological Survey modular ground-water model—The ground-water flow process: USGS Techniques and Methods 6-A16, https://doi.org/10.3133/tm6A16.

Harrison, J.E., Cressman, E.R., and Whipple, J.W., 1992, Geologic and structure maps of the Kalispell 1° x 2° quadrangle, Montana, and Alberta and British Columbia: USGS Miscellaneous Investigations Series Map I-2267, 2 sheets, scale 1:250,000.

Heath, R.C., 1983, Basic ground-water hydrology: USGS Water Supply Paper 2220, https://doi.org/10.3133/wsp2220.

Jenkins, C.T., 1968, Computation of rate and volume of stream depletion by wells: U.S. Geological Survey Techniques of Water-Resources Investigations, Book 4, ch. D1, available at https://pubs.usgs.gov/twri/twri4d1/pdf/twri_4-D1_a.pdf [Accessed June 2024].

Kendy, E., and Tresch, R.E., 1996, Geographic, geologic, and hydrologic summaries of intermontane basins of the northern Rocky Mountains, Montana: USGS Water-Resources Investigations Report 96-4025, 233 p., https://doi.org/10.3133/wri964025.

Konizeski, R.L., Brietkrietz, A., and McMurtrey, R.G., 1968, Geology and ground water resources of the Kalispell Valley, northwestern Montana: Montana Bureau of Mines and Geology Bulletin 68, 42 p., 5 sheets.

LaFave, J.I., Smith, L.N., and Patton, T.W., 2004, Ground-water resources of the Flathead Lake Area: Flathead, Lake, and parts of Missoula and Sanders counties. Part A–Descriptive overview:

Montana Bureau of Mines and Geology Montana Ground-Water Assessment Atlas 2-A, 144 p.

Myse, T., Bobst, A., and Rose, J., 2023, Analyses of three constant-rate aquifer tests, East Flathead Valley, northwest Montana: Montana Bureau of Mines and Geology Open-File Report 757, 44 p.

Nash, J.E., and Sutcliffe, J.V., 1970, River flow forecasting through conceptual models, Part I—A discussion of principles: Journal of Hydrology., v. 10, p. 282–290, https://doi.org/10.1016/0022-1694(70)90255-6.

Noble, R.A., and Stanford, J.A., 1986, Ground-water resources and water quality of the unconfined aquifers in the Kalispell Valley, Montana: Montana Bureau of Mines and Geology Open-File Report 177, 112 p.

PRISM Climate Group, 2015, Precipitation Yearly Normal for 1981–2010 from PRISM, available at http://prism.oregonstate.edu; https://geoinfo.msl.mt.gov/ [Accessed 12/31/20].

RockWare, 2015, RockWorks 17 User's Manual; Golden, Colo., , 4086 p. https://www.rockware.com/downloads/documentation/rockworks/rockworks17.pdf [Accessed June 2023].

Rose, J., 2018, Three-dimensional hydrostratigraphic model of the subsurface geology, Flathead Valley, Kalispell, Montana: Montana Bureau of Mines and Geology Open-File Report 703, 44 p., 1 sheet.

Rose, J., Bobst, A., and Gebril, A., 2022, Hydrogeologic investigation of the deep alluvial aquifer, Flathead Valley, Montana: Montana Bureau of Mines and Geology Report of Investigation 32, 44 p.

Smith, L.N., 2004a, Surficial geologic map of the upper Flathead River valley (Kalispell valley) area, Flathead County, northwestern Montana: Montana Bureau of Mines and Geology Montana Ground-Water Assessment Atlas 2-B-06, 1 sheet, scale 1:70,000.

Smith, L.N., 2004b, Altitude of and depth to the bedrock surface: Flathead Lake Area, Flathead and Lake Counties, Montana: Montana Bureau of Mines and Geology Montana Ground-Water Assessment Atlas 2-B-07, 1 sheet, scale 1:150,000.

Smith, L.N., 2004c, Depth to deep alluvium of the deep aquifer in the Kalispell valley: Flathead County, Montana: Montana Bureau of Mines and Geology Montana Ground-Water Assessment Atlas 2-B-08, 1 sheet, scale 1:63,360.

Smith, L.N., 2004d, Thickness of the confining unit in the Kalispell valley, Flathead County, Montana: Montana Bureau of Mines and Geology Montana Ground-Water Assessment Atlas 2-B-09, 1 sheet, scale 1:100,000.

Smith, L.N., 2004e, Thickness of shallow alluvium, Flathead Lake Area, Flathead, Lake, Missoula, and Sanders counties, Montana: Montana Bureau of Mines and Geology Montana Ground-Water Assessment Atlas 2-B-11, 1 sheet, scale 1:100,000.

Smith, L.N., 2004f, Late Pleistocene stratigraphy and implications for deglaciation and subglacial processes of the Flathead Lobe of the Cordilleran Ice Sheet, Flathead Valley, Montana, USA: Sedimentary Geology, v. 165, p. 295–332, https://doi.org/10.1016/j.sedgeo.2003.11.013.

Stickney, M.C., 1980, Seismicity and gravity studies of faulting in the Kalispell Valley, northwest Montana: University of Montana, Missoula, Mont., M.S. Thesis, 82 p.

Theis, C.V., 1940, The source of water derived from wells: Civil Engineering, v. 10, no. 5, p. 277–280, available at https://water.usgs.gov/ogw/pubs/Theis-1940.pdf [Accessed June 2024].

United States Census Bureau, 2021, County Population Totals: 2010–2020, available at https://www.census.gov/programs-surveys/popest/technical-documentation/research/evaluation-estimates/2020-evaluation-estimates/2010s-counties-total.html [Accessed June 2024].

United States Bureau of Reclamation (USBOR), 2022, Precipitation data from the Creston Montana AgriMet Weather Station (crsm), available at https://www.usbr.gov/pn/agrimet/agrimetmap/crsmda.html [Accessed February 2023].

Uthman, W., Waren, K., and Corbett, M., 2000, A reconnaissance ground water investigation in the upper Flathead River valley area: Montana Bureau of Mines and Geology Open-File Report 414, 151 p.

Vuke, S.M., Porter, K.W., Lonn, J.D., and Lopez, D.A., 2007, Geologic map of Montana: Montana

Bureau of Mines and Geology Geologic Map 62, 73 p., 2 sheets, scale 1:500,000.

Watershed Sciences Inc., 2010, Remote sensing data collection, Flathead Basin, MT: Submitted to Stephen Story, Montana DNRC, available at https://montana.maps.arcgis.com/apps/MapSeries/index.html?appid=55cc886ec7d2416d85beca68d05686f4 [Accessed June 2024].

Whitlock, C., Cross, W., Maxwell, B., Silverman, N., and Wade, A.A., 2017, 2017 Montana Climate Assessment: Bozeman and Missoula, Mont.: Montana State University and University of Montana, Montana Institute on Ecosystems, 318 p., https://doi.org/10.15788/m2ww8w.

Winter, T.C., Harvey, J.W., Franke, O.L. and Alley, W.M., 1998, Groundwater and surface water a single resource: U.S. Geological Survey Circular 1139, available at https://pubs.usgs.gov/circ/1998/1139/report.pdf [Accessed June 2024].

APPENDIX A
WELLS MONITORED

Appendix A. Wells monitored (sorted by well number).

Well No.	GWIC ID	Depth (ft)	Hydrogeologic Unit (HGU)	Calibration Target	Model Layer	WQ
1	85605	64	Shallow Aquifer			
2	148188	518	Deep Aquifer	X	4	X
3	148187	157	Intermediate Aquifer	X	2	X
4	219805	162	Intermediate Aquifer	X	2	
5	85628	149	Intermediate Aquifer	X	2	X
6	85652	183	Deep Aquifer			
7	85656	169	Deep Aquifer	X	4	
8	85649	160	Intermediate Aquifer	X	2	
9	310812	218	Deep Aquifer	X	4	
10	122756	210	Deep Aquifer	X	4	
11	85669	40	Shallow Aquifer	X	1	
12	305674	NR	Shallow Aquifer			X
13	301628	240	Deep Aquifer	X	4	X
14	85687	40	Shallow Aquifer			
15	158200	170	Bedrock			X
16	305482	NR	Deep Aquifer			
17	85774	152	Intermediate Aquifer	X	2	
18	176091	145	Intermediate Aquifer	X	2	
19	85730	91	Intermediate Aquifer	X	2	X
20	164733	145	Intermediate Aquifer	X	2	
21	173515	193	Deep Aquifer	X	4	
22	305675	168	Deep Aquifer	X	4	
23	268043	178	Deep Aquifer	X	4	
24	152953	78	Shallow Aquifer	X	1	
25	215682	180	Deep Aquifer	X	4	
26	83503	149	Deep Aquifer	X	4	
27	139610	151	Deep Aquifer	X	4	
28	310809	238	Deep Aquifer	X	4	
29	209308	175	Deep Aquifer	X	4	X
30	284671	501	Deep Aquifer	X	4	
31	83431	552	Deep Aquifer	X	4	
32	83435	340	Deep Aquifer			X
33	180242	204	Deep Aquifer	X	4	
34	188169	173	Deep Aquifer	X	4	
35	291347	198	Deep Aquifer	X	4	
36	310814	79	Shallow Aquifer	X	1	
37	310813	319	Deep Aquifer	X	4	
38	83538	200	Intermediate Aquifer			X
39	83586	121	Shallow Aquifer	X	1	
40	83579	627	Deep Aquifer	X	4	
41	244505	600	Deep Aquifer			

Appendix A—*Continued.*

Well No.	GWIC ID	Depth (ft)	Hydrogeologic Unit (HGU)	Calibration Target	Model Layer	WQ
42	311096	4.8	Shallow Aquifer	X	1	
43	262175	180	Deep Aquifer	X	4	
44	215007	241	Deep Aquifer	X	4	
45	218164	200	Deep Aquifer	X	4	
46	310811	319	Deep Aquifer	X	4	
47	219773	81	Shallow Aquifer	X	1	
48	83633	190	Deep Aquifer			
49	194711	219	Deep Aquifer	X	4	
50	274595	221	Deep Aquifer	X	4	
51	301923	400	Deep Aquifer	X	4	X
52	294592	8.2	Shallow Aquifer	X	1	
53	83571	188	Intermediate Aquifer	X	2	X
54	83719	160	Intermediate Aquifer	X	2	X
55	83716	338	Deep Aquifer	X	4	X
56	238895	221	Deep Aquifer	X	4	X
57	83713	194	Intermediate Aquifer	X	2	
58	83651	184	Intermediate Aquifer			
59	240258	215	Deep Aquifer	X	4	X
60	240260	193	Intermediate Aquifer	X	2	
61	150702	110	Shallow Aquifer			
62	305676	122	Intermediate Aquifer	X	2	
63	83690	100	Intermediate Aquifer	X	2	
64	194713	361	Deep Aquifer	X	4	
65	205926	148	Bedrock			
66	83662	120	Bedrock			X
67	286781	200	Deep Aquifer			
68	132462	525	Deep Aquifer	X	4	
69	83752	195	Intermediate Aquifer	X	2	X
70	311098	9	Shallow Aquifer	X	1	
71	209505	102	Shallow Aquifer	X	1	
72	83789	119	Shallow Aquifer	X	1	X
73	82262	208	Deep Aquifer	X	4	
74	308707	238	Deep Aquifer			
75	304306	153	Intermediate Aquifer	X	2	X
76	304311	NR	Shallow Aquifer	X	1	
77	244906	241	Deep Aquifer	X	4	X
78	258145	198	Deep Aquifer	X	4	
79	310776	300	Deep Aquifer	X	4	
80	304307	183	Deep Aquifer	X	4	
81	81678	132	Intermediate Aquifer	X	2	
82	304313	210	Intermediate Aquifer	X	2	X

Appendix A—*Continued.*

Well No.	GWIC ID	Depth (ft)	Hydrogeologic Unit (HGU)	Calibration Target	Model Layer	WQ
83	255030	310	Deep Aquifer	X	4	
84	157098	157	Intermediate Aquifer	X	2	
85	201436	100	Shallow Aquifer	X	1	X
86	310774	280	Deep Aquifer	X	4	
87	214653	160	Ablation Till	X	2	
88	304314	80	Shallow Aquifer	X	1	
89	81636	75	Bedrock			
90	194666	33	Shallow Aquifer	X	1	
91	82288	180	Intermediate Aquifer	X	2	X
92	262325	480	Deep Aquifer	X	4	X
93	262323	217	Intermediate Aquifer	X	2	X
94	262324	66	Shallow Aquifer	X	1	X
95	82279	486	Deep Aquifer	X	4	X
96	304310	295	Deep Aquifer	X	4	X
97	81675	225	Deep Aquifer			
97	301129	260	Deep Aquifer	X	4	
99	143314	178	Intermediate Aquifer	X	2	
100	166458	43	Shallow Aquifer	X	1	
101	86672	214	Shallow Aquifer	X	1	
102	194672	719	Deep Aquifer	X	4	X
103	318263	640	Deep Aquifer			X
104	318265	50	Shallow Aquifer			
105	318266	300	Intermediate Aquifer			X
106	298493	58	Shallow Aquifer	X	1	
107	81861	531	Deep Aquifer	X	4	
108	148762	420	Deep Aquifer	X	4	
109	296866	220	Intermediate Aquifer			
110	81781	166	Intermediate Aquifer	X	2	X
111	152923	499	Deep Aquifer	X	4	X
112	304304	353	Deep Aquifer	X	4	
113	304312	281	Deep Aquifer	X	4	
114	131551	279	Deep Aquifer			
115	261280	174	Intermediate Aquifer	X	2	
116	81775	140	Shallow Aquifer	X	1	X
117	311097	123	Shallow Aquifer	X	1	
118	293105	8	Shallow Aquifer			
119	300217	NR	Shallow Aquifer			
120	300216	NR	Shallow Aquifer			
121	176653	198	Deep Aquifer			X
122	304315	51	Shallow Aquifer	X	1	X
123	310816	180	Intermediate Aquifer	X	2	X

Appendix A—*Continued.*

Well No.	GWIC ID	Depth (ft)	Hydrogeologic Unit (HGU)	Calibration Target	Model Layer	WQ
124	310815	280	Deep Aquifer	X	4	
125	318274	300	Deep Aquifer			X
126	318275	56	Shallow Aquifer			X
127	310777	200	Bedrock			
128	154810	132	Mountain Front			
129	81530	171	Mountain Front			
130	168372	135	Shallow Aquifer	X	1	
131	302090	259	Intermediate Aquifer			
132	242978	1122	Bedrock			X
133	81711	340	Bedrock			
134	242593	120	Shallow Aquifer			
135	244618	200	Deep Aquifer	X	4	
136	241511	321	Deep Aquifer	X	4	
137	132433	132	Shallow Aquifer	X	1	
138	302541	NR	Shallow Aquifer	X	1	
139	81551	410	Deep Aquifer	X	4	
140	120789	110	Intermediate Aquifer			
141	132078	390	Intermediate Aquifer			
142	132436	273	Deep Aquifer	X	4	X
143	81875	200	Intermediate Aquifer	X	2	
144	304309	140	Mountain Front			

Note. WQ indicates that water quality data are available. NR indicates that the value was not reported.

APPENDIX B
SURFACE-WATER MONITORING SITES

Appendix B. Surface-water monitoring sites (sorted by site number).

Site No.	GWIC ID	Site Name	Type	Agency	Stage	Discharge	WQ
1	307785	FLATHEAD RIVER AT COLUMBIA FALLS * USGS GAUGE 12363000	STREAM	USGS	X	X	X
2	304694	FLATHEAD RIVER BLW PRESSENTINE FISHING ACCESS	STREAM	MBMG	X		X
3	307792	FLATHEAD RIVER NEAR KALISPELL * USGS GAUGE 12363500	STREAM	USGS	X	X	X
4	321084	FLATHEAD RIVER AT FOYS BEND NR KALISPELL * USGS GAUGE 12366500	STREAM	USGS	X	X	
5	307786	FLATHEAD RIVER NEAR BIGFORK * USGS GAUGE 12369000	STREAM	USGS	X	X	X
6	321083	FLATHEAD LAKE AT POLSON * USGS GAUGE 12371550	LAKE	USGS	X		X
7	307787	MOORING CREEK AT ELK PARK RD	STREAM	MBMG			X
8	307788	MOORING CREEK AT SAMPSONS * DNRC GAUGE 76LJ 005	STREAM	DNRC	X	X	X
9	321081	MOORING CREEK AT BLACKMER ROAD * DNRC GAUGE 76LJ 004	STREAM	DNRC	X	X	
10	304710	MOORING CREEK AT LAKE BLAINE INLET * BLW YOEMAN HALL RD	LAKE	MBMG	X	X	X
11	304707	HEMLER CREEK AT HANDKERCHIEF CREEK DR	STREAM	MBMG	X	X	X
12	307790	HEMLER CREEK * DNRC GAUGE 76LJ 003	STREAM	DNRC	X	X	X
13	307789	BLAINE CREEK AT OUTLET OF LAKE BLAINE * DNRC GAUGE 76LJ 002	STREAM	DNRC	X	X	X
14	321079	BLAINE CREEK AT MSU AG STATION * DNRC GAUGE 76LJ 001	STREAM	DNRC	X	X	X
15	256986	JESSUP MILL POND	POND	MBMG	X		X
16	262326	MILL CREEK BLW CRESTON HATCHERY * DNRC GAUGE 76LJ 07500	STREAM	DNRC	X	X	X
17	307794	MILL CREEK AT HWY 35	STREAM	MBMG	X	X	X
18	307796	MILL CREEK AT RIVERSIDE ROAD	STREAM	MBMG	X	X	X
19	307795	MILL CREEK ABOVE ROSE CREEK	STREAM	MBMG			X
20	256831	LOST CREEK	STREAM	MBMG	X	X	X
21	302482	TRAIL CREEK AT PETERS RIDGE ROAD * USFS	STREAM	MBMG	X	X	X
22	302483	MILL CREEK AT PETERS RIDGE ROAD * USFS	STREAM	MBMG	X	X	X
23	305404	MILL CREEK LOWER ABV FOOTHILL DR * MBMG	STREAM	MBMG	X	X	X
24	302485	BROWNS GULCH AT PETERS RIDGE ROAD * USFS	STREAM	MBMG	X	X	X
25	305405	BROWNS GULCH LOWER ABV FOOTHILL DR * MBMG	STREAM	MBMG	X	X	X
26	302486	PETERS CREEK AT PETERS RIDGE ROAD * USFS	STREAM	MBMG	X	X	X
27	307791	UNNAMED POND * BETWEEN LAKE BLAINE AND FLATHEAD RIVER	POND	MBMG			X

Note. WQ indicates that water-quality data are available.

APPENDIX C

PRELIMINARY GROUNDWATER BUDGET

APPENDIX C: TABLE OF CONTENTS

INTRODUCTION

A preliminary groundwater budget was developed for the valley-fill aquifers to provide initial estimates of reasonable ranges for the magnitude, timing, and geographic distribution of the major groundwater inflows and outflows within the study area. This budget provided insight into the magnitude and timing of sources and sinks of groundwater, and aided in development of numerical groundwater models. Monitoring data collected from June 2019 to December 2020 were used to develop some components of the budget; however, the budget was developed to represent long-term average values (e.g., 30-yr normals). Each water budget component was estimated on both a monthly and annual basis (table C1).

This appendix provides details on how the preliminary groundwater budget components were derived. A water budget for the Swan Mountain Block was developed to estimate the amount and timing of groundwater and surface-water inflow from the Swan Block to the east side of the valley-fill aquifer (fig. C1). The inflows from the mountain block were combined with other inputs and outputs to develop an overall groundwater budget for the unconsolidated valley-fill aquifers on the east side of the Flathead Valley (fig. C1).

SWAN BLOCK WATER BUDGET

The Swan Mountain Block includes 17,272 acres between the mountain front and the top of the Swan Range, along the east side of the study area (fig. C2). Recharge to the valley-fill aquifers from the Swan Mountain Block occurs from mountain block recharge (MBR; groundwater inflow from the mountain block to the valley aquifers), and surficial mountain front recharge (MFR_s, stream infiltration at the mountain front; Markovich and others, 2019; fig. C1). Note that MBR and MFR_s are conceptually combined in the main text of this report, and referred to as mountain front recharge (MFR; Wilson and Guan, 2004; Markovich and others, 2019).

The water budget for the Swan Block was estimated based on a volumetric balance within the mountain block between precipitation (PCP), actual evapotranspiration (AET), surface-water runoff (RO), and groundwater recharge (RCH; fig. C1). That is:

$$PCP = AET + RO + RCH. \qquad \text{eq. C1}$$

Analysis was conducted on a drainage basis (fig. C2). The areas between drainages along the mountain front, known as mountain front facets (MFFs; Markovich and others, 2019), were also digitized so that the entire mountain block was included. Drainages in the Swan Mountain Block were defined based on the USGS 1/3 arc-second digital elevation model (DEM; ~10 m resolution). An accumulation map was developed using the ArcMap > Spatial Analyst > Hydrology > "Flow Direction" and "Flow Accumulation" tools. Pore points, which are the points where water flows out of an area, were established at the mountain front for stream elements that had more than 10,000 contributing cells (fig. C2, table C2). Since the cells are 10 m x 10 m, the drainage areas above the pore points were greater than 100 hectares (247 acres). This provided pore points at all USGS National Hydrography Dataset (NHD; USGS, 2019) flowlines, which are based on "blue lines" from 1:24,000-scale topographic maps, plus two other small drainages. Drainage polygons for each pore point were defined using the ArcMap > Spatial Analyst > Hydrology > "Watershed" tool, and manual digitization. This resulted in a total of 21 drainage polygons that cover 81% of the area, and 21 MFFs (fig. C2, table C2).

Precipitation (*PCP*)

Long-term average precipitation values were obtained for each drainage or MFF in the Swan Block from the PRISM (parameter-elevation regressions on independent slopes model) 1981–2010 normal precipitation values dataset (PRISM Climate Group, 2015; https://prism.oregonstate.edu/). Results for each drainage and MFF are on table C2. The reported normal precipitation values within the Swan Block ranged from 22 in/yr near the valley bottom to over 70 in/yr at the top of the ridge (fig. C3). The area-weighted average precipitation for the Swan Block was 45.8 in/yr.

Actual Evapotranspiration (*AET*)

AET is the amount of water that is actually evaporated or transpired by vegetation to the atmosphere. Because *AET* is limited by water availability, it is not the same as potential evapotranspiration (*PET*). *AET* was estimated using the MOD16 *AET* algorithm (Mu and others, 2007, 2011; https://www.ntsg.umt.edu/project/modis/mod16.php). These estimates are based on MODIS satellite data and meteorological data. The datasets provide *AET* estimates over 1 km^2 pixels. This
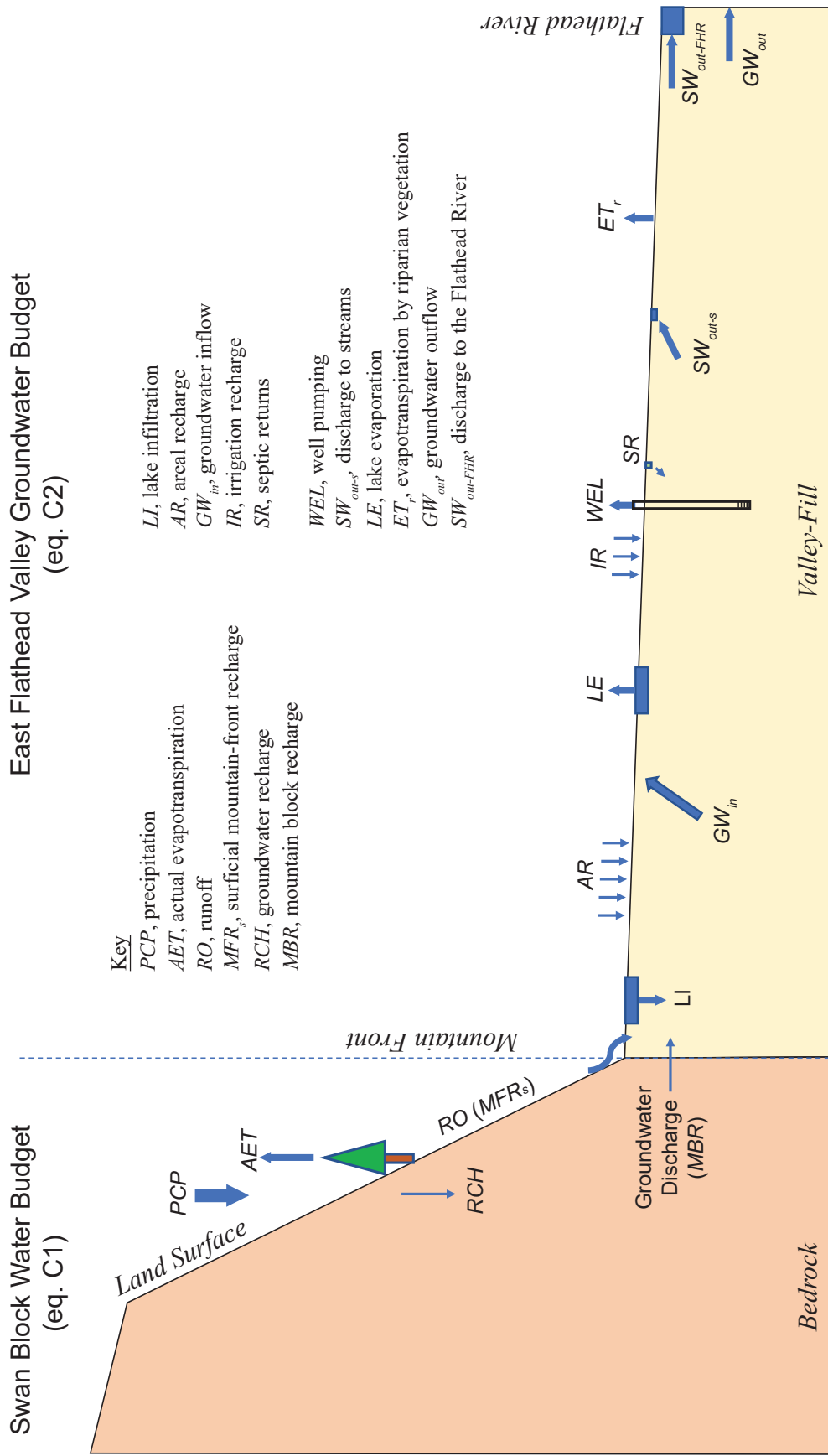
Figure C1. Schematic diagram of water budget components for the Swan Mountain Block and the East Flathead Valley. Designations in parentheses (*MFR*$_s$ and *MBR*) reflect that the runoff (*RO*) and groundwater discharge, which are outputs from the mountain block, are inputs to the valley ground-water budget.

Table C1. Preliminary Groundwater Budget for the East Flathead Valley (ac-ft; long-term average values).

	O	N	D	J	F	M	A	M	J	J	A	S	Annual BE	10% ε	LBE	UBE
MBR	891	863	891	891	812	891	863	891	863	891	891	863	10,503	1,050	9,452	11,553
MFR_s	886	796	703	504	404	518	1,433	4,695	6,156	3,152	1,311	841	21,399	2,140	19,259	23,539
LI	536	518	536	536	488	536	518	536	518	536	536	518	6,311	631	5,680	6,942
GW_{in}	878	850	878	878	800	878	850	878	850	878	878	850	10,346	1,035	9,311	11,380
AR	728	705	728	728	663	728	705	728	705	728	728	705	8,578	858	7,720	9,435
IR	0	0	0	0	0	0	0	0	917	1,334	896	548	3,695	370	3,326	4,065
SR	59	57	59	59	54	59	57	59	57	59	59	57	693	69	624	762
Total Inflows*	3,978	3,788	3,795	3,595	3,222	3,610	4,425	7,787	10,065	7,578	5,299	4,381	61,524	2,833	58,691	64,358
WEL	228	181	180	182	166	185	183	398	2,129	3,829	2,773	470	10,903	1,090	9,813	11,994
SW_{out-s}	2,354	2,279	2,354	2,354	2,146	2,354	2,279	2,354	2,279	2,354	2,354	2,279	27,741	2,774	24,967	30,515
LE	91	29	14	14	30	75	141	293	326	421	345	199	1,977	198	1,779	2,175
ET_r	34	0	0	0	0	45	46	77	78	109	109	73	572	57	515	629
Residual Outflow (GW_{out} + $SW_{out-FHR}$)	1,726	1,670	1,726	1,726	1,572	1,726	1,670	1,726	1,670	1,726	1,726	1,670	20,330	2,033	18,297	22,363
Total Outflows*	4,433	4,158	4,274	4,276	3,915	4,384	4,318	4,849	6,482	8,438	7,307	4,690	61,524	3,614	57,910	65,138
Change in Storage	-455	-370	-478	-681	-693	-774	107	2,938	3,583	-860	-2,008	-309	0	0	0	0

Estimated Uncertainty for Annual Budget

Note. BE, best estimate; e, error; LBE, lower bound estimate; UBE, upper bound estimate.
*Error for totals calculated using root mean square error propagation.
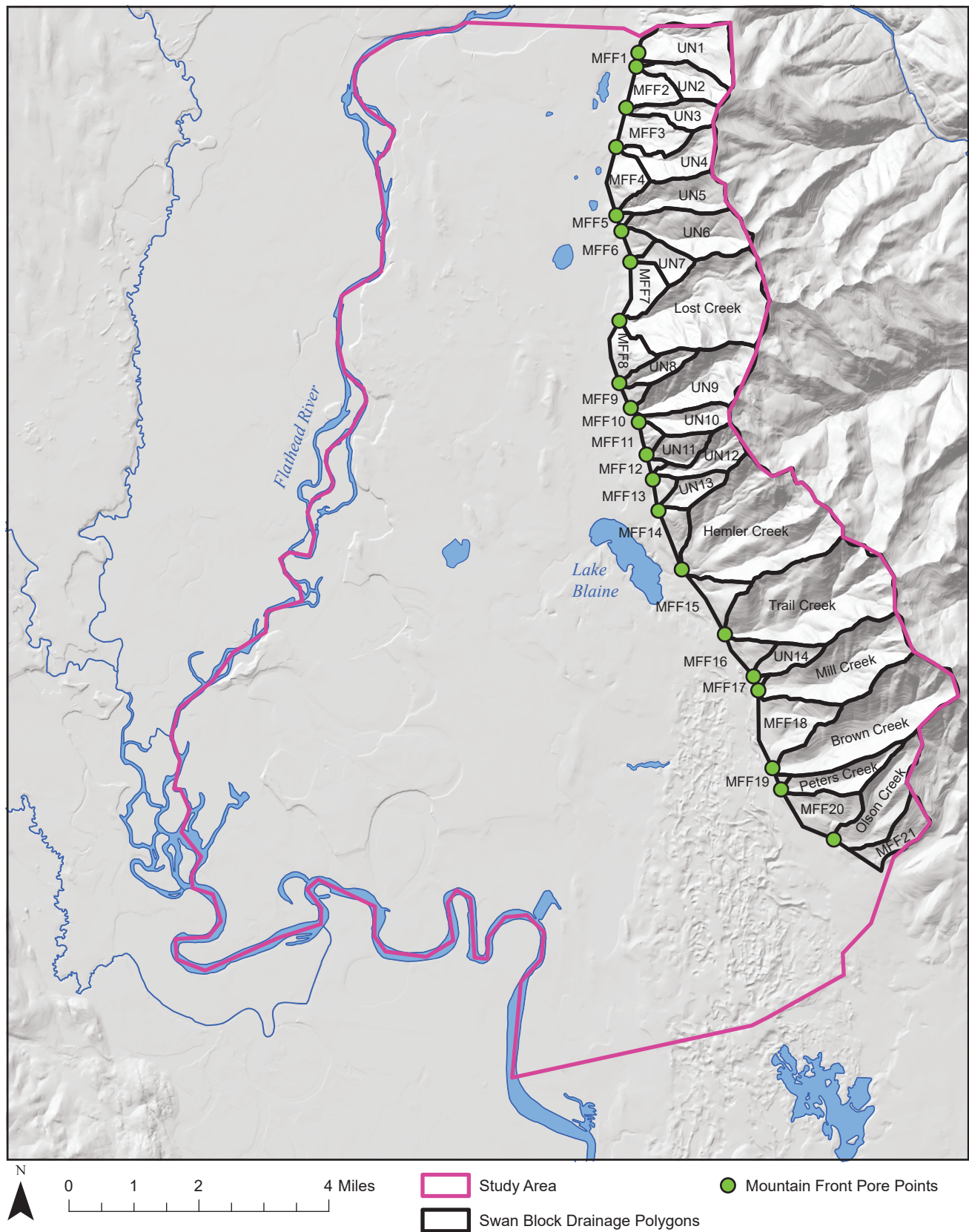
Figure C2. Drainages and mountain front facets (*MFFs*) in the Swan Block were defined based on the 10 m DEM. These areas were used to estimate *MBR* and *MFR*$_s$ to the valley aquifers. Stream discharge (*RO*) was calculated at the mountain front pore points (MF Pore Points).

Table C2. Summary of Swan Block Water Budgets

Name	Acres	PCP	AET	Raw RO	Raw RCH	Adj RO	Adj RCH	PCP	AET	Adj RO	Adj RCH
				(acre-ft/yr)					(in/yr)		
Drainages											
UN1	572	2,107	1,009	1,183	-85	1,098	0	44	21	23	0
UN2	303	1,237	544	798	-105	693	0	49	22	27	0
UN3	250	1,049	464	678	-93	585	0	50	22	28	0
UN4	403	1,708	761	784	163	784	163	51	23	23	5
UN5	462	1,960	837	861	262	861	262	51	22	22	7
UN6	655	2,963	1,157	1,169	637	1,169	637	54	21	21	12
UN7	198	755	343	620	-208	412	0	46	21	25	0
Lost Creek	1,490	7,088	2,563	3,017	1,508	3,017	1,508	57	21	24	12
UN8	197	690	325	498	-133	365	0	42	20	22	0
UN9	774	3,610	1,318	1,942	350	1,942	350	56	20	30	5
UN10	286	1,216	478	778	-40	738	0	51	20	31	0
UN11	211	721	344	525	-148	377	0	41	20	21	0
UN12	322	1,404	550	842	12	842	12	52	20	31	0.4
UN13	206	638	369	217	52	217	52	37	22	13	3
Hemler Creek*	2,023	8,335	3,749	3,113	1,473	3,113	1,473	49	22	18	9
Trail Creek	1,813	7,920	3,579	2,908	1,433	2,908	1,433	52	24	19	9
UN14	208	573	421	133	19	133	19	33	24	8	1
Mill Creek	1,084	4,585	2,152	1,430	1,003	1,430	1,003	51	24	16	11
Brown Creek	1,481	5,962	2,970	2,315	677	2,315	677	48	24	19	5
Peters Creek	366	1,010	740	330	-60	270	0	33	24	9	0
Olson Creek	645	1,963	1,277	319	367	319	367	37	24	6	7
Mountain Front Facets											
MFF1	13	32	23	—	9	—	9	29	21	—	8
MFF2	213	633	357	—	276	—	276	36	20	—	16
MFF3	331	1,087	602	—	485	—	485	39	22	—	18
MFF4	242	610	376	—	234	—	234	30	19	—	12

Table C2. Summary of Swan Block Water Budgets—*Continued*.

Name	Acres	PCP	AET	Raw RO	Raw RCH	Adj RO	Adj RCH	PCP	AET	Adj RO	Adj RCH
				(acre-ft/yr)					(in/yr)		
MFF5	23	57	37	—	20	—	20	30	20	—	11
MFF6	93	261	162	—	99	—	99	34	21	—	13
MFF7	238	721	410	—	311	—	311	36	21	—	16
MFF8	228	579	351	—	228	—	228	30	18	—	12
MFF9	62	156	96	—	60	—	60	30	19	—	12
MFF10	6	15	10	—	5	—	5	29	19	—	10
MFF11	72	181	107	—	74	—	74	30	18	—	12
MFF12	28	67	47	—	20	—	20	29	20	—	9
MFF13	74	165	126	—	39	—	39	27	20	—	6
MFF14	151	330	253	—	77	—	77	26	20	—	6
MFF15	207	460	380	—	80	—	80	27	22	—	5
MFF16	143	296	274	—	22	—	22	25	23	—	2
MFF17	16	31	31	—	0	—	0	23	23	—	0
MFF18	515	1,207	996	—	211	—	211	28	23	—	5
MFF19	20	38	37	—	1	—	1	23	22	—	1
MFF20	364	804	685	—	119	—	119	26	23	—	4
MFF21	286	767	589	—	178	—	178	32	25	—	7

Note. Shaded italic indicates values adjusted to prevent negative R values.

*During high flows Hemler Creek discharges some of its water to Lake Blaine, so MFR_s were calculated as the RO shown here, minus the volume flowing past the gage, plus the infiltration estimated between the gage and Lake Blaine (MFR_s = 3,113 − 2,570 + 380 = 923 acre-ft/yr).
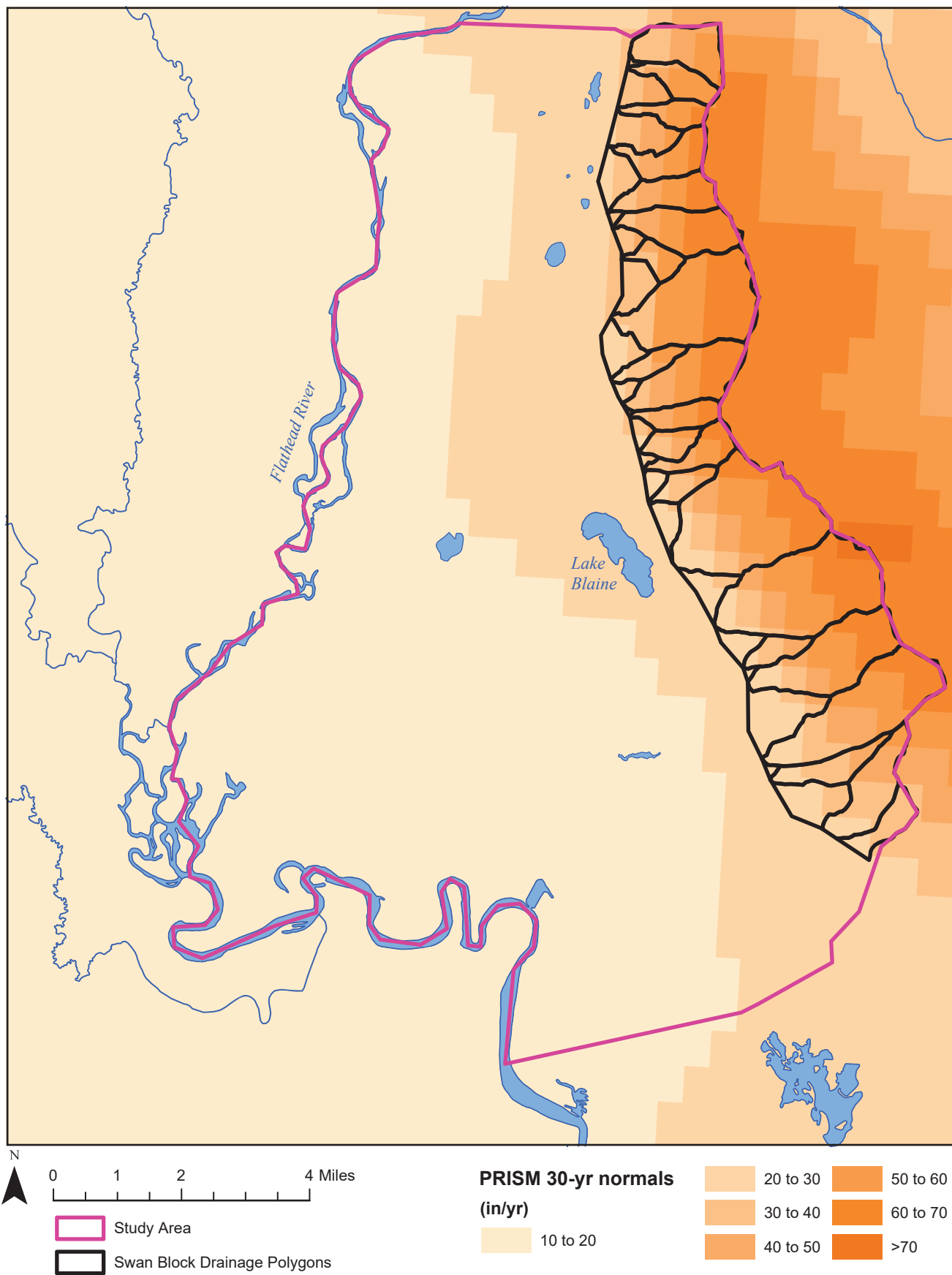
Figure C3. Average annual precipitation within the study area varied from 15 in in the valley bottom to 70 in at the top of the Swan Range. Average annual precipitation within the Swan Block ranged from 22 to over 70 in. Precipitation values based on PRISM 1981–2010 normals (PRISM Climate Group, 2015).

is an energy balance approach based on the Penman–Monteith equation (Monteith, 1965) that has been calibrated to many flux sites in natural vegetation regimes. This approach should provide reasonably accurate estimates of *AET* in areas of complex topography and varied natural vegetation types (D. Ketchum; MT-DNRC, written commun., 2021). The MOD16 average annual *AET* estimates for the Swan Block were calculated based on satellite data collected from 2001 to 2010 (Mu and others, 2011), and they show that mean *AET* values for the drainages and MFFs range from 17 to 25 in/yr, with higher values for those areas at higher elevations, and with higher precipitation (figs. C3, C4, table C2).

Runoff (*RO*)

Streamflows were monitored at eight sites within the Swan Block, with four near the mountain front, and four further upstream in the central portion of the block (fig. C5, table C3). The monitoring data used in this analysis were collected from April to November 2020. Discharge records were used to estimate the total amount of water that flowed past each station per month and over water year 2020 (WY20). Precipitation at the Creston Agrimet station and Noisy SNOWTEL sites was 89.1% and 93.0% of 1981–2010 normal precipitation values, respectively, so the observed yields from WY20 were multiplied by 1.099 (the inverse of the average percent precipitation during those years relative to normal) to provide an estimate of the long-term average annual yields for these sites (table C3).

StreamStats (McCarthy and others, 2016) was used to estimate average monthly runoff from gaged and ungaged drainages. The USGS developed the StreamStats program for Montana to provide users with access to an assortment of analytical tools for water-resources planning and management. It can be accessed at http://water.usgs.gov/osw/streamstats/. This web-based program uses historical records and regional regression equations to estimate streamflow statistics. The regression equations incorporate physical and climatic characteristics of the drainage basin such as drainage area, mean annual precipitation, and land cover.

The estimated long-term (~30 yr) average *RO* values based on our monitoring were compared to the values developed for these sites using the StreamStats program (table C3, fig. C6). The StreamStats model consistently overestimated flows. This overestimate

appears to be due to higher rates of groundwater recharge within the Swan Block than was normally the case for those sites used to develop the regional regression equations. Since this relationship was reasonably consistent between watersheds (fig. C6), it was used to adjust the StreamStats model results to estimate the streamflow at each pore point (fig. C2, table C2). As shown in table C2 and discussed below, these estimates were slightly adjusted in some watersheds to prevent the calculated groundwater recharge being less than zero.

Groundwater Recharge (*RCH*)

Groundwater recharge was estimated based on an annual water budget equation for each drainage and mountain front facet (table C2, eq. C1). This approach provided initial *RCH* estimates (Raw *RCH* in table C2); however, in some smaller drainages, the resulting *RCH* values were negative. Since negative *RCH* values are not physically reasonable, the *RO* values (which are believed to be the most uncertain part of the calculation) were lowered in those areas so that *RCH* would not be less than zero. The total for the resulting *RO* values (Adj *RO* in table C1) was 96% of the original estimate, and the resulting total *RCH* value (Adj *RCH* in table C1) was 109% of the original estimate.

These calculations are also helpful in understanding the fate of precipitation in the Swan Block (table C2). The area-weighted average precipitation was 45.8 in/yr. Evapotranspiration caused 48% of that water (22.2 in/yr) to return to the atmosphere within the Swan Block. Streams carried 36% of that water to the mountain front (16.4 in/yr), and the estimated groundwater recharge in the Swan Block accounted for 16% of precipitation (7.3 in/yr).

EAST VALLEY GROUNDWATER BUDGET

Long-term average annual and monthly groundwater budgets were developed for the combined unconsolidated basin-fill aquifers in the East Flathead Valley (table C1). This includes all of the hydrogeologic units above the semi-consolidated Tertiary Sediments (i.e. the shallow, intermediate, and deep aquifers, plus confining units). The eastern boundary is at the Swan Mountain Front, and the western boundary is at the Flathead River (fig. C2). The northern boundary
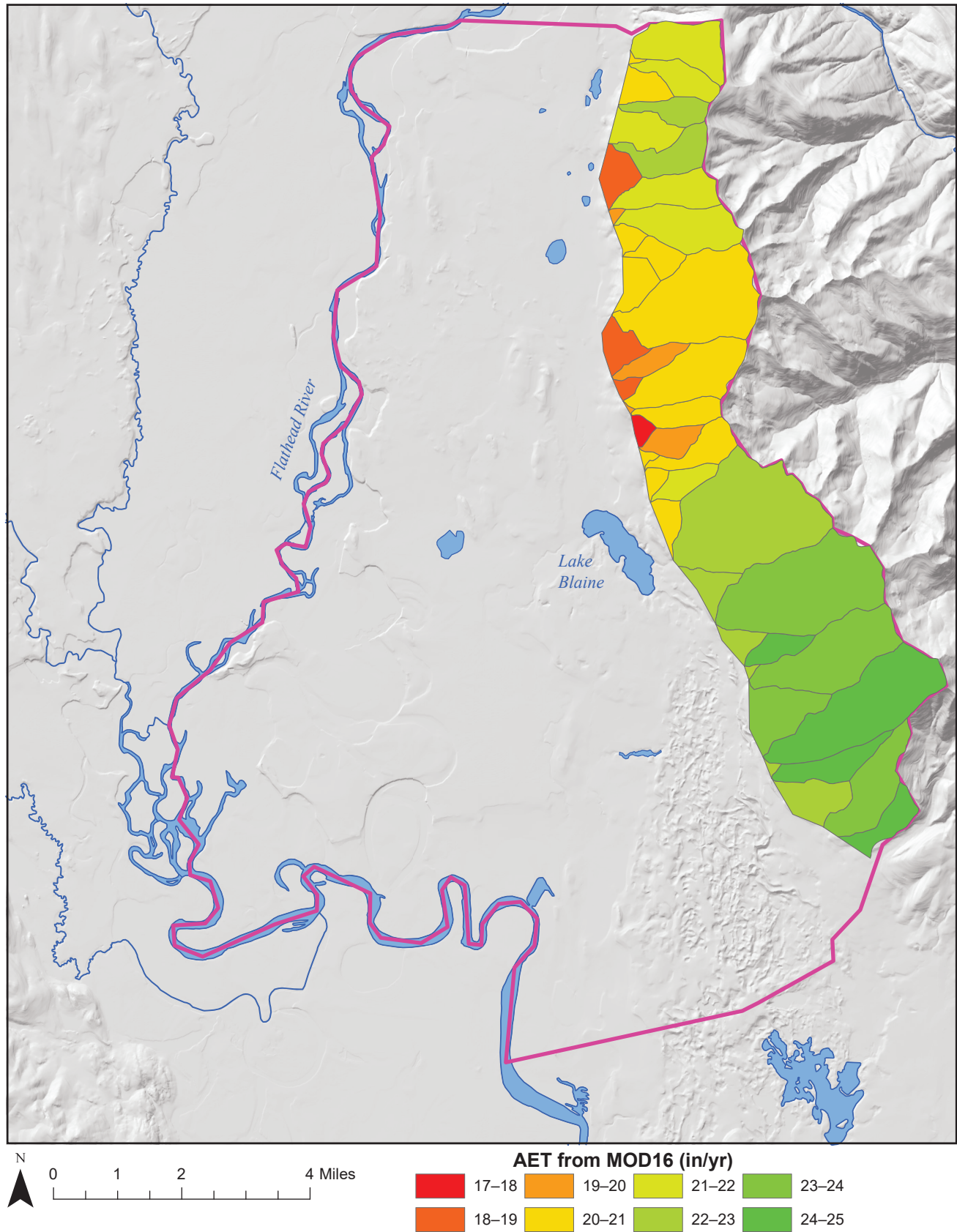
Figure C4. Average annual actual evapotranspiration (*AET*) within the drainages and *MFF*$_S$ in the Swan Block ranged from 17 to 25 in. AET values were based on MOD16 2001–2010 average values (https://www.ntsg.umt.edu/project/modis/mod16.php).
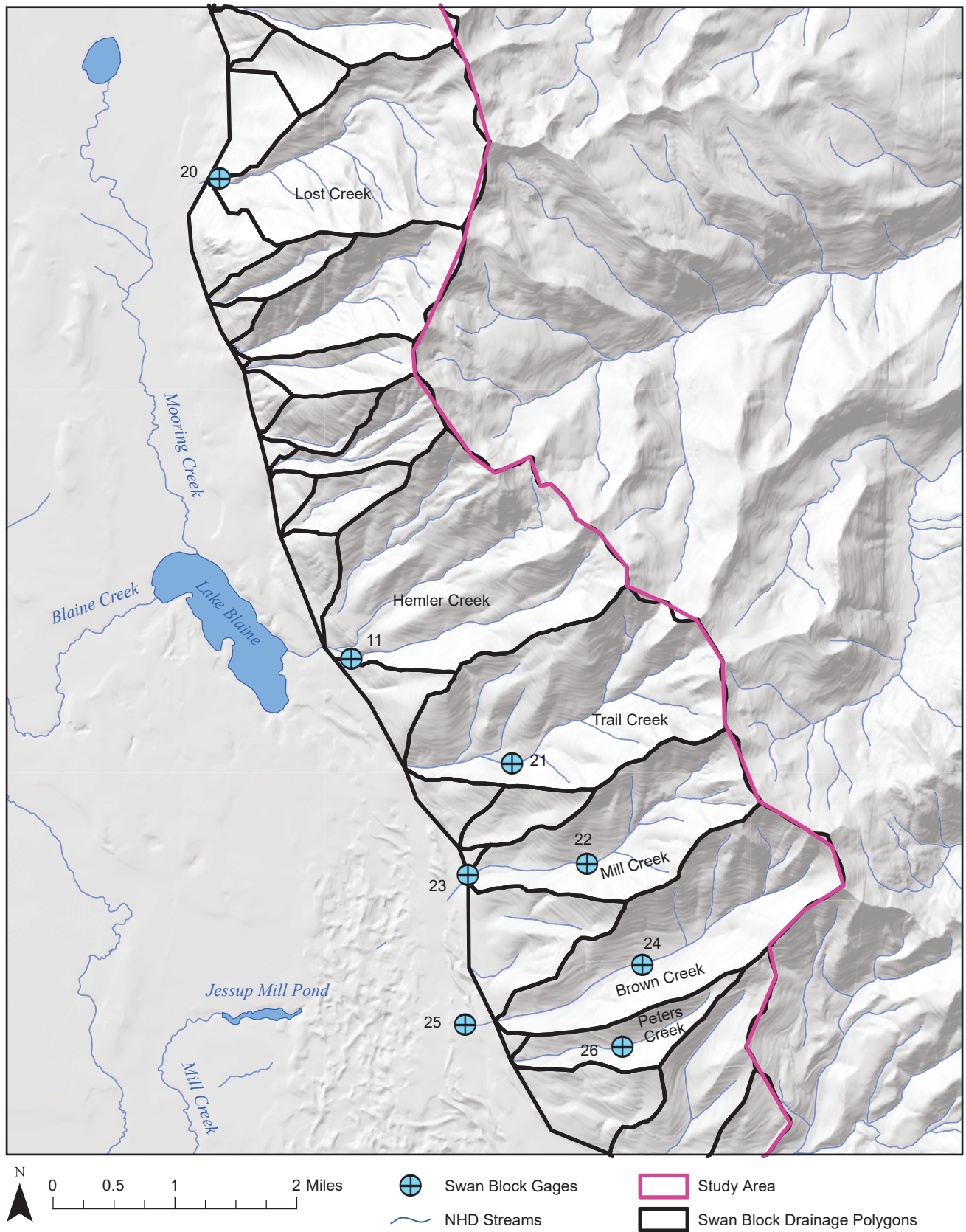
Figure C5. MBMG-monitored stream gages in the Swan Block. See table C3 and appendix B for additional site details. Labels are site numbers.

Table C3. Mountain block surface-water monitoring.

Site	Site No.	Drainage Area (acre)	WY2020 Obs Yield (acre-ft/yr)	Estimated Long-Term Average Yield (acre-ft/yr)	StreamStats Yield from Mean Annual Flow (acre-ft/yr)
Lost Creek	20	1,408	2,689	2,956	4,144
Hemler Creek above South Fork	11	704	1,471	1,616	1,898
Trail Creek	21	1,152	1,728	1,899	3,941
Upper Mill Creek	22	768	1,275	1,401	2,746
Lower Mill Creek	23	1,088	1,550	1,704	3,463
Upper Browns Gulch	24	960	2,061	2,265	3,398
Lower Browns Gulch	25	1,472	2,064	2,268	4,173
Peters Creek	26	218	16	18	531

Note. See appendix B and MBMG's GWIC database for additional site details.

follows a groundwater flow line (a hydraulic no-flow boundary; fig. C2; LaFave and others, 2004; Rose and others, 2022). The southern boundary follows a surface divide, which is also a groundwater divide in the shallow aquifers. In the deep aquifer, groundwater flow is across the southern boundary due to a bedrock high (northern extension of the Mission Range) forming a flow barrier along the west side of this boundary, near the Flathead River (Rose and others, 2022). This flow barrier forces groundwater in the deep aquifer from the Swan Valley to flow further north before turning west into the main Flathead Valley. While this budget is not inherently spatially explicit, where possible geographic and stratigraphic information was retained to aid in developing the numerical models.

The groundwater budget for the East Flathead Valley is represented by equation C2:

$$MBR + MFR_s + GW_{in} + LI + AR + IR + SR =$$

$$WEL + SW_{out\text{-}s} + LE + ET_r + GW_{out} + SW_{out\text{-}FHR} \pm \Delta S,$$

where (using units of acre-ft/yr for this analysis):

Inflows

MBR is mountain block recharge;

MFR_s is surficial mountain-front recharge;

GW_{in} is groundwater inflow;

LI is lake infiltration;

AR is areal recharge;

IR is irrigation recharge; and

SR is septic returns.

Outflows

WEL is well pumping;

$SW_{out\text{-}s}$ is discharge to streams;

LE is lake evaporation;

ET_r is evapotranspiration by riparian vegetation;

GW_{out} is groundwater outflow from the study area;

$SW_{out\text{-}FHR}$ is discharge to the Flathead River; and

ΔS is changes in storage (for the monthly budgets).

Inflows

The surface-water and groundwater flows out of the Swan Block (RO and RCH) flow into the east Flathead Valley. These inputs flow into the aquifer system via mountain block recharge (MBR), surficial mountain-front recharge (MFR_s), and lake infiltration (LI). Differentiating between MBR and MFR_s is important since MBR is assumed to occur at a near-constant rate, while MFR_s is strongly influenced by snowmelt. Also, MFR_s provides recharge to the shallow alluvial aquifers along stream channels, while recharge from the MBR occurs along the entire interface between the bedrock and the valley-fill aquifers (although likely not uniformly).
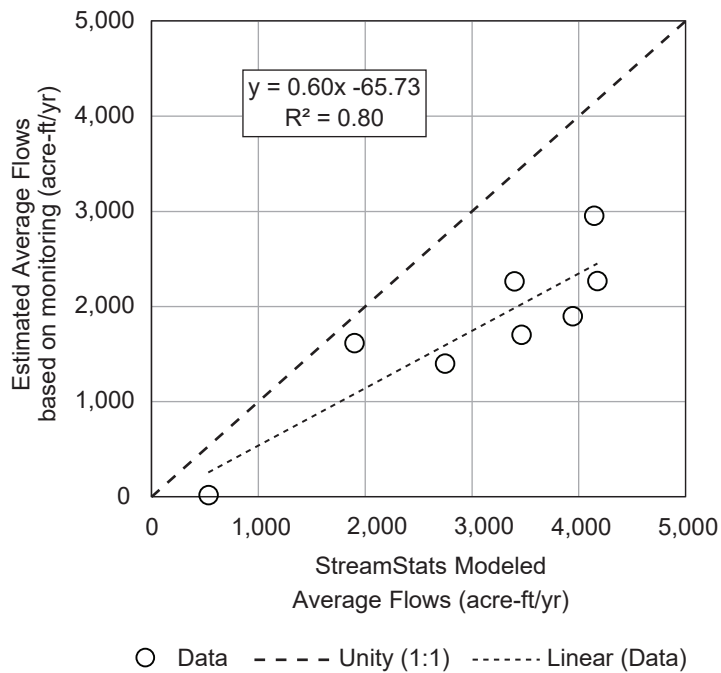
Figure C6. Comparison of our monitoring data to estimated flows from the USGS StreamStats program.

Mountain Block Recharge (MBR)

As discussed above, *MBR* is "the subsurface inflow of groundwater to the lowland aquifer that comes directly from the mountain block" (Wilson and Guan, 2004; Markovich and others, 2019). This includes groundwater inflow from the bedrock and from the "fingers/lenses of alluvium underlying the mountain streams" (Markovich and others, 2019). *MBR* includes both diffuse and focused *MBR* (Markovich and others, 2019), which are not differentiated in our study. *MBR* also includes groundwater inflow from the infiltration of non-channelized water from the MFFs above the mountain front fault (aka "front-slope flow"; Markovich and others, 2019).

MBR was estimated by assuming that over the long term (~30 years), the groundwater discharge to the valley aquifer will be equal to the *RCH* in the mountain block. That is, net changes in storage are negligible on a long-term basis, and there are no other significant sources or sinks in the mountain block. The adjusted recharge (Adj *RCH)* values in table C2 are the annual *MBR* values for each drainage and MFF, and they total 10,503 acre-ft/yr. Monthly *MBR* values were calculated assuming that *MBR* enters the valley aquifers at a near-constant rate, so the annual totals were distributed by the number of days in each month (table C1).

To provide for the geographic distribution of *MBR*, flux segments were defined along the mountain front, which generally begin and end at the midpoints of adjacent MFFs (fig. C7). Each segment was assigned the *MBR* from the drainage upgradient from it, and half of the *MBR* from each of the adjacent MFFs (table C4).

While this approach provides an estimate of the amount of *MBR*, it provides no information on how to proportion it vertically, since the inflow will occur along the entire interface between the valley aquifers and the mountain block (though likely not uniformly). This vertical segregation of mountain block recharge was part of the calibration process for the numerical groundwater flow models.

Surface Mountain Front Recharge (MFR_s)

The streams draining the Swan Mountain Block other than Hemler Creek all infiltrate at the mountain front, and defined channels do not extend beyond the mountain front zone (fig. C5). Therefore, for all drainages except Hemler Creek, annual *MFR* was assumed to be equal to the estimated adjusted *RO* (Adj *RO* in table C2). The percentage of the annual flow for each month was distributed based on the observed flows at Browns Gulch (table C5). This stream infiltration occurs into the shallowest aquifers (layer 1 of the numerical models) near the pore points (fig. C2).

Hemler Creek provides flow into Lake Blaine during high flows in the spring and early summer of most years. Analysis of monitoring data and modeled flows based on the adjusted StreamStats values suggest that about 100 acre-ft/mo (1.7 cfs) infiltrates from Hemler Creek over the 0.34-mi reach between the mountain front and Lake Blaine (4.9 cfs/mi) when the whole reach is wetted. During months where the flow was estimated to be less than 100 acre-ft, all the water is assumed to infiltrate prior to reaching Lake Blaine (table C5).

Lake Infiltration (LI)

Lake Blaine receives inflow from Hemler Creek on the east and Mooring Creek on the north. When lake levels are high enough, water will flow out the spillway into Blaine Creek (fig. C5). DNRC monitoring at the spillway (2017–2021) shows that outflow
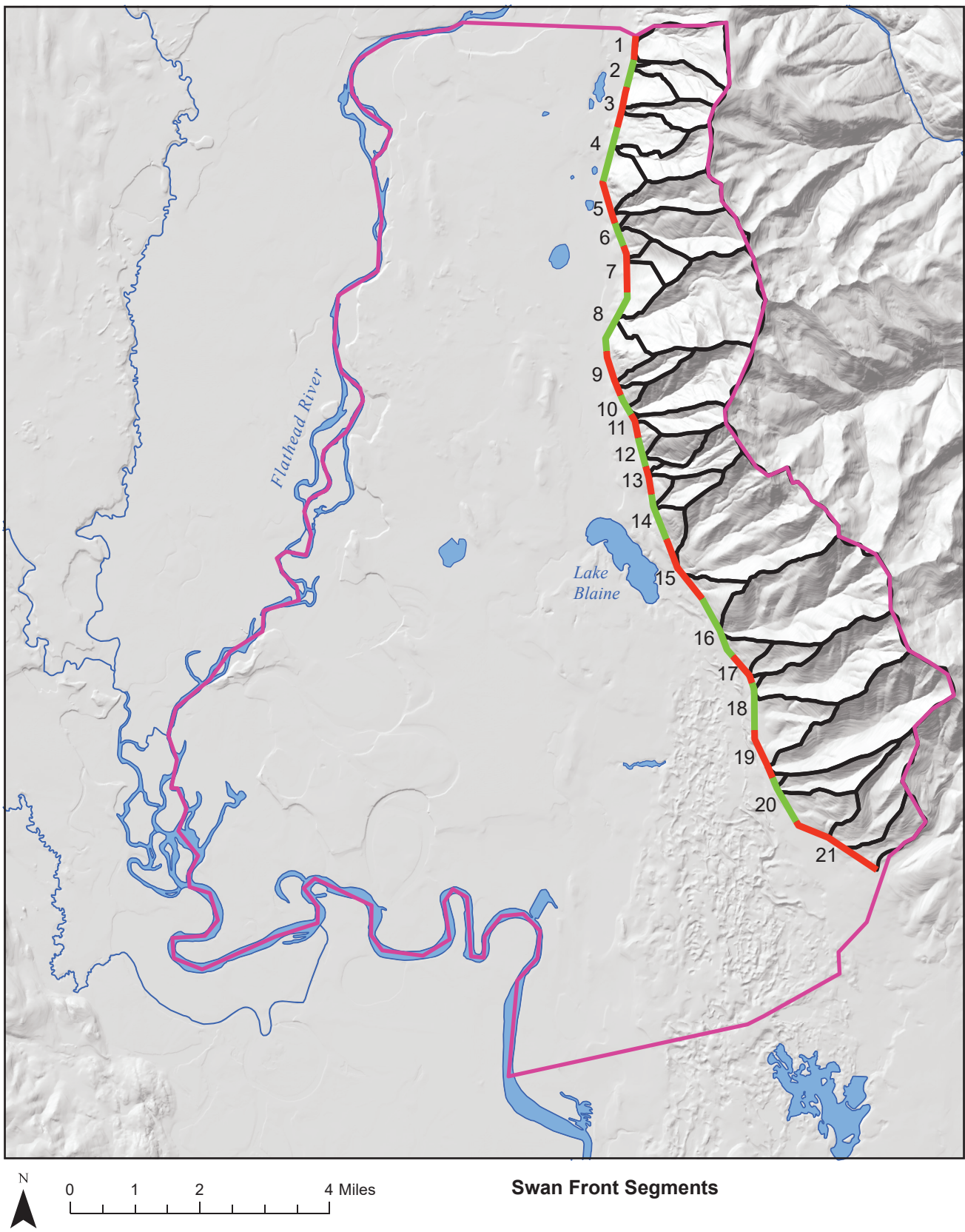
Figure C7. Mountain Front Segments for the distribution of MBR.

Table C4. MBR by mountain front segment and month.

Segment	Annual MBR	O	N	D	J	F	M	A	M	J	J	A	S
							(acre-ft)						
1	5	0.4	0.4	0.4	0.4	0.3	0.4	0.4	0.4	0.4	0.4	0.4	0.4
2	143	12.1	11.7	12.1	12.1	11.0	12.1	11.7	12.1	11.7	12.1	12.1	11.7
3	381	32.3	31.3	32.3	32.3	29.4	32.3	31.3	32.3	31.3	32.3	32.3	31.3
4	523	44.3	42.9	44.3	44.3	40.4	44.3	42.9	44.3	42.9	44.3	44.3	42.9
5	389	33.0	32.0	33.0	33.0	30.1	33.0	32.0	33.0	32.0	33.0	33.0	32.0
6	696	59.1	57.2	59.1	59.1	53.8	59.1	57.2	59.1	57.2	59.1	59.1	57.2
7	205	17.4	16.8	17.4	17.4	15.9	17.4	16.8	17.4	16.8	17.4	17.4	16.8
8	1,777	150.8	146.0	150.8	150.8	137.4	150.8	146.0	150.8	146.0	150.8	150.8	146.0
9	144	12.2	11.8	12.2	12.2	11.1	12.2	11.8	12.2	11.8	12.2	12.2	11.8
10	382	32.5	31.4	32.5	32.5	29.6	32.5	31.4	32.5	31.4	32.5	32.5	31.4
11	40	3.4	3.2	3.4	3.4	3.1	3.4	3.2	3.4	3.2	3.4	3.4	3.2
12	47	4.0	3.9	4.0	4.0	3.6	4.0	3.9	4.0	3.9	4.0	4.0	3.9
13	41	3.5	3.4	3.5	3.5	3.2	3.5	3.4	3.5	3.4	3.5	3.5	3.4
14	110	9.3	9.0	9.3	9.3	8.5	9.3	9.0	9.3	9.0	9.3	9.3	9.0
15	1,552	131.7	127.4	131.7	131.7	120.0	131.7	127.4	131.7	127.4	131.7	131.7	127.4
16	1,484	126.0	121.9	126.0	126.0	114.8	126.0	121.9	126.0	121.9	126.0	126.0	121.9
17	30	2.6	2.5	2.6	2.6	2.3	2.6	2.5	2.6	2.5	2.6	2.6	2.5
18	1,108	94.1	91.0	94.1	94.1	85.7	94.1	91.0	94.1	91.0	94.1	94.1	91.0
19	783	66.4	64.3	66.4	66.4	60.5	66.4	64.3	66.4	64.3	66.4	66.4	64.3
20	60	5.1	4.9	5.1	5.1	4.6	5.1	4.9	5.1	4.9	5.1	5.1	4.9
21	604	51.3	49.6	51.3	51.3	46.7	51.3	49.6	51.3	49.6	51.3	51.3	49.6
Total	10,503	891	863	891	891	812	891	863	891	863	891	891	863

only occurred following periods of above-average precipitation. Outflow occurred in 2017 and 2018, following high-precipitation water years in 2016 and 2017 (112% and 127% of average, respectively, based on data from the Creston Agrimet Station). There was no outflow to Blaine Creek in 2019, 2020, or 2021. In water years 2018, 2019, 2020, and 2021, annual precipitation totals were 98%, 93%, 89%, and 101% of average (based on data from the Creston Agrimet Station). Therefore, during WY20 water entered Lake Blaine from the creeks and due to direct precipitation, and was removed by either infiltration or evaporation. Thus, the Blaine Lake water budget for WY20 is:

$$LI = C_{in} + PCP - Evap \pm \Delta S, \qquad \text{eq. C3}$$

where (using acre-ft/yr):

LI is lake infiltration;

C_{in} is creek inflow;

PCP is precipitation;

$Evap$ is lake evaporation; and

ΔS is change in lake storage.

This assumes that any surface runoff into the lake that is not from the creeks is negligible. This is consistent with the assumption that RO from the MFFs is also negligible. The effect is that any precipitation in excess of AET is assumed to recharge groundwater where the precipitation falls (see areal recharge below), while if it actually ran off it would still provide the same amount of groundwater recharge, but it would be as lake infiltration rather than areal recharge.

Creek Inflow (C_{in})

Monitoring on Mooring Creek and Hemler Creek (sites 8 and 12, appendix B) in WY20 shows that the discharge to Lake Blaine was about 5,200 acre-ft (an average of 7.2 cfs) from Mooring Creek, and about

Table C5. MFRs from the Swan Block, by month.

Pour Point	Annual MFRs	O	N	D	J	F	M	A	M	J	J	A	S
Monthly Distribution		3.9%	3.5%	3.1%	2.3%	1.8%	2.3%	6.5%	22.4%	29.6%	14.9%	5.9%	3.7%
							(acre-ft)						
UN1	1,098	43	39	34	25	20	26	71	246	325	164	65	41
UN2	693	27	24	22	16	13	16	45	156	205	103	41	26
UN3	585	23	21	18	13	11	14	38	131	173	87	35	22
UN4	784	30	28	24	18	14	18	51	176	232	117	46	29
UN5	861	33	30	27	20	16	20	56	193	255	128	51	32
UN6	1,169	45	41	36	27	22	27	76	262	346	174	69	43
UN7	412	16	14	13	9	8	10	27	92	122	61	24	15
Lost Creek	3,017	117	106	94	68	56	70	196	677	892	450	178	112
UN8	365	14	13	11	8	7	9	24	82	108	54	22	14
UN9	1,942	76	68	61	44	36	45	126	436	574	289	115	72
UN10	738	29	26	23	17	14	17	48	166	218	110	44	27
UN11	377	15	13	12	9	7	9	25	85	111	56	22	14
UN12	842	33	30	26	19	16	20	55	189	249	126	50	31
UN13	217	8	8	7	5	4	5	14	49	64	32	13	8
Hemler Creek	*923*	*89*	*78*	*65*	*39*	*26*	*41*	*100*	*100*	*100*	*100*	*100*	*83*
Trail Creek	2,908	113	102	91	66	54	68	189	653	860	433	172	108
UN14	133	5	5	4	3	2	3	9	30	39	20	8	5
Mill Creek	1,430	56	50	45	32	26	33	93	321	423	213	85	53
Brown Creek	2,315	90	81	72	53	43	54	151	520	685	345	137	86
Peters Creek	270	10	9	8	6	5	6	18	61	80	40	16	10
Olson Creek	319	12	11	10	7	6	7	21	72	94	48	19	12
Total MFRs	21,399	886	796	703	504	404	518	1,433	4,695	6,156	3,152	1,311	841

1,800 acre-ft (2.5 cfs on average, after accounting for downstream infiltration) from Hemler Creek. Therefore, the total inflow from creeks was about 7,000 acre-ft.

Precipitation (PCP)

The area of Lake Blaine varies through the year, but has a maximum area of about 385 acres. It is assumed that any precipitation that falls in this maximum area (even if the lake is at a lower level) will flow into the lake. During WY20 the Creston Agrimet station received a total of 14.7 in of precipitation. Thus, the total water added to the lake by direct precipitation in WY20 was about 471 acre-ft.

Evaporation (Evap)

The evaporation from Lake Blaine was estimated for WY20 using Sentinel 2 enhanced vegetation index (EVI) data, and potential evapotranspiration values from the Creston Agrimet station. The EVI data were used to estimate the area of the lake for each month, with EVI values less than 0.1 indicating open water. The grass PET values from the Creston Agriment sta-

tion were multiplied by 1.1 to provide an estimate of the free water surface evaporation rate (Jensen, 2010). The surface area of the lake ranged from 292 to 385 acres, and total evaporation was 31.6 in. This resulted in the total annual calculated evaporation from Lake Blaine being 947 acre-ft.

Change in Lake Storage (ΔS)

Measured stages and Sentinel 2 EVI data were used to evaluate changes in the amount of water stored in Lake Blaine during WY20. These data showed that from October 2019 to October 2020 the area of the lake increased from 334 to 369 acres (an increase of 35 acres), and the stage increased by 0.6 ft. This increase in water level was estimated to increase the amount of water stored in the lake by 212 acre-ft.

Summary Lake Infiltration

Lake infiltration for WY20 was calculated as the residual of the lake water budget (eq. C3). That is:

$$LI = 7{,}000 \text{ acre-ft} + 471 \text{ acre-ft} - 947 \text{ acre-ft} \quad \text{eq. C4}$$
$$- \ 212 \text{ acre-ft} = 6{,}311 \text{ acre-ft}.$$

This equates to an average infiltration rate of 0.045 ft/d through the fine-grained sediments over the area of the lake. We assumed that this infiltration rate is constant through the year, and monthly values are assigned based on the number of days in each month (table C1).

There likely is a slight seasonal pattern to the infiltration since the lake area and stage were highest in July following snowmelt, then decreased following a near-linear pattern until December, stayed at that low level until May, and then increased again as snowmelt filled the lake. Throughout the year the area of the lake varied from 292 to 385 acres, and the stage of the lake increased from a winter baseline level of about 2,992 ft-amsl to a maximum level of 2,997 ft-amsl in July.

Groundwater Inflow to the Study Area (GW_in)

There is groundwater flow into the study area in the deep aquifer along the southern boundary. The potentiometric surface of the deep aquifer and mapped bedrock elevations show that in the southeast corner of the study area, groundwater flows north into the study area through the deep aquifer (see fig. G4 in appendix G). In the shallow aquifer flow is parallel to the southern boundary (fig. G1). Groundwater in the shallow aquifer flows to the west so we assumed no flow into the study area.

The amount of groundwater flow entering the study area was estimated as a Darcy Flux:

$$Q = KiA, \qquad \text{eq. C5}$$

where:

Q is discharge (ft^3/d);

K is hydraulic conductivity (ft/d);

i is potentiometric surface gradient along flow (ft/ft); and

A is cross-sectional area of the aquifer perpendicular to flow (ft^2).

Hydraulic conductivity (K) was estimated from aquifer tests and literature values for sand and gravel. Gradient (i) was based on monitoring data (see fig. 4 of the main body of this report, and appendix A). Cross-sectional area (A) was determined from well logs used to interpret the geometry of the aquifer in the southeast portion of the study area. The following parameters were used in the initial estimation of flow:

K is 100 ft/d;

i is (40 ft)/(36,500 ft) = 0.00109 = 1.09 x10^{-3} ft/ft; and

A is 11,258,883 ft^2.

The above parameters resulted in an initial discharge estimate (Q) of 1,233,850 ft^3/d (10,346 acre-ft/yr) through the deep aquifer in the southeast corner of the study area. This inflow was assumed to be evenly distributed throughout the year (table C1).

Areal Recharge (AR)

Areal recharge was estimated as the difference between precipitation and the combined total of AET and runoff. To evaluate AR we began by comparing the total AET during WY20 to the observed precipitation at the Creston Agrimet station (14.7 in. in WY20).

To estimate AET we obtained EVI data from the Sentinel 2 satellites from the Climate Engine website (http://climateengine.org/). EVI is an indication of vegetation health, and is calculated from red, near-infrared, and blue reflectance values (Nagler and others, 2009).

The data from the Sentinel 2 satellites have a 10 m pixel resolution, and the satellites provide imagery every 5 days. We used the climate engine website to obtain the mean monthly EVI imagery for the study area from March to October 2020. The Sentinel 2 data are more appropriate than the MOD16 approach (with 1,000 m pixels) used in the mountain block since the valley is relatively flat, and has more heterogeneous land cover.

EVI values were rescaled so that values from 0 to 1 spanned from bare ground to well-watered crops by using the following equation (Choudhury and others, 1994; Nagler and others, 2005, 2009; Glenn and others, 2010):

$$EVI^* = 1 - \left[\frac{EVI_{max} - EVI}{EVI_{max} - EVI_{min}}\right], \qquad \text{eq. C6}$$

where:

EVI^* is the normalized EVI value for a particular pixel;

EVI is raw EVI value for a particular pixel;

EVI_{max} is EVI value for well-watered crops; and

EVI_{min} is EVI value for bare ground.

For each month's image EVI_{max} was obtained by evaluating the highest values for irrigated fields and EVI_{min} was obtained from large areas of bare ground, including gravel quarries and talus slopes. These values were used to create monthly $EVI*$ rasters. Areal recharge was evaluated on non-irrigated cropland. A total of 365 fields (14,326 acres) were identified using the Montana Department of Revenue's final land use layer (MDOR, 2019). The mean $EVI*$ values from the monthly $EVI*$ rasters were extracted to each of the non-irrigated polygons.

The monthly mean $EVI*$ values were combined with the monthly PET value for alfalfa from the Creston Agrimet station to estimate the monthly AET for each area using the equation (Glenn and others, 2010):

$$AET = PET \, (EVI*). \qquad \text{eq. C7}$$

The monthly values for March to October were summed to obtain the total AET during the 2020 growing season (assuming AET is zero during November–February). The PET value for 2020 was 34.41 in. While this value is more than double the actual precipitation (14.7 in), plants in non-irrigated areas rarely have sufficient water to transpire at the PET rate.

AET values in the analyzed non-irrigated polygons averaged 11.2 in. Thus, on average, precipitation exceeds AET by about 3.5 in/yr. Note that in irrigated areas (8,622 acres), this water is accounted for in the irrigation recharge calculation, and over Lake Blaine (385 acres), this water is accounted for in the lake infiltration calculation. This leaves 68,620 acres receiving areal recharge. If we assume that the ratio of runoff to infiltration in non-irrigated areas is similar to that in wild flood areas (NRCS, 1997; Smesrud and Madison, 2007), about 43% of this excess water will infiltrate. This results in a calculated AR of 8,578 acre-ft/yr (a mean rate of 0.00034 ft/d; 10.2% of precipitation; table C1). Since the timing of movement of water through the unsaturated zone is difficult to predict without detailed monitoring and modeling, it is assumed that the rate of recharge to the groundwater is constant throughout the year, so AR was split between months based on the number of days in each month (table C3). We assumed this recharge enters the shallowest aquifer.

Irrigation Recharge (IR)

Irrigation recharge occurs when the amount of water applied to crops (including precipitation) exceeds AET and runoff. This includes fields that are irrigated from groundwater as well as surface water, so there is not a direct link to the irrigation well pumping rates discussed below. Irrigation recharge by month was estimated based on the irrigation method efficiency (flood, pivot, or sprinkler) and acreage from the final land units (FLU) layer, and AET based on Sentinel 2 EVI data.

Irrigation efficiency represents the portion of the applied water that is consumptively used by plants (AET). Center pivot irrigation typically has an efficiency of about 80%, with 20% of the applied water infiltrating below the root zone and providing irrigation recharge (NRCS, 1997). Sprinkler irrigation is typically about 70% efficient, with 30% of the water infiltrating to groundwater (NRCS, 1997). Flood irrigation is highly variable; however, it is typically about 30% efficient, with 40% of the applied water running off and about 30% infiltrating (NRCS, 1997; Smesrud and Madison, 2007).

The irrigation method for each field was based on the Montana Department of Revenue's FLU coverage (MDOR, 2019). Slight modifications were made based on 2019 NAIP aerial photographs (downloaded from https://nris.msl.mt.gov/), and field recognzance.

The AET for irrigated fields was calculated using the same approach discussed in the AR section, using the EVI values from Sentinel 2 imagery. These AET values were then used with irrigation efficiencies to estimate irrigation recharge. Irrigation recharge was estimated as follows:

$$IR_{pivot} = (20/80)*AET = 25\% \text{ of } AET, \qquad \text{eq. C8}$$

$$IR_{sprinkler} = (30/70)*AET = 43\% \text{ of } AET, \text{ and} \quad \text{eq. C9}$$

$$IR_{flood} = (30/30)*AET = 100\% \text{ of } AET. \qquad \text{eq. C10}$$

Note that for flood irrigation it is assumed that 40% of the applied water runs off, so the fractions do not equal 100.

Of the 8,622 irrigated acres, 1,950 acres are pivot irrigated, 5,999 acres are sprinkler irrigated, and 673 acres are flood irrigated. In the pivot-, sprinkler-, and

flood-irrigated fields the mean *AET* values were 12.1, 11.8, and 11.9 in/yr, respectively. The total calculated *IR* was 3,695 acre-ft/yr, which was applied June to September based on the distribution of *AET* during those months (table C1).

Septic Returns (SR)

While wells pump groundwater, a substantial portion of the water used inside homes and businesses is not consumed, but returns to the groundwater system through septic systems. This includes water used for toilets, bathing, cooking, and cleaning. While pumping rates for wells vary due to irrigation uses in the warmer months, the amount of water returned to the groundwater system by septic systems is fairly constant. Based on data from the Townview subdivision near Helena, MT (Bobst and others, 2014), a reasonable estimate of septic returns is about 168 gpd/home. There are 3,585 homes within the study area (MSL, 2019), for an overall septic return rate of 602,280 gpd (675 acre-ft/yr). In addition, there are 97 other occupied structures in the study area (primarily commercial and retail sites), which we assumed discharged septic effluent at rates similar to homes, resulting in an additional 16,296 gpd (18 acre-ft/yr) of septic returns, for an overall total of 693 acre-ft/yr. This recharges the uppermost aquifer, and was distributed by month based on the number of days in each month (table C1).

Outflows

Well Pumping (WEL)

Domestic Wells

The GWIC database showed 2,607 domestic wells (http://mbmggwic.mtech.edu/). An average pumping rate per well of 603 gpd was used to estimate average annual pumping (Bobst and others, 2014; Helena area). Monthly average pumping rates were also estimated (based on Bobst and others, 2014; Helena area) and ranged from 173 to 1,510 gpd per residence. These calculations suggest a total of about 1,762 acre-ft/yr pumped via domestic wells.

Public Water Supply Wells

There were 37 public water supply wells identified in the study area. The amount of water supplied by each public water supply well was based on the number of residences served by the well (Montana DEQ Drinking Water Watch database; http://sdwisdww.mt.gov:8080/DWW/). Nearly every homeowner's association (HOA) with multiple wells reports the total number of homes in the HOA as connections for each well, which results in residences being counted repeatedly. To correct for this, air photos were used to determine the actual number of homes in each HOA, which showed 578 connections to public water supply wells. Similar to individual domestic wells, the annual and monthly rates per residence were estimated (Bobst and others, 2014), resulting in an annual rate of 391 acre-ft/yr.

Irrigation Wells

There were 21 irrigation wells identified in the study area using GWIC (http://mbmggwic.mtech.edu), the DNRC water rights database (http://wrqs.dnrc.mt.gov), remote sensing, and areal imagery. In most cases each of these wells supply water to several fields. The amount of water pumped by each irrigation well was based on the area irrigated (acres from FLU), and the amount of irrigation water applied (*IW*; inches).

Each irrigated field was associated with an irrigation well using the DNRC water rights database and MBMG GWIC well records. The total amount of pumping needed to irrigate the fields was summed to provide a pumping schedule for each well.

The amount of water applied was estimated based on *AET*, *IR* to the groundwater system, and effective precipitation (P_e). Since all the fields with groundwater as the source were irrigated using sprinkler or pivot systems, it was assumed that there was no runoff. Therefore, the monthly linear flux for each field was estimated by:

$$IW = (AET + IR) - P_e, \qquad \text{eq. C11}$$

where all terms are in inches.

The same process used to estimate monthly *AET* values for non-irrigated areas was also used for each irrigated field (see areal recharge section). That is, for each field, 2020 EVI values from Sentinel 2 satellite imagery and *PET* values from the Creston Agrimet station were used to estimate *AET*.

Irrigation recharge (*IR*) was estimated using the same approach as in the Irrigation Recharge section for inflows. That is, the efficiency of the irrigation method was used along with the *AET* to estimate the amount of water percolating through the root zone.

Effective precipitation (P_e) is the amount of moisture available for use by plants. For instance, water that evaporates or runs off cannot be used by plants since it does not reach the root zone. Since crop needs can be satisfied in part by effective precipitation, this reduces the amount of water that needs to be applied from the irrigation wells. P_e was estimated for 2020 using meteorological data from the Creston Agrimet station following the approach specified in the Soil Conservation Service's National Irrigation Handbook (SCS, 1993, p. 2-146 to 2-153).

The total area irrigated with wells in the study area includes 1,641 acres of pivot irrigation and 1,179 acres of sprinkler irrigation. Area-weighted average *IW* values were 28.4 in/yr. The total calculated pumping for irrigation wells was 6,679 acre-ft/yr. Pumping was applied in June, July, and August, with the distribution based in the Montana Irrigation Guide for Creston, using alfalfa in a normal year (NRCS, 1996).

Commercial and Industrial Wells

Pumping rates for commercial and industrial wells were based on water rights for each well. For the commercial and industrial wells the annual total diversion volume was distributed throughout the year based on the number of days in each month for a total pumping amount of 2,072 acre-ft/yr.

In summary, all types of wells are estimated to pump about 10,903 acre-ft/yr from aquifers in the study area (table C3). Of that total, about 61% is used for irrigated agriculture, 19% is for commercial or industrial uses, and 20% is for domestic use.

Discharge to Streams ($SW_{out\text{-}s}$)

Groundwater discharges to Mill Creek and Mooring Creek. Groundwater discharge to Blaine Creek was considered; however, DNRC monitoring data (site 14; appendix B; fig. 2 in the main body of this report) from WY20 show that streamflow only occurred in direct response to precipitation (see GWIC for data). This suggests that groundwater discharges to Blaine Creek are likely negligible.

The largest groundwater outflow to streams is the discharge of many springs through the bottom of Jessup Mill Pond. The outflow from Jessup Mill Pond is Mill Creek (site 16; appendix B). It should be noted that there is also a Mill Creek in the Swan Block that flows out to the valley approximately 1.5 mi north-east of Jessup Mill Pond; however, they are not connected by a surface channel. The USFWS Creston Fish Hatchery uses some of the water from Jessup Mill Pond in its operations, and monitoring site 16 was established on Mill Creek at the downstream end of the hatchery operations. This site has been monitored from 2011 to present by the MBMG (GWIC 262326) and the DNRC (SWAMP ID 76LJ 07500). The flow is stable, reflecting the groundwater-fed nature of the stream. Mean monthly flow from 2011 to 2021 ranged from 23.4 cfs in February to 32.0 cfs in June, and the average annual flow rate is 26.6 cfs (from https://mbmg.mtech.edu/WaterEnvironment/SWAMP; on 3/1/21). We assume the groundwater discharge rate is near constant, so the lowest flows reflect the groundwater discharge, and higher flows reflect a combination of groundwater, surface runoff, and soil water discharge. Thus, the total annual groundwater discharge to Jessup Mill Pond was calculated as 16,916 acre-ft, based on the lowest mean monthly flow rate.

As Mill Creek flows from Jessup Mill Pond to the Flathead River, monitoring shows additional net stream gains (sites 17–19; appendix B). Along this 3.9-mi reach, net stream gains of about 3 cfs/mi occur, which results in an overall gain of 8,476 acre-ft/yr.

Mooring Creek also receives groundwater discharge. Some of the groundwater discharged into Mooring Creek flows back into the aquifer through the bottom of Lake Blaine (see Lake Infiltration section). The gaging station at the Lake Blaine inlet (site 10; appendix B) was affected by high lake stages, so it was not possible to calculate continuous stream discharge at that site. Instead we used data from the DNRC gage approximately 1.7 mi upstream from the lake (site 8; appendix B). The mean monthly flows at this site in WY20 varied from 3.24 to 24.8 cfs. Assuming that the lowest flow rates reflect the groundwater inflows, while higher flows are supplemented by surface runoff and soil water inflows, this results in a calculated discharge of 2,349 acre-ft/yr.

In total, groundwater discharges to surface waters other than the Flathead River account for about 27,741 acre-ft/yr (table C1). These discharge rates are assumed to be near constant, so this total was distributed by month based on the number of days in each month (table C1).

Lake Evaporation (LE)

Evaporation from lakes other than Lake Blaine are included in this budget since groundwater monitoring near the lakes shows that groundwater levels and lake levels are very similar. This suggests a direct connection between the lakes and the shallow aquifer. Evaporation from Lake Blaine was included in the "Lake Infiltration from Lake Blaine" calculation. The other lakes are primarily in the Many Lakes area. They are pothole lakes without channelized inflow or outflow, so it is assumed that they are fed by and discharge to groundwater. The area of the lakes was determined by extracting lakes greater than 2 acres in size from the USGS National Hydrography Dataset (NHD; USGS, 2015). This resulted in 49 water bodies with a total delineated area of 601 acres. Areal and satellite imagery shows that the areas of the lakes are not constant, with the largest areas in the spring when groundwater levels are high, and then shrinking over the summer as groundwater levels drop. Since this same pattern is seen at Lake Blaine, the pattern of Lake Blaine area change was used to estimate the seasonal changes in the area of the other lakes. This caused the total lake area to vary in size from 455 to 601 acres.

The monthly lake areas were combined with monthly free water evaporation rates to estimate the monthly groundwater evaporation from the lakes. The free water evaporation rates were based on multiplying grass reference ET rates by 1.1 (Jensen, 2010). Grass reference ET rates were obtained for the Creston Agrimet station (https://www.usbr.gov/pn/agrimet/etsummary.html). This resulted in calculated evaporation rates ranging from 14 acre-ft in January to 421 acre-ft in July, and a total of 1,977 acre-ft/yr evaporated (table C1).

Riparian Evapotranspiration (ET_r)

Evapotranspiration of groundwater by riparian vegetation was calculated based on the AET in areas identified as riparian. There are about 4,878 acres of riparian vegetation in the study area (MNHP, 2017). The two most common community types are Emergent Wetlands and Riparian Forested, which account for 45% and 41% of the total, respectively (table C6). Emergent Wetlands are also called marsh, meadow, fen, prairie pothole, and slough (Cowardin and others, 1979). Riparian Forested areas contain woody obligate and facultative wetland species, such as willow and cottonwood.

AET was estimated for each riparian polygon using an approach similar to that used to estimate crop AET, except that the normalized difference vegetation index (NDVI) was used instead of EVI. The EVI approach appears to produce reasonable values within agricultural areas with relatively homogeneous and dense vegetation. Using the EVI approach within the riparian polygons resulted in AET values that were unreasonably low (less than precipitation). The low AET values from the EVI approach were likely due to the presence of water (which returns a negative EVI value), or bare ground (e.g., dry ponds). When NDVI was used instead of EVI, the average AET value was 16.1 in/yr, which is somewhat higher than precipitation (14.7 in/yr). Therefore, the amount of groundwater consumed by riparian vegetation (ET_r) was estimated to be 572 acre-ft/yr (table C6). This annual total was distributed by month based on the temporal distribution of calculated PET at the Creston Agrimet station.

Residual Outflow ($GW_{out} + SW_{out-FHR}$)

Groundwater outflow from the study area (GW_{out}) and groundwater discharge to the Flathead River and

Table C6. Riparian areas.

Community Type	Acres	% of Total	Area Weighted Mean AET (in/yr)	AET-PCP (in/yr)	ET_r (acre-ft/yr)
Freshwater Emergent Wetland	2,181	45%	15.2	0.51	92
Freshwater Forested Wetland	47	1%	15.1	0.38	1
Freshwater Scrub-Shrub Wetland	273	6%	15.2	0.55	12
Riparian Emergent	347	7%	16.9	2.20	64
Riparian Forested	1,979	41%	17.1	2.39	395
Riparian Scrub-Shrub	50	1%	16.6	1.89	8
Total	4,878	100%	16.1	1.41	572

associated springs ($SW_{out-FHR}$) are grouped together in this analysis as residual outflows. These water budget components were combined because these outflows are poorly constrained by monitoring data. Darcy flux calculations can be used to estimate groundwater outflow, but the thickness and hydraulic conductivity (K) of the deep aquifer are poorly constrained, and the entire residual could easily be accounted for by groundwater outflow. Similarly, the difference in streamflows in the Flathead River could be used to estimate groundwater outflow to the river; however, the Flathead River has a minimum mean monthly flow of 5,250 cfs (USGS Station 12363000; Flathead River at Columbia Falls, MT) and measurement errors make it difficult to quantify changes in discharge of less than ~5%, so changes of less than 262 cfs are within the margin of error (Carter and Anderson, 1963; Cey and others, 1998). Therefore, separating these budget components would be arbitrary.

For the annual budget, residual outflow was calculated as the difference between quantified inflows and outflows, since long-term groundwater monitoring suggests that on an annual basis ΔS is near zero. This was a total of 20,330 acre-ft/yr (28 cfs). Monthly budgets assumed that residual outflow occurs at a constant rate, so it was distributed based on the number of days in each month (table C1).

Changes in storage (ΔS)

Changes in storage are important in the monthly budgets; however, based on long-term groundwater-level monitoring data, they appear to be near zero on an annual basis. On a monthly basis ΔS was calculated as the residual from the other water budget components for that month (table C1).

SUMMARY

The total amount of groundwater moving through the East Flathead study area is about 60,000 acre-ft/yr (table C1, fig. C8). The Swan Mountain Block is an important source of water, with groundwater inflow from the Swan Block, infiltration of streams at the mountain front, and infiltration of water from Lake Blaine (which obtains most of its water from the Swan Block) together accounting for 62% of the recharge to the valley-fill aquifer. Groundwater inflow along the southern boundary (17%), areal recharge (14%), and irrigation recharge (6%) are the other main sources of groundwater recharge. Most groundwater leaving the area discharges to local streams (45%), is extracted by wells (18%), flows to the Flathead River, or flows out of the area as groundwater to downgradient portions of the shallow and deep aquifers (33%, combined).

Inflows

Legend:
- Mountain Block Recharge (*MBR*)
- Lake Infiltration (*LI*)
- Areal Recharge (*AR*)
- Septic Returns (*SR*)
- Surficial Mountain-Front Recharge (*MFR*$_s$)
- Groundwater Inflow (*GW*$_{in}$)
- Irrigation Recharge (*IR*)

Outflows

Legend:
- Well Pumping (*WEL*)
- Lake Evaporation (*LE*)
- Residual Outflow (*GW*$_{out}$+*SW*$_{out}$-*FHR*)
- Discharge to Streams (*SW*$_{out-s}$)
- Riparian Evapotranspiration (*ET*$_r$)
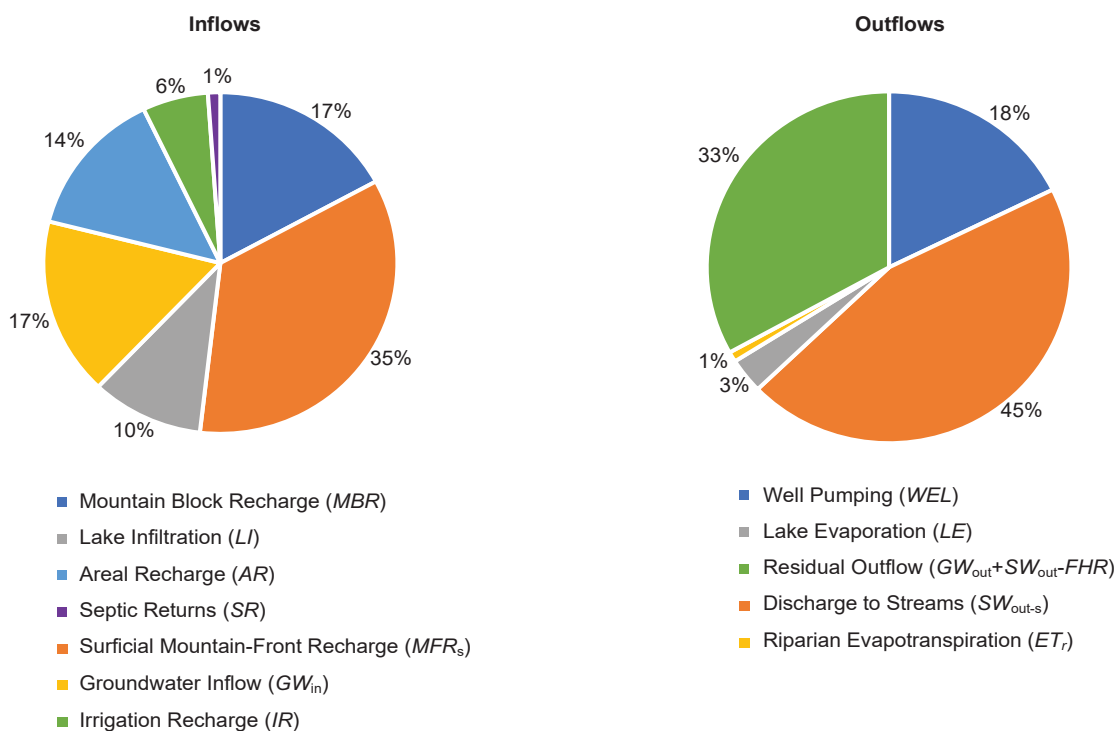
Figure C8. A summary of the average annual preliminary groundwater budget for the East Flathead Study Area.

REFERENCES

Bobst, A., Waren, K., Swierc, J., and Madison, J.D., 2014, Hydrogeologic investigation of the North Hills study area, Lewis and Clark County, Montana, Technical Report: Montana Bureau of Mines and Geology Open-File Report 654, 376 p.

Carter, R.W., and Anderson, I.E., 1963, Accuracy of current meter measurements: Journal of Hydraulics Division, Proceedings of ASCE, v. 4, no. 1, p. 105–115.

Cey, E.E., Rudolph, D.L., Parkin, G.W. and Aravena, R., 1998, Quantifying groundwater discharge to a small perennial stream in southern Ontario, Canada: Journal of Hydrology, v. 210, no. 1–4, p. 21–37.

Choudhury, B., Ahmed, N., Idso, S., Reginato, R., and Daughtry, C., 1994, Relations between evaporation coefficients and vegetation indices studied by model simulations: Remote Sensing of Environment, no. 50, p. 1–17.

Cowardin, L.M., Carter, V., Golet, F. C. E., and LaRoe, T., 1979, Classification of wetlands and deepwater habitats of the United States: U.S. Department of the Interior, Fish and Wildlife Service, Jamestown, ND: Northern Prairie Wildlife Research Center Online, available at http://www.npwrc.usgs.gov/resource/wetlands/classwet/index.htm [Accessed June 2024].

Glenn, E.P., Nagler, P.L., and Huete, A.R., 2010, Vegetation index methods for estimating evapotranspiration by remote sensing: Surveys in Geophysics, no. 31, p. 531–555, https://doi.org/10.1007/s10712-010-9102-2.

Jensen, M.E., 2010, Estimating evaporation from water surfaces, in Proceedings of the CSU/ARS Evapotranspiration Workshop, p. 1–27.

LaFave, J.I., Smith, L.N., and Patton, T.W., 2004, Ground-water resources of the Flathead Lake Area: Flathead, Lake, and parts of Missoula and Sanders counties. Part A—Descriptive overview: Montana Bureau of Mines and Geology Montana Ground-Water Assessment Atlas 2-A, 144 p.

Markovich, K.H., Manning, A.H., Condon, L.E., and McIntosh, J.C., 2019, Mountain-block recharge: A review of current understanding: Water Resources Research, v. 55, no. 11, p. 8278–8304.

McCarthy, P.M., Dutton, D.M., Sando, S.K., and Sando, R., 2016, Montana StreamStats—A method for retrieving basin and streamflow characteristics in Montana: U.S. Geological Survey Scientific Investigations Report 2015–5019–A, 16 p., http://dx.doi.org/10.3133/sir20155019A.

Montana Department of Revenue (MDOR), 2019, Revenue Final Land Unit (FLU) Classification, available from https://msl.mt.gov/geoinfo/ [Accessed 7/29/2019].

Montana Natural Heritage Program (MNHP), 2017, Montana Landcover Framework Map Service, available from https://nris.msl.mt.gov/ [Accessed 3/8/21].

Montana State Library (MSL), 2019, Montana Structures/Addresses Framework, available from https://msl.mt.gov/geoinfo/ [Accessed 12/11/20].

Monteith, J.L., 1965, Evaporation and Environment, in Symposia of the society for experimental biology: Cambridge University Press (CUP) Cambridge, v. 19, p. 205–234.

Mu, Q., Heinsch, F. A., Zhao, M., and Running, S.W., 2007, Development of a global evapotranspiration algorithm based on MODIS and global meteorology data: Remote Sensing of Environment, v. 111, p. 519–536, https://doi.org/10.1016/j.rse.2007.04.015.

Mu, Q., Zhao, M., and Running, S.W., 2011, Improvements to a MODIS global terrestrial evapotranspiration algorithm: Remote Sensing of Environment, v. 115, p.1781–1800.

Nagler, P.L., Cleverly, J., Glenn, E., Lampkin, D., Huete, A., and Wan, Z., 2005, Predicting riparian evapotranspiration from MODIS vegetation indices and meteorological data: Remote Sensing of Environment, v. 94, no. 1, p. 17–30.

Nagler, P.L., Morino, K., Murray, R.S., Osterberg, J., and Glenn, E.P., 2009, An empirical algorithm for estimating agricultural and riparian evapotranspiration using MODIS enhanced vegetation index and ground measurements of ET. I. Description of method: Remote Sensing, v. 1, no. 4, p. 1273–1297.

PRISM Climate Group, 2015, Precipitation yearly normal for 1981–2010 from PRISM, available from http://prism.oregonstate.edu; https://geoinfo.msl.mt.gov/ [Accessed 12/31/20].

Rose, J., Bobst, A., and Gebril, A., 2022, Hydrogeo-
logic investigation of the deep alluvial aquifer,
Flathead Valley, Montana: Montana Bureau of
Mines and Geology Report of Investigation 32,
44 p.

Smesrud, J., and Madison, M., 2007, Wild flood to
graded border irrigation for water and energy con-
servation in the Klamath Basin: USCID Fourth
International Conference, p. 751–758.

USDA Natural Resources Conservation Service
(NRCS), 1996, Montana Irrigation Guide, avail-
able at https://www.nrcs.usda.gov/Internet/FSE_
DOCUMENTS/stelprdb1250160.pdf [Accessed
12/10/20].

USDA Natural Resources Conservation Service
(NRCS), 1997, National Engineering Handbook
Part 652: Irrigation Guide, available at https://
www.nrcs.usda.gov/Internet/FSE_DOCU-
MENTS/nrcs144p2_033068.pdf [Accessed
12/10/20].

USDA Soil Conservation Service (SCS), 1993, Na-
tional Engineering Handbook Part 623: Chap-
ter 2–Irrigation Water Requirements, available
at https://www.wcc.nrcs.usda.gov/ftpref/wntsc/
waterMgt/irrigation/NEH15/ch2.pdf [Accessed
8/27/21].

U.S. Geological Survey, 2019, National Hydrography
Dataset (ver. USGS National Hydrography Data-
set Best Resolution (NHD) for Hydrologic Unit
(HU) 4-2001 (published 20191002)), available
at https://www.usgs.gov/national-hydrography/
access-national-hydrography-products [Accessed
October 10, 2020].

Wilson, J.L., and Guan, H., 2004, Mountain-block hy-
drology and mountain-front recharge: Groundwa-
ter recharge in a desert environment: The South-
western United States, no. 9, p. 113–137.

APPENDIX D

AQUIFER TESTS
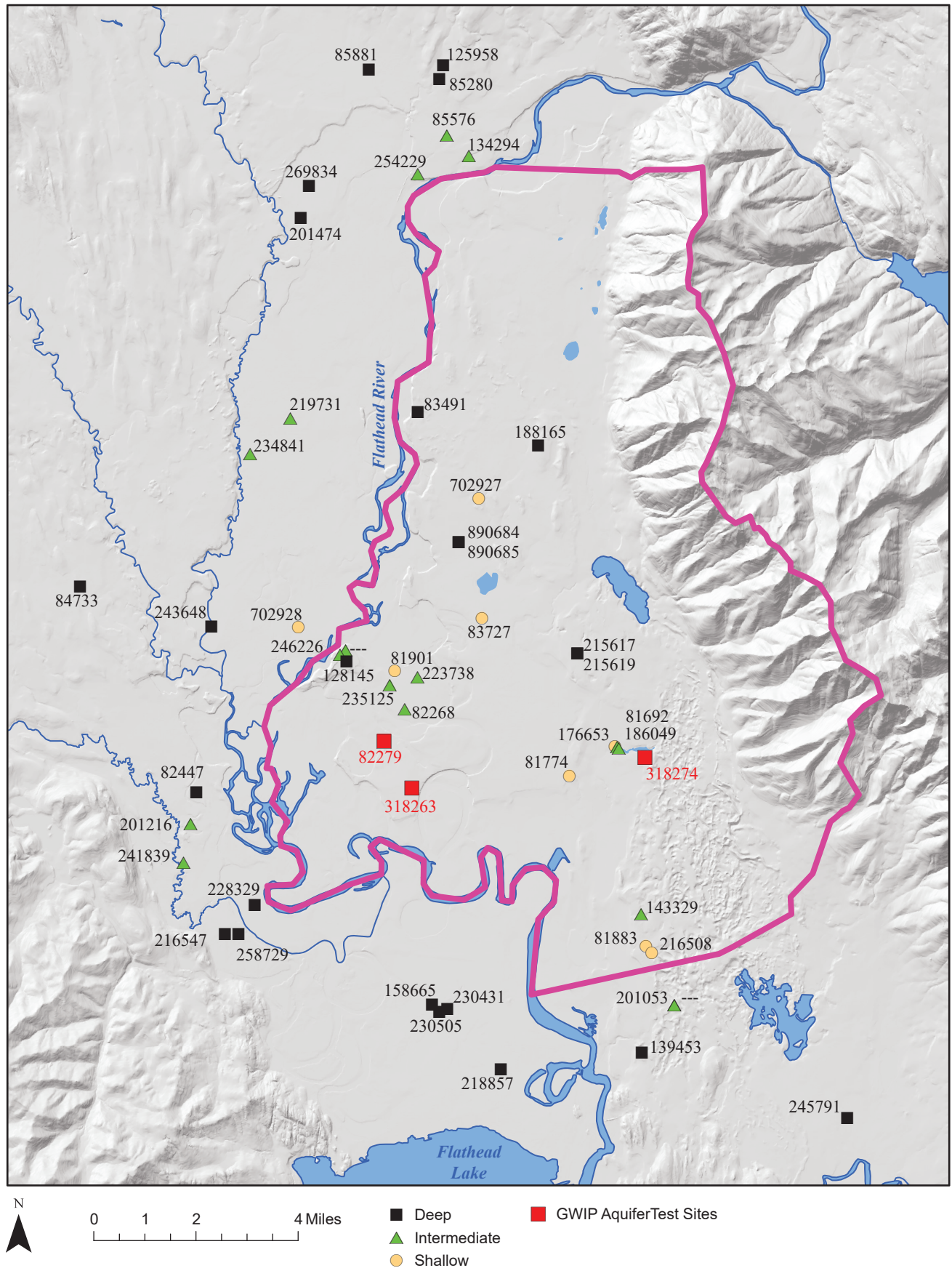
Figure D1. Locations and GWIC IDs of wells with aquifer test information from previous studies, and the locations of aquifer tests by GWIP in the East Flathead study area (Myse and others, 2023). Pink outline shows the East Flathead Study Area.

Table D1. Previous aquifer tests (from DNRC records).

GWIC ID	Latitude	Longitude	Well Depth (ft)	Screen Length (ft)	Transmissivity (ft²/d)	Storativity	Hydraulic Conductivity, K (ft/d)	HGU
702928	48.2275	-114.2561	100	17	510		20	Shallow
81901	48.2169	-114.2141	110	10	48		3.2	Shallow
81883	48.1430	-114.1005	140	20	14,301		476.7	Shallow
702927	48.2672	-114.1827	142	17	110		4.3	Shallow
81774	48.1900	-114.1372	163	17	375		14.7	Shallow
83727	48.2333	-114.1783	195	17	16,711		655.3	Shallow
186049	48.1991	-114.1186	198	17	16,000		627.5	Shallow
216508	48.1412	-114.0978	201	12	1,300		72.2	Shallow
176653	48.1990	-114.1177	202	14	8,740		416.2	Intermediate
246226	48.2219	-114.2355	207	22	2,197		66.6	Intermediate
201216	48.1699	-114.2968	216	17	635		24.9	Intermediate
—	48.2204	-114.2377	220	12	2,382	2.50E-04	132.3	Intermediate
235125	48.2127	-114.2158	222	10	2,930	8.50E-05	195.3	Intermediate
85576	48.3697	-114.2056	231	35	21,200		403.8	Intermediate
219731	48.2866	-114.2649	235	80	15,551	8.19E-03	129.6	Intermediate
143329	48.1520	-114.1033	260	15	649		28.8	Intermediate
82268	48.2061	-114.2088	264	16	455		19	Intermediate
254229	48.3581	-114.2170	270	16	22,000		916.7	Intermediate
223738	48.2154	-114.2042	280	14	8,420	1.70E-04	401	Intermediate
201053	48.1266	-114.0869	286	84	18,637	1.40E-01	147.9	Intermediate
—	48.1266	-114.0869	286	38	4,350		76.3	Intermediate
241839	48.1587	-114.2988	287	26	45,962		1,178.50	Intermediate
81692	48.1986	-114.1169	300	131	7,273	2.60E-03	37	Intermediate
234841	48.2758	-114.2811	300	10	828	5.00E-03	55.2	Intermediate
134294	48.3642	-114.1957	304	65	30800	4.26E-04	315.9	Intermediate
82447	48.1790	-114.2952	306	12	5,342		296.8	Deep
139453	48.1126	-114.0995	310	65	49,788		510.6	Deep
245791	48.0974	-114.0108	322	54	4,500	1.20E-03	55.6	Deep
216547	48.1392	-114.2794	346	82	980	1.00E-04	7.9	Deep
228329	48.1479	-114.2675	350	58	31,416	1.20E-05	361.1	Deep
188165	48.2833	-114.1588	356	120	2,203		12.2	Deep
85881	48.3871	-114.2406	378	10	62	2.50E-05	4.2	Deep
215617	48.2248	-114.1369	395	39	559	1.70E-03	9.6	Deep
84733	48.2352	-114.3499	400	65	20,880	2.00E-04	214.2	Deep
230505	48.1208	-114.1864	400	65	17,200	3.30E-05	176.4	Deep
243648	48.2262	-114.2931	420	37	12,420	4.80E-05	223.8	Deep
258729	48.1394	-114.2736	421	78	9,255	5.70E-04	79.1	Deep
158665	48.1227	-114.1897	448	15	28,946		1,286.50	Deep
83491	48.2907	-114.2109	454	251	17,480		46.4	Deep
128145	48.2187	-114.2348	489	24	2,102		58.4	Deep
201474	48.3438	-114.2657	543	78	13,100	3.50E-03	112	Deep
269834	48.3530	-114.2630	602	22	1,686	9.00E-03	51.1	Deep
230431	48.1218	-114.1831	640	65	28,946	2.62E-04	296.9	Deep
215619	48.2248	-114.1369	654	109	860		5.3	Deep
218857	48.1055	-114.1589	685	17	5,331		209.1	Deep
890684	48.2545	-114.1902	690	65	17300		177.4	Deep
890685	48.2545	-114.1902	690	99	16,711	1.50E-03	112.5	Deep
85280	48.3855	-114.2103	734	65	162		1.7	Deep
125958	48.3896	-114.2090	743	23	160	3.50E-02	4.6	Deep
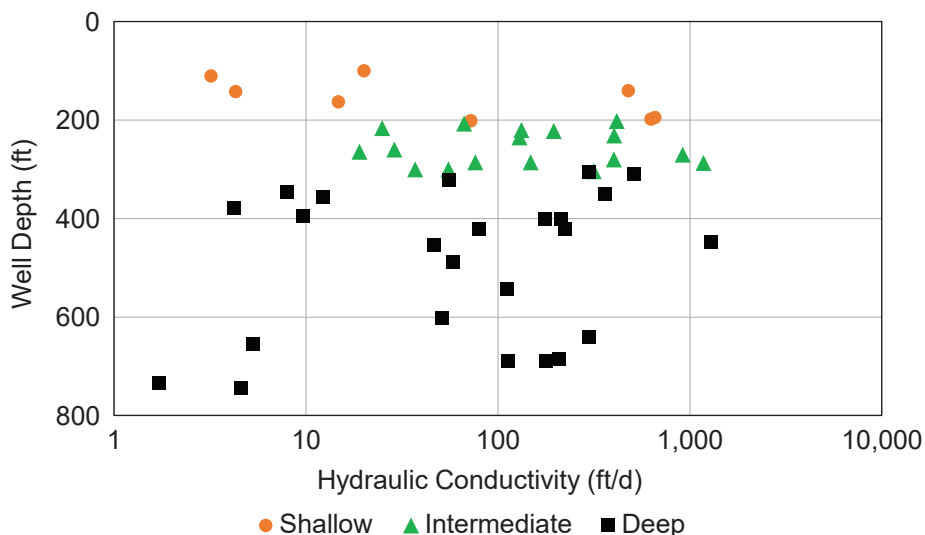
Figure D2. Aquifer test results by well depth and aquifer.

Table D2. Summary of hydraulic conductivity (K) from previous aquifer tests (ft/d)

HGU	n	Min	Max	25th Percentile	Median	75th Percentile	Geometric Mean
Shallow Aquifers	8	3	655	12	46	514	52
Intermediate Aquifers	17	19	1,179	55	132	401	135
Deep Aquifer	24	2	1,287	12	96	217	61

Table D3. Wells used for GWIP aquifer tests.

GWIC ID	Name	Latitude (deg. N)	Longitude (deg. W)	Measuring Point Elevation (ft-amsl)	Total Depth (ft-bgs)	Screen Interval (ft)	Distance from PW (ft)	Comments
Foy's Bend								
318263	Quigley Deep	48.167212	114.233313	2909.51	640	610 - 630	—	Deep Pumping Well
318266	Quigley Intermediate	48.167260	114.233177	2910.55	300	295 - 300	33	Intermediate Observation Well
318265	Quigley Shallow	48.167241	114.233235	2910.04	50	40 - 50	56	Shallow Observation Well
Jessup Mill Pond								
318274	Ottey PW	48.196797	114.105436	2987.99	300	278-298	—	Deep Pumping Well
304315	Ottey House Well	48.196493	114.105899	2972.10	52	Open Bottom	188	Shallow Observation Well
310815	Ottey 280	48.196444	114.105578	2973.07	280	Open Bottom	202	Deep Observation Well
310816	Ottey 180	48.196439	114.105584	2972.99	180	Open Bottom	203	Intermediate Observation Well
Jaquette Road								
82279	Ken Smith	48.196594	114.216836	2950.83	486	438-478	—	Deep Pumping Well
262323	MBMG Intermediate	48.196536	114.216977	2948.73	217	Open Bottom	40	Top of Deep Observation Well
262324	MBMG Shallow	48.196553	114.216916	2948.46	66	56-66	24	Shallow Observation Well
262325	MBMG Deep	48.196591	114.217362	2952.02	480	Open Bottom	128	Deep Observation Well
128155	Ken Smith - Domestic	48.196858	114.218400	2926.65	417	363-416	393	Deep Observation Well
197798	Fairmont Egan School #3	48.196995	114.221201	2941.60	298	Open Bottom	1,078	Deep Observation Well
143331	Bill and Linda Arlint	48.189944	114.219203	2951.50	200	Open Bottom	2,494	Deep Observation Well

Note. ft-amsl, feet above mean sea level; ft-bgs, feet below ground surface. Horizontal Datum, NAD83; Vertical Datum, NAVD88.

APPENDIX E

GEOLOGIC MODEL WELLS

Appendix E. Wells used to construct the Geologic Model (sorted by GWIC ID).

GWIC ID	Latitude	Longitude	Geo Method	Ground Surface Altitude (ft, amsl)	Depth (ft)
80685	48.1315	-114.1523	TRS-SEC	2903	283
80694	48.1214	-114.1485	TRS-SEC	2906	345
80696	48.1104	-114.1567	TRS-SEC	2899	652
81528	48.2202	-114.0712	TRS-SEC	3600	218
81530	48.1976	-114.0711	SUR-GPS	3217	171
81548	48.1880	-114.0600	MAP	3247	120
81551	48.1698	-114.0629	NAV-GPS	3140	410
81565	48.1697	-114.0433	MAP	3211	270
81579	48.1686	-114.0394	MAP	3229	162
81591	48.1675	-114.0286	MAP	3253	137
81611	48.1434	-114.0452	TRS-SEC	3049	162
81635	48.2210	-114.0858	TRS-SEC	3100	380
81636	48.2168	-114.0744	SUR-GPS	3321	75
81655	48.2249	-114.1417	MAP	3048	187
81657	48.2215	-114.1402	MAP	3046	273
81665	48.2247	-114.1930	MAP	2963	64
81673	48.1977	-114.1880	TRS-SEC	2970	267
81678	48.2058	-114.1369	MAP	2968	132
81693	48.1995	-114.1155	NAV-GPS	2951	95
81711	48.1931	-114.0733	SUR-GPS	3180	340
81766	48.1863	-114.1319	MAP	2919	407
81772	48.1898	-114.1461	SUR-GPS	2958	500
81775	48.1900	-114.1413	SUR-GPS	2958	140
81792	48.1811	-114.2016	TRS-SEC	2958	215
81794	48.1756	-114.1965	TRS-SEC	2906	356
81800	48.1732	-114.1409	TRS-SEC	2930	254
81843	48.1542	-114.0814	NAV-GPS	3055	100
81862	48.1585	-114.1990	TRS-SEC	2899	753
81875	48.1518	-114.0980	NAV-GPS	3057	200
81919	48.2247	-114.2382	TRS-SEC	2912	102
82279	48.1966	-114.2168	SUR-GPS	2949	486
82285	48.1911	-114.2027	TRS-SEC	2968	212
82288	48.1919	-114.2361	SUR-GPS	2945	180
82458	48.1740	-114.2893	TRS-SEC	2917	245
82496	48.1758	-114.2812	TRS-SEC	2923	301
82498	48.1759	-114.2461	TRS-SEC	2913	690
82505	48.1702	-114.2029	TRS-SEC	2918	375
82515	48.1569	-114.2300	TRS-SEC	2908	407
82518	48.1606	-114.2664	TRS-SEC	2915	288
82636	48.1461	-114.2500	TRS-SEC	2903	300
82650	48.1406	-114.2068	TRS-SEC	2909	810

Appendix E—*Continued*.

GWIC ID	Latitude	Longitude	Geo Method	Ground Surface Altitude (ft, amsl)	Depth (ft)
83424	48.2997	-114.1300	MAP	3091	250
83425	48.3005	-114.1308	MAP	3087	200
83431	48.3012	-114.1424	MAP	3050	552
83435	48.3015	-114.1369	SUR-GPS	3045	340
83491	48.2907	-114.2109	TRS-SEC	3051	454
83512	48.2843	-114.1972	TRS-SEC	3054	173
83535	48.2908	-114.1731	MAP	3060	200
83538	48.2858	-114.1708	SUR-GPS	3056	200
83574	48.2830	-114.1426	TRS-SEC	3030	439
83579	48.2743	-114.1371	MAP	3030	627
83633	48.2602	-114.1737	NAV-GPS	3009	190
83640	48.2677	-114.1358	TRS-SEC	3012	597
83642	48.2650	-114.1426	TRS-SEC	3055	405
83644	48.2631	-114.1508	TRS-SEC	3080	445
83651	48.2550	-114.1409	NAV-GPS	3052	184
83662	48.2542	-114.1151	NAV-GPS	3089	120
83666	48.2519	-114.1194	MAP	3034	139
83690	48.2495	-114.1395	NAV-GPS	3037	100
83713	48.2469	-114.1694	NAV-GPS	3024	194
83716	48.2475	-114.1838	SUR-GPS	2986	338
83725	48.2282	-114.1041	NAV-GPS	3077	125
83732	48.2272	-114.1642	MAP	2981	86
83752	48.2399	-114.1492	NAV-GPS	3006	195
83789	48.2400	-114.1283	NAV-GPS	3082	120
83794	48.2268	-114.1309	MAP	3068	155
83797	48.2260	-114.1208	MAP	3067	140
83808	48.2325	-114.1091	MAP	3088	120
83826	48.2322	-114.1088	MAP	3086	124
83999	48.2807	-114.2261	TRS-SEC	2952	126
84458	48.2269	-114.2226	TRS-SEC	2925	20
85474	48.3618	-114.1530	MAP	3042	215
85475	48.3624	-114.1479	MAP	3095	284
85480	48.3574	-114.1505	TRS-SEC	3090	284
85481	48.3583	-114.1465	TRS-SEC	3090	620
85547	48.3670	-114.1811	TRS-SEC	3017	131
85557	48.3604	-114.1784	TRS-SEC	3000	60
85615	48.3505	-114.1808	MAP	3081	164
85628	48.3429	-114.1852	SUR-GPS	3058	149
85649	48.3462	-114.1669	NAV-GPS	3076	160
85652	48.3470	-114.1753	NAV-GPS	3070	183
85669	48.3460	-114.1525	NAV-GPS	3074	40

Appendix E—*Continued*.

GWIC ID	Latitude	Longitude	Geo Method	Ground Surface Altitude (ft, amsl)	Depth (ft)
85673	48.3538	-114.1399	TRS-SEC	3069	342
85689	48.3442	-114.1450	SUR-GPS	3074	308
85703	48.3469	-114.1311	MAP	3076	71
85708	48.3413	-114.1344	MAP	3103	120
85711	48.3356	-114.1480	TRS-SEC	3075	445
85730	48.3329	-114.1605	NAV-GPS	3069	91
85737	48.3283	-114.1652	MAP	3071	223
85774	48.3296	-114.1857	NAV-GPS	3070	152
85780	48.3415	-114.2095	MAP	2986	217
85781	48.3408	-114.2047	MAP	2985	84
85856	48.3229	-114.1480	TRS-SEC	3050	455
86294	48.3459	-114.2271	TRS-SEC	2987	158
120789	48.1793	-114.0501	NAV-GPS	3242	110
122756	48.3479	-114.1509	NAV-GPS	3072	210
125938	48.2358	-114.2122	NAV-GPS	2968	64
125969	48.3255	-114.1841	MAP	3071	142
125971	48.3266	-114.1605	MAP	3068	143
127407	48.1858	-114.0944	MAP	2968	38
132078	48.1783	-114.0356	NAV-GPS	3357	390
132433	48.1639	-114.0910	NAV-GPS	3074	132
132436	48.1567	-114.1044	NAV-GPS	3064	273
132453	48.2821	-114.1303	TRS-SEC	3055	1026
132462	48.2380	-114.1538	NAV-GPS	3006	525
134960	48.3451	-114.1536	NAV-GPS	3069	171
139537	48.2050	-114.1144	MAP	2968	90
141608	48.1879	-114.0924	NAV-GPS	2987	80
141616	48.2755	-114.1188	MAP	3335	405
141690	48.3555	-114.1822	MAP	3007	100
143170	48.2022	-114.1734	TRS-SEC	2971	316
143314	48.2010	-114.1349	NAV-GPS	2985	178
143349	48.3508	-114.2116	TRS-SEC	2990	100
143354	48.2722	-114.1640	TRS-SEC	3057	580
148187	48.3481	-114.1969	SUR-GPS	3043	157
148188	48.3482	-114.1990	SUR-GPS	3045	518
148189	48.3469	-114.1991	SUR-GPS	3043	342
148484	48.3288	-114.1622	MAP	3075	240
148755	48.2225	-114.0825	MAP	3171	224
148762	48.1817	-114.1751	NAV-GPS	2954	420
149273	48.1750	-114.0352	MAP	3318	200
150702	48.2507	-114.1387	NAV-GPS	3032	110
152923	48.1857	-114.1572	NAV-GPS	2956	499

Appendix E—*Continued*.

GWIC ID	Latitude	Longitude	Geo Method	Ground Surface Altitude (ft, amsl)	Depth (ft)
152925	48.1734	-114.1234	NAV-GPS	2906	158
152961	48.2261	-114.1200	MAP	3064	203
154872	48.1625	-114.0216	MAP	3174	414
156650	48.2856	-114.1306	TRS-SEC	3057	298
156652	48.2503	-114.1909	TRS-SEC	2982	702
157098	48.2269	-114.1082	NAV-GPS	3063	157
158200	48.3432	-114.1296	SUR-GPS	3202	170
158599	48.2385	-114.2057	NAV-GPS	3001	118
164337	48.3105	-114.1320	TRS-SEC	3080	248
164733	48.3238	-114.1677	NAV-GPS	3072	145
167049	48.1497	-114.1094	TRS-SEC	2958	203
168372	48.1845	-114.1065	NAV-GPS	2999	135
168384	48.1787	-114.0906	NAV-GPS	2981	60
168471	48.1595	-114.1311	TRS-SEC	2904	167
172621	48.2784	-114.1303	TRS-SEC	3080	500
172626	48.2270	-114.1611	MAP	3003	357
172627	48.2373	-114.1051	NAV-GPS	3022	67
173488	48.2242	-114.2049	TRS-SEC	2918	140
173515	48.3135	-114.1986	NAV-GPS	3065	193
176034	48.3614	-114.2040	TRS-SEC	3055	214
176038	48.2848	-114.1425	TRS-SEC	3030	299
176085	48.3557	-114.1399	TRS-SEC	3070	278
176091	48.3288	-114.1746	NAV-GPS	3074	145
176653	48.1990	-114.1177	MAP	2948	198
176654	48.1971	-114.1168	SUR-GPS	2947	198
176896	48.2192	-114.2327	TRS-SEC	2982	341
182314	48.2073	-114.1073	TRS-SEC	3000	170
187856	48.2866	-114.1343	TRS-SEC	3025	363
188125	48.1950	-114.1571	TRS-SEC	2966	315
188130	48.1556	-114.1143	TRS-SEC	2955	218
188172	48.2461	-114.1270	NAV-GPS	3038	41
188286	48.1208	-114.0930	TRS-SEC	2975	207
194635	48.1971	-114.0873	NAV-GPS	2979	100
194699	48.2830	-114.1317	TRS-SEC	3045	319
194711	48.2605	-114.1666	NAV-GPS	3035	219
194718	48.2428	-114.1451	NAV-GPS	3007	98
197798	48.1970	-114.2212	NAV-GPS	2944	298
200815	48.2349	-114.1739	TRS-SEC	2980	170
200818	48.2365	-114.1060	TRS-SEC	3030	660
200851	48.2446	-114.2493	TRS-SEC	2934	250
200962	48.2566	-114.1358	TRS-SEC	3018	673

Appendix E—*Continued*.

GWIC ID	Latitude	Longitude	Geo Method	Ground Surface Altitude (ft, amsl)	Depth (ft)
201042	48.1345	-114.0529	TRS-SEC	3037	100
201436	48.2073	-114.1149	NAV-GPS	2985	100
205926	48.2565	-114.1149	MAP	3100	148
206068	48.3327	-114.2116	TRS-SEC	2977	164
206321	48.3098	-114.1943	MAP	3063	179
206484	48.3148	-114.1413	TRS-SEC	3045	377
211096	48.2355	-114.1071	MAP	3006	60
214004	48.3287	-114.2353	TRS-SEC	2978	184
214653	48.2157	-114.1060	NAV-GPS	3023	160
215007	48.2599	-114.1954	NAV-GPS	3007	241
215616	48.1480	-114.0179	TRS-SEC	3116	236
215619	48.2248	-114.1369	TRS-SEC	3054	654
216891	48.1950	-114.1198	NAV-GPS	2935	120
217695	48.1877	-114.0927	TRS-SEC	3010	500
217812	48.2419	-114.2534	TRS-SEC	2929	340
219773	48.2586	-114.1758	NAV-GPS	3003	81
219805	48.3447	-114.1948	NAV-GPS	3042	162
220005	48.3582	-114.1275	NAV-GPS	3129	140
220323	48.2603	-114.1147	NAV-GPS	3169	145
220614	48.3400	-114.1844	TRS-SEC	3061	208
220618	48.2105	-114.1286	TRS-SEC	2992	255
220871	48.2708	-114.1203	NAV-GPS	3143	74
221135	48.3533	-114.1458	NAV-GPS	3085	315
221136	48.2061	-114.1893	NAV-GPS	2932	220
222175	48.2772	-114.1654	NAV-GPS	3044	260
222591	48.3057	-114.1703	NAV-GPS	3058	120
222592	48.3066	-114.1688	NAV-GPS	3056	156
222636	48.2365	-114.1290	NAV-GPS	3070	240
222729	48.3414	-114.1693	NAV-GPS	3065	80
222974	48.1734	-114.0929	NAV-GPS	3047	99
223157	48.3402	-114.1303	TRS-SEC	3268	602
223461	48.2997	-114.1633	SUR-GPS	3053	167
223737	48.1958	-114.0694	NAV-GPS	3198	190
223738	48.2154	-114.2042	NAV-GPS	2939	280
223739	48.2154	-114.2036	NAV-GPS	2936	280
223849	48.2081	-114.1978	NAV-GPS	2934	160
224048	48.1674	-114.0960	NAV-GPS	3078	254
224393	48.2162	-114.1429	NAV-GPS	2978	220
224610	48.2496	-114.1408	NAV-GPS	3044	171
224612	48.2289	-114.0958	NAV-GPS	3088	120
224634	48.1858	-114.0839	NAV-GPS	3065	200

Appendix E—*Continued.*

GWIC ID	Latitude	Longitude	Geo Method	Ground Surface Altitude (ft, amsl)	Depth (ft)
224670	48.1652	-114.1464	NAV-GPS	2904	180
224675	48.3363	-114.1697	NAV-GPS	3075	220
224677	48.1624	-114.1981	NAV-GPS	2899	680
224839	48.2162	-114.1017	NAV-GPS	3026	120
225107	48.2908	-114.1488	NAV-GPS	3061	140
225259	48.3368	-114.1700	NAV-GPS	3075	80
225263	48.3584	-114.1701	NAV-GPS	3016	150
226527	48.1752	-114.0789	NAV-GPS	3095	240
227402	48.2507	-114.1850	NAV-GPS	2983	260
227807	48.2625	-114.1956	NAV-GPS	3011	159
227809	48.2044	-114.1333	NAV-GPS	3011	198
228892	48.2786	-114.1690	NAV-GPS	3047	157
228894	48.3103	-114.1698	NAV-GPS	3060	183
230280	48.3101	-114.1574	NAV-GPS	3058	140
230457	48.2487	-114.1403	NAV-GPS	3037	296
230460	48.3261	-114.1666	NAV-GPS	3071	260
231696	48.2203	-114.1197	NAV-GPS	3053	279
232307	48.2293	-114.0892	NAV-GPS	3182	360
232311	48.2917	-114.1433	NAV-GPS	3033	80
234416	48.1500	-114.0639	NAV-GPS	3081	158
234503	48.2841	-114.1531	NAV-GPS	3116	289
234504	48.2839	-114.1531	NAV-GPS	3119	293
235121	48.1661	-114.1003	NAV-GPS	3028	260
235122	48.3449	-114.1701	NAV-GPS	3058	160
235125	48.2127	-114.2158	NAV-GPS	2936	220
235126	48.2080	-114.0767	NAV-GPS	3191	240
235127	48.2145	-114.1870	NAV-GPS	2966	200
235129	48.3333	-114.2029	NAV-GPS	3032	120
235262	48.1986	-114.2767	NAV-GPS	2910	240
235537	48.2238	-114.1877	NAV-GPS	2987	80
235539	48.2320	-114.1046	NAV-GPS	3071	142
235864	48.3457	-114.1866	NAV-GPS	3043	160
236810	48.2395	-114.1276	NAV-GPS	3076	318
236929	48.2091	-114.1397	NAV-GPS	2972	80
237105	48.1456	-114.0106	NAV-GPS	3117	440
237972	48.3656	-114.1394	NAV-GPS	3086	320
238520	48.2420	-114.1225	NAV-GPS	3077	120
238521	48.3344	-114.1794	NAV-GPS	3076	140
238523	48.3176	-114.1696	NAV-GPS	3070	100
238620	48.3067	-114.1684	NAV-GPS	3058	180
238660	48.2286	-114.0950	NAV-GPS	3106	128

Appendix E—*Continued.*

GWIC ID	Latitude	Longitude	Geo Method	Ground Surface Altitude (ft, amsl)	Depth (ft)
238800	48.1228	-114.1306	NAV-GPS	2897	257
238895	48.2499	-114.1833	NAV-GPS	2982	221
239270	48.3507	-114.1725	TRS-SEC	3080	241
239337	48.2126	-114.1855	NAV-GPS	2962	300
239360	48.1763	-114.1111	NAV-GPS	2924	140
239386	48.2167	-114.1448	NAV-GPS	2970	180
239390	48.2946	-114.1525	NAV-GPS	3056	175
239392	48.1678	-114.0315	NAV-GPS	3257	220
239557	48.2402	-114.2472	NAV-GPS	2931	128
239589	48.2292	-114.1489	NAV-GPS	3005	260
239590	48.2289	-114.1489	NAV-GPS	3006	260
240256	48.1848	-114.0849	NAV-GPS	3044	200
240258	48.2514	-114.1388	NAV-GPS	3041	215
240260	48.2514	-114.1384	NAV-GPS	3038	193
240372	48.2537	-114.2377	NAV-GPS	2938	218
240843	48.3104	-114.1567	NAV-GPS	3058	200
240844	48.3099	-114.1563	NAV-GPS	3055	200
241511	48.1669	-114.0919	NAV-GPS	3066	321
241547	48.3218	-114.1789	TRS-SEC	3065	241
241710	48.3104	-114.1567	NAV-GPS	3058	200
241711	48.3099	-114.1563	NAV-GPS	3055	200
241994	48.3264	-114.1642	NAV-GPS	3070	152
242066	48.1950	-114.1625	TRS-SEC	2968	377
242093	48.2249	-114.1055	NAV-GPS	3061	160
242282	48.1847	-114.1028	NAV-GPS	2960	117
242297	48.1965	-114.0721	NAV-GPS	3188	200
242591	48.3022	-114.1500	NAV-GPS	3048	396
242592	48.3022	-114.1557	NAV-GPS	3046	78
242593	48.1690	-114.1333	NAV-GPS	2905	120
242614	48.2500	-114.1625	NAV-GPS	3013	253
242679	48.2513	-114.1462	NAV-GPS	3044	158
242680	48.1753	-114.0298	NAV-GPS	3361	280
242682	48.1718	-114.0380	NAV-GPS	3271	160
242978	48.1886	-114.0778	NAV-GPS	3066	1122
243241	48.2761	-114.1925	NAV-GPS	3059	247
243856	48.2368	-114.1585	NAV-GPS	2998	400
243857	48.2363	-114.1568	NAV-GPS	2998	400
243863	48.1595	-114.0094	NAV-GPS	3268	160
244079	48.3519	-114.2228	NAV-GPS	2987	183
244208	48.3573	-114.1300	NAV-GPS	3109	385
244505	48.2756	-114.1370	NAV-GPS	3024	600

Appendix E—*Continued*.

GWIC ID	Latitude	Longitude	Geo Method	Ground Surface Altitude (ft, amsl)	Depth (ft)
244618	48.1678	-114.1094	NAV-GPS	2978	200
244711	48.1414	-114.1452	NAV-GPS	2905	620
244906	48.2103	-114.1581	NAV-GPS	2974	241
245273	48.1532	-114.0653	NAV-GPS	3074	260
245445	48.2017	-114.0904	NAV-GPS	3011	185
245557	48.2901	-114.1625	NAV-GPS	3054	180
245558	48.3267	-114.1659	NAV-GPS	3074	255
245559	48.3497	-114.1426	NAV-GPS	3079	380
245773	48.1967	-114.0955	NAV-GPS	2985	100
246396	48.3020	-114.1463	NAV-GPS	3046	580
246710	48.2888	-114.1461	NAV-GPS	3053	120
247674	48.2371	-114.1196	NAV-GPS	3070	369
247886	48.2105	-114.2013	NAV-GPS	2935	173
248333	48.2599	-114.1599	NAV-GPS	3045	80
248537	48.2486	-114.1653	NAV-GPS	3016	234
249238	48.3365	-114.2342	NAV-GPS	2980	169
249242	48.2266	-114.1561	SUR-GPS	2988	234
249300	48.2826	-114.1560	NAV-GPS	3134	240
249552	48.1550	-114.2017	SUR-GPS	2905	750
249704	48.3546	-114.1998	NAV-GPS	3040	160
250059	48.3385	-114.1617	NAV-GPS	3069	200
250060	48.3392	-114.1630	NAV-GPS	3067	240
250548	48.1843	-114.0709	NAV-GPS	3147	800
251533	48.3139	-114.1480	TRS-SEC	3050	509
251545	48.3366	-114.1637	NAV-GPS	3076	200
252585	48.1848	-114.1034	NAV-GPS	2990	158
252617	48.2061	-114.0927	TRS-SEC	3019	200
253686	48.2440	-114.1235	NAV-GPS	3012	115
253827	48.2273	-114.1113	NAV-GPS	3065	140
253838	48.2006	-114.0792	NAV-GPS	3110	360
254252	48.1825	-114.0986	NAV-GPS	2961	120
254835	48.3579	-114.1753	NAV-GPS	3014	80
255030	48.2200	-114.1232	NAV-GPS	3053	310
255908	48.1500	-114.0416	SUR-GPS	3138	348
256263	48.2411	-114.1178	NAV-GPS	3015	58
256464	48.2716	-114.1246	NAV-GPS	3110	720
257046	48.2301	-114.1095	NAV-GPS	3088	220
257290	48.1738	-114.0880	NAV-GPS	3063	170
257784	48.1559	-114.2744	NAV-GPS	2906	220
258145	48.2147	-114.1467	NAV-GPS	2971	198
258308	48.2616	-114.1599	MAP	3044	56

Appendix E—*Continued.*

GWIC ID	Latitude	Longitude	Geo Method	Ground Surface Altitude (ft, amsl)	Depth (ft)
258729	48.1394	-114.2736	NAV-GPS	2920	484
259246	48.2083	-114.0791	NAV-GPS	3143	188
260131	48.1675	-114.1519	NAV-GPS	2902	357
262174	48.3301	-114.1978	NAV-GPS	3050	200
262175	48.2662	-114.1997	NAV-GPS	3030	180
262176	48.3494	-114.1581	NAV-GPS	3083	205
262680	48.1839	-114.0713	TRS-SEC	3100	883
264162	48.2727	-114.1372	MAP	3026	43
265586	48.3604	-114.1262	NAV-GPS	3256	465
268208	48.3218	-114.1898	TRS-SEC	3143	300
271370	48.2919	-114.1748	NAV-GPS	3075	218
271371	48.3025	-114.1855	NAV-GPS	3076	227
271372	48.2942	-114.1980	NAV-GPS	3047	153
274654	48.2564	-114.2201	TRS-SEC	2935	237
275914	48.3544	-114.1784	NAV-GPS	3085	180
276577	48.2360	-114.1209	MAP	3073	305
276840	48.3404	-114.1739	NAV-GPS	3073	179
276874	48.2014	-114.1322	NAV-GPS	3007	212
277927	48.2042	-114.1977	NAV-GPS	2927	238
278159	48.2317	-114.1199	NAV-GPS	3072	219
278187	48.1532	-114.1059	MAP	3037	257
278712	48.3497	-114.1547	NAV-GPS	3070	226
279019	48.2064	-114.1141	TRS-SEC	2977	240
279308	48.1520	-114.2102	SUR-GPS	2906	780
281275	48.2821	-114.2072	NAV-GPS	3048	189
281276	48.2010	-114.1959	NAV-GPS	2969	276
281729	48.2105	-114.1149	NAV-GPS	3010	275
281779	48.1716	-114.1674	SUR-GPS	2907	222
281848	48.3297	-114.1662	NAV-GPS	3079	265
282334	48.1987	-114.0697	MAP	3258	240
282629	48.1938	-114.1218	SUR-GPS	2934	215
283261	48.1794	-114.0688	MAP	3182	937
284182	48.1519	-114.2034	NAV-GPS	2905	760
284671	48.3022	-114.1486	MAP	3050	501
284856	48.2675	-114.1305	TRS-SEC	3020	420
285037	48.1419	-114.0664	NAV-GPS	3135	200
285412	48.3627	-114.1377	NAV-GPS	3073	118
286001	48.2185	-114.1196	MAP	3049	205
286069	48.1717	-114.1317	NAV-GPS	2926	144
286762	48.2950	-114.1752	NAV-GPS	3060	178
286781	48.2366	-114.1989	NAV-GPS	2987	200

Appendix E—*Continued*.

GWIC ID	Latitude	Longitude	Geo Method	Ground Surface Altitude (ft, amsl)	Depth (ft)
287113	48.2222	-114.1040	NAV-GPS	3046	115
287177	48.2093	-114.0787	NAV-GPS	3145	200
288050	48.2072	-114.0824	NAV-GPS	3098	100
288266	48.3183	-114.1627	TRS-SEC	3064	240
288970	48.3077	-114.1521	TRS-SEC	3045	421
289963	48.1526	-114.0976	NAV-GPS	3057	265
290238	48.3444	-114.1604	MAP	3059	178
290360	48.2071	-114.0805	NAV-GPS	3117	560
291347	48.2882	-114.1786	NAV-GPS	3064	198
291819	48.2333	-114.1156	NAV-GPS	3075	180
292084	48.1953	-114.1035	TRS-SEC	2995	240
292238	48.2416	-114.1181	NAV-GPS	3009	100
292239	48.1702	-114.0387	MAP	3257	178
292473	48.1854	-114.2862	NAV-GPS	2950	320
292871	48.2955	-114.1545	NAV-GPS	3054	138
292900	48.1513	-114.1053	NAV-GPS	3023	118
292921	48.1363	-114.1411	NAV-GPS	2905	298
293209	48.3315	-114.1854	NAV-GPS	3071	200
293719	48.1897	-114.1416	NAV-GPS	2957	140
293982	48.3309	-114.1734	NAV-GPS	3073	152
293989	48.3375	-114.1720	NAV-GPS	3075	200
294121	48.2638	-114.1963	NAV-GPS	3012	80
294783	48.3261	-114.1811	NAV-GPS	3071	220
294949	48.1827	-114.0785	NAV-GPS	3087	231
295222	48.1823	-114.0826	NAV-GPS	3101	153
295542	48.2073	-114.1127	TRS-SEC	2981	240
295569	48.2368	-114.2085	NAV-GPS	2981	180
296370	48.2105	-114.1854	NAV-GPS	2960	280
296371	48.3283	-114.1463	NAV-GPS	3055	480
296586	48.2254	-114.1727	SUR-GPS	2982	137
296587	48.2254	-114.1712	SUR-GPS	2982	205
296748	48.2955	-114.2066	NAV-GPS	3044	150
296770	48.1330	-114.0931	NAV-GPS	3007	180
296820	48.3309	-114.1749	NAV-GPS	3073	138
296866	48.1766	-114.1696	NAV-GPS	2902	220
297465	48.2307	-114.1203	NAV-GPS	3071	158
298165	48.1921	-114.0927	NAV-GPS	2988	80
298166	48.1767	-114.0741	NAV-GPS	3104	320
298174	48.3164	-114.1886	NAV-GPS	3116	280
298925	48.3522	-114.1540	NAV-GPS	3083	220
298950	48.3595	-114.1585	MAP	3058	157

Appendix E—*Continued*. .

GWIC ID	Latitude	Longitude	Geo Method	Ground Surface Altitude (ft, amsl)	Depth (ft)
298952	48.1899	-114.1410	MAP	2958	160
299286	48.3011	-114.2102	TRS-SEC	3047	204
299755	48.3569	-114.1556	NAV-GPS	3086	240
299865	48.3399	-114.1446	NAV-GPS	3083	440
300199	48.3407	-114.1458	NAV-GPS	3092	329
300654	48.1648	-114.2782	SUR-GPS	2922	295
300696	48.2680	-114.1827	NAV-GPS	3039	220
300976	48.3442	-114.1622	NAV-GPS	3058	180
301129	48.2010	-114.1604	NAV-GPS	2970	260
301158	48.3479	-114.1412	MAP	3075	405
301628	48.3456	-114.1510	NAV-GPS	3066	240
302090	48.1865	-114.0768	NAV-GPS	3094	259
302161	48.3122	-114.1684	NAV-GPS	3061	176
302335	48.2220	-114.0791	TRS-SEC	3200	323
302608	48.3546	-114.1903	MAP	3075	136
302787	48.2408	-114.1005	MAP	3120	350
302837	48.3329	-114.1520	TRS-SEC	3070	440
303448	48.3551	-114.1551	NAV-GPS	3080	236
303504	48.2109	-114.0761	NAV-GPS	3209	199
303513	48.1379	-114.0345	NAV-GPS	3050	120
303516	48.3478	-114.1579	NAV-GPS	3080	225
303582	48.2326	-114.1203	NAV-GPS	3074	170
303583	48.2326	-114.1174	NAV-GPS	3077	180
303585	48.2690	-114.1737	NAV-GPS	3062	260
303586	48.2950	-114.1479	NAV-GPS	3040	120
303737	48.3097	-114.1765	NAV-GPS	3066	220
303927	48.1859	-114.1080	NAV-GPS	2956	47
304325	48.2912	-114.1869	TRS-SEC	3050	205
304509	48.2174	-114.2382	TRS-SEC	2995	303
304547	48.2189	-114.1706	NAV-GPS	2981	140
307344	48.1498	-114.1389	NAV-GPS	2908	320
308287	48.1280	-114.0590	NAV-GPS	3027	160
309486	48.3638	-114.2134	SUR-GPS	3056	290
310804	48.1200	-114.1245	NAV-GPS	2898	640
311657	48.2096	-114.2105	NAV-GPS	2932	220
890685	48.2545	-114.1902	MAP	2991	690

Note. amsl, above mean sea level.

APPENDIX F

MODEL CONSTRUCTION

Table F1. Drain and river conductance values.

Reach	Layer	Calibrated Conductance (ft^2/d)
Drain 1	1	362
Drain 2	1	164,655
Drain 3	1	1,159
Drain 41	4	100
Drain 42	4	135
Drain 43	4	19.5
Drain 44	4	1.24
Drain 45	4	78.7
Drain 46	4	4.03
Drain 47	4	0.19
River 1	1	102
River 2	1	68.2
River 3	1	4.77
River 4	1	237
River 5	1	419
River 6	1	457
River 7	1	621
River 8	1	467
River 9	1	704
River 10	1	240

Note. See figs. F11 and F12 for the locations of these reaches.
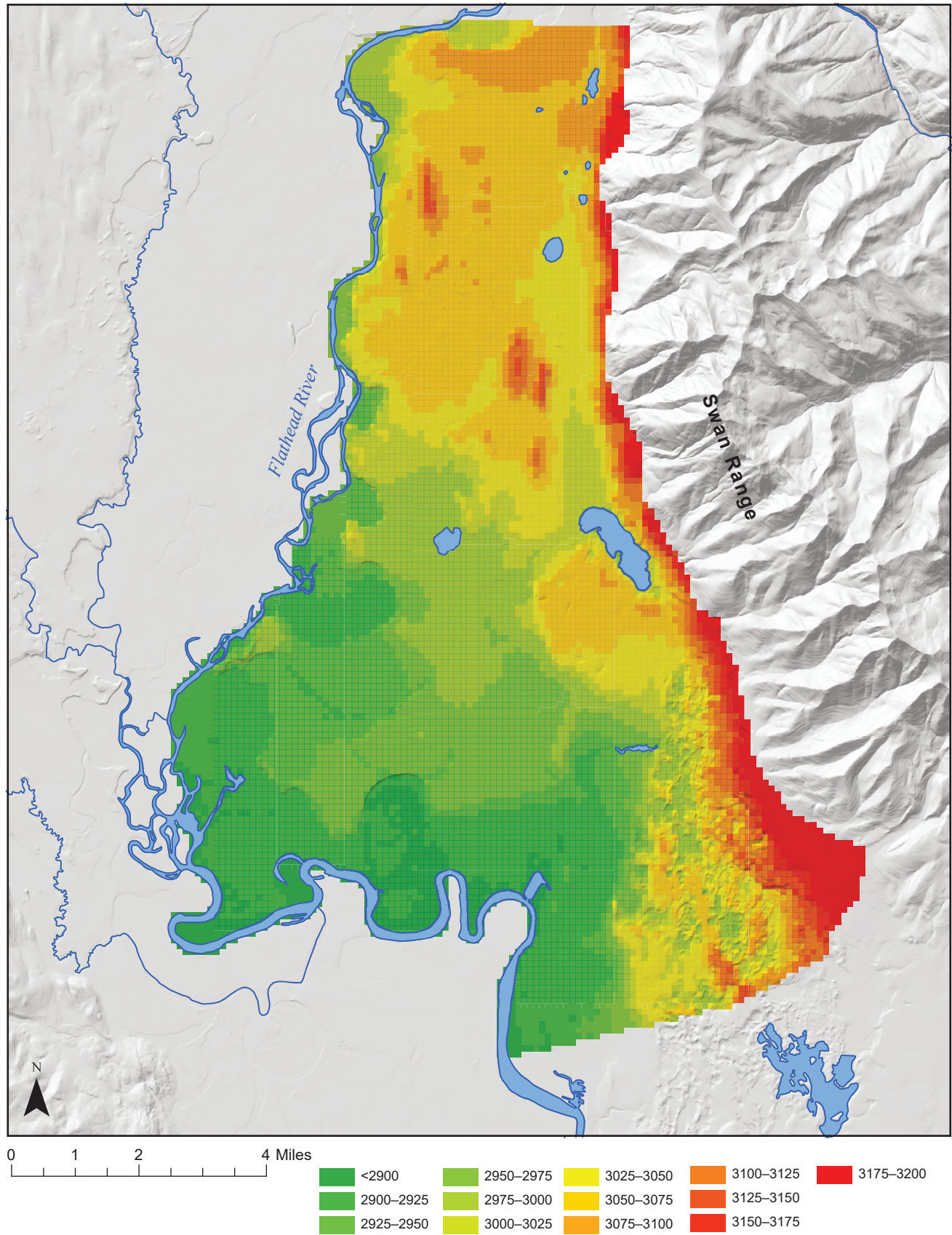
Figure F1. Surface elevations (ft-amsl) of the model grid, defined from LiDAR data.
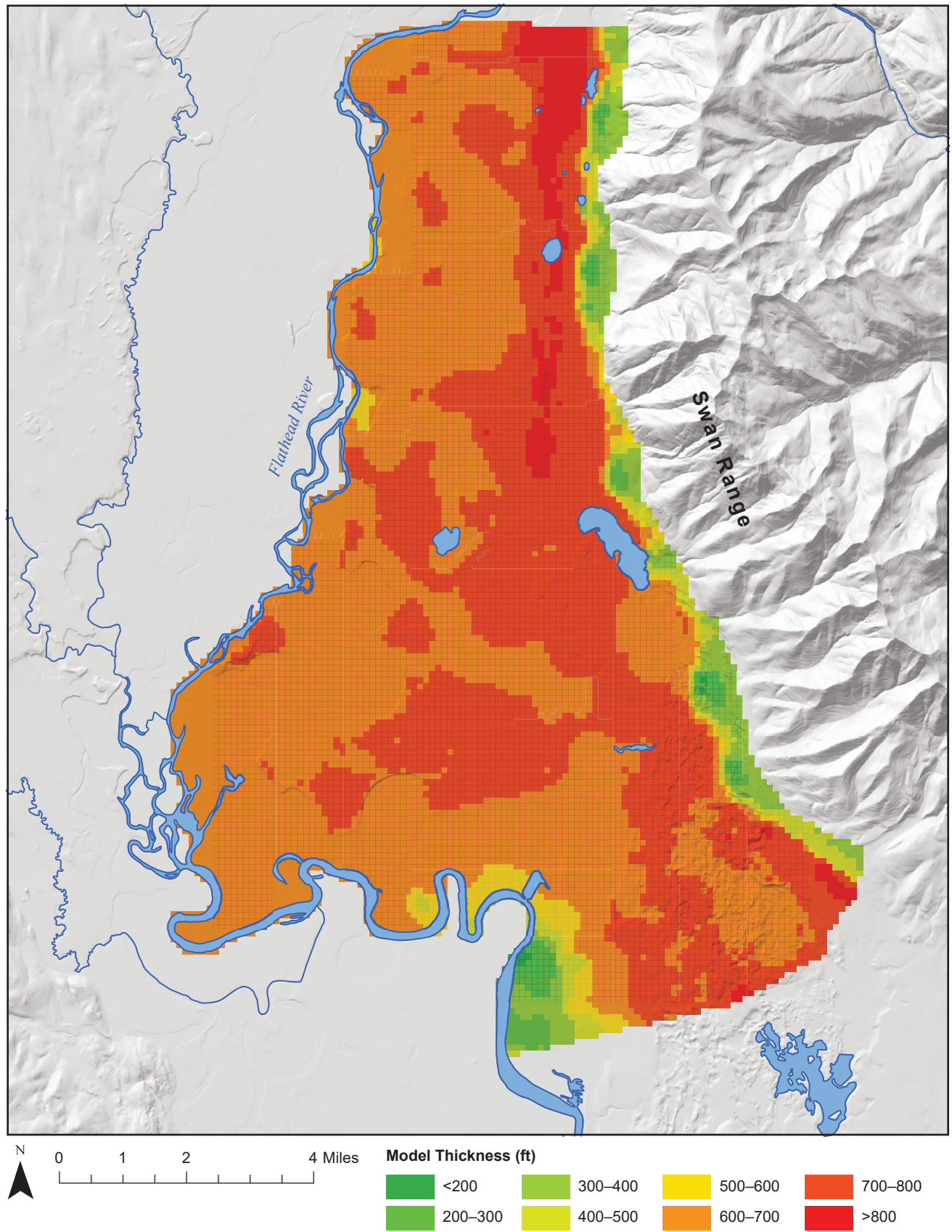
Figure F2. Total thickness of all modeled layers (ft).
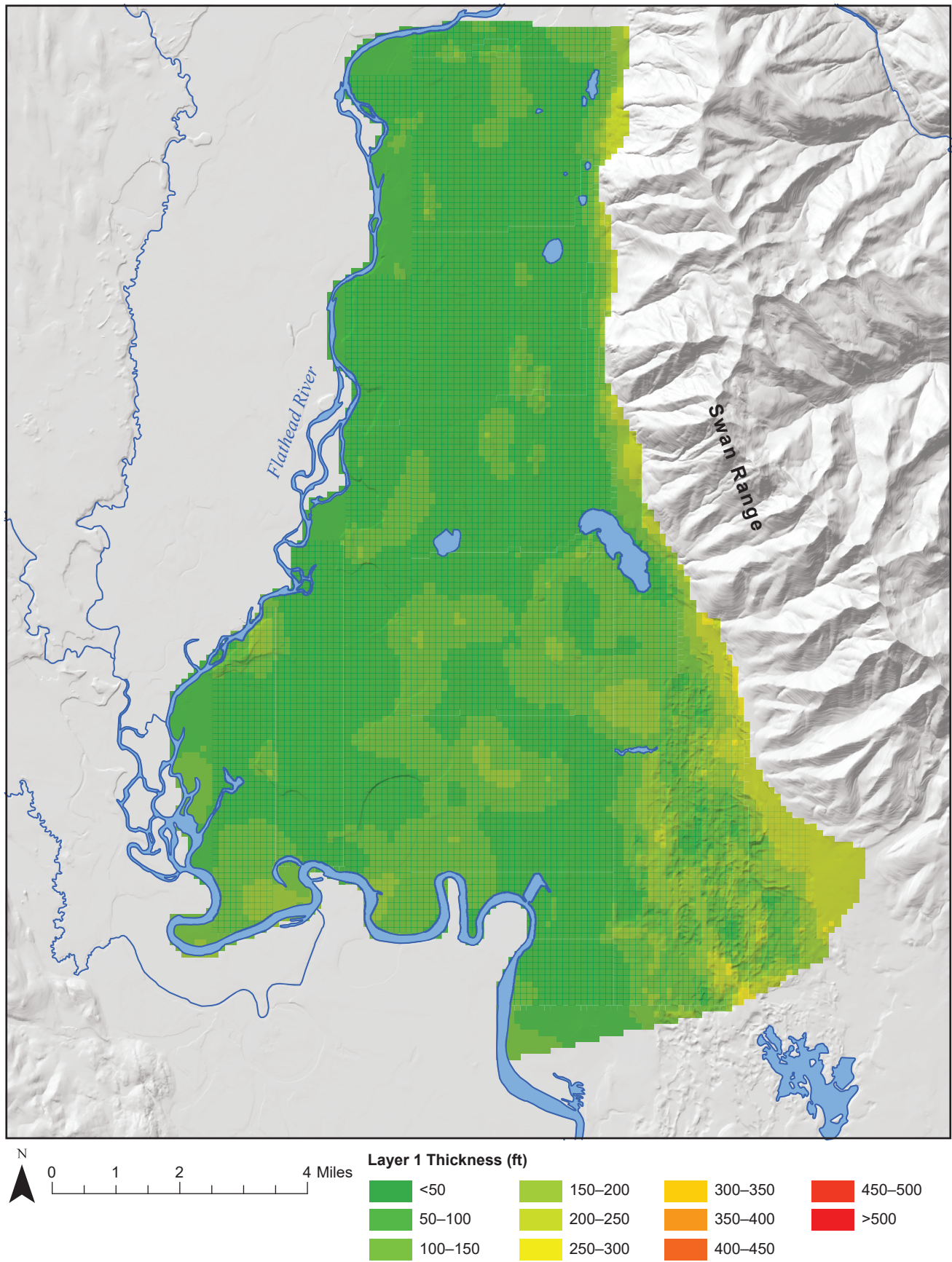
Figure F3. Model Layer 1 thickness (ft).
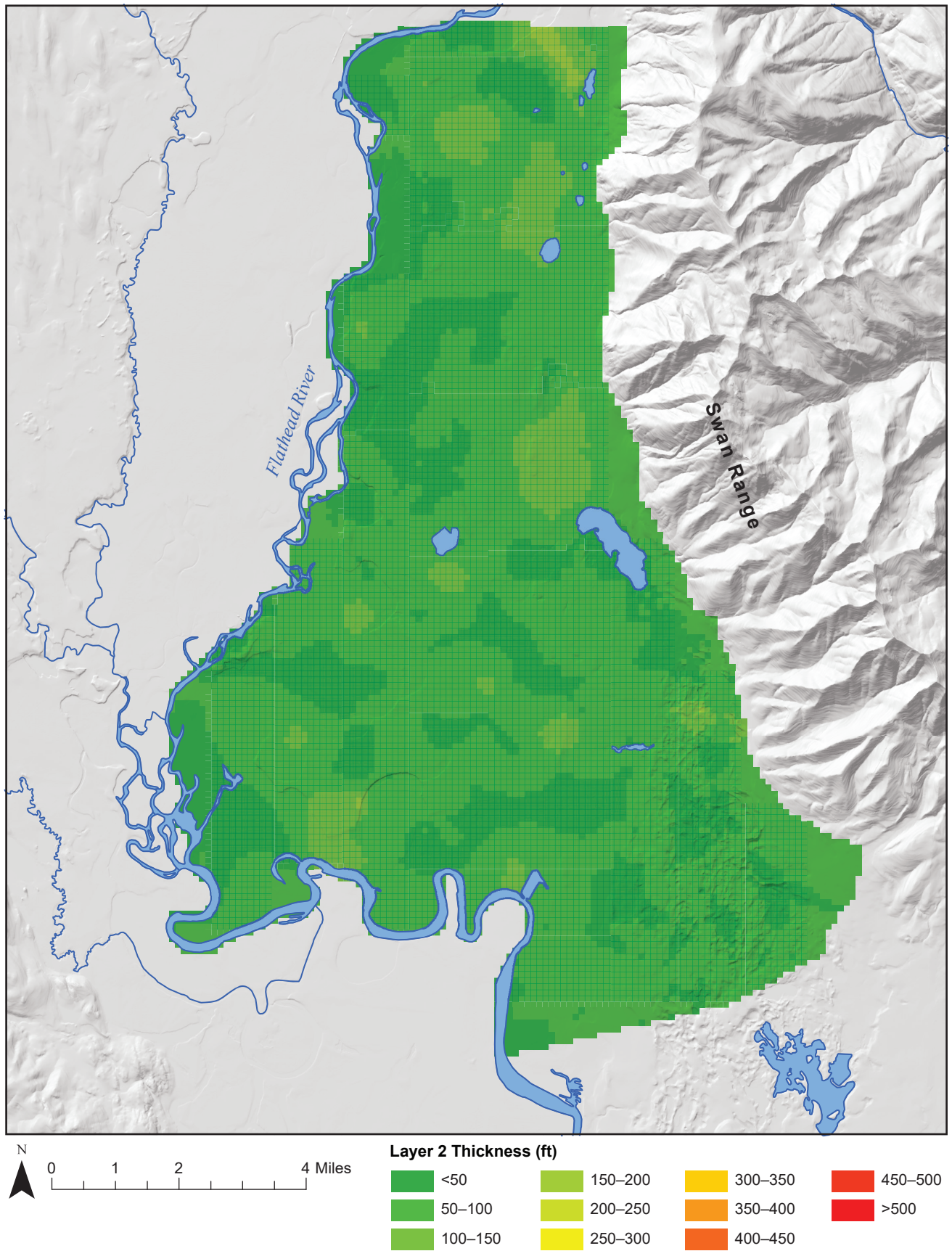
Figure F4. Model Layer 2 thickness (ft).
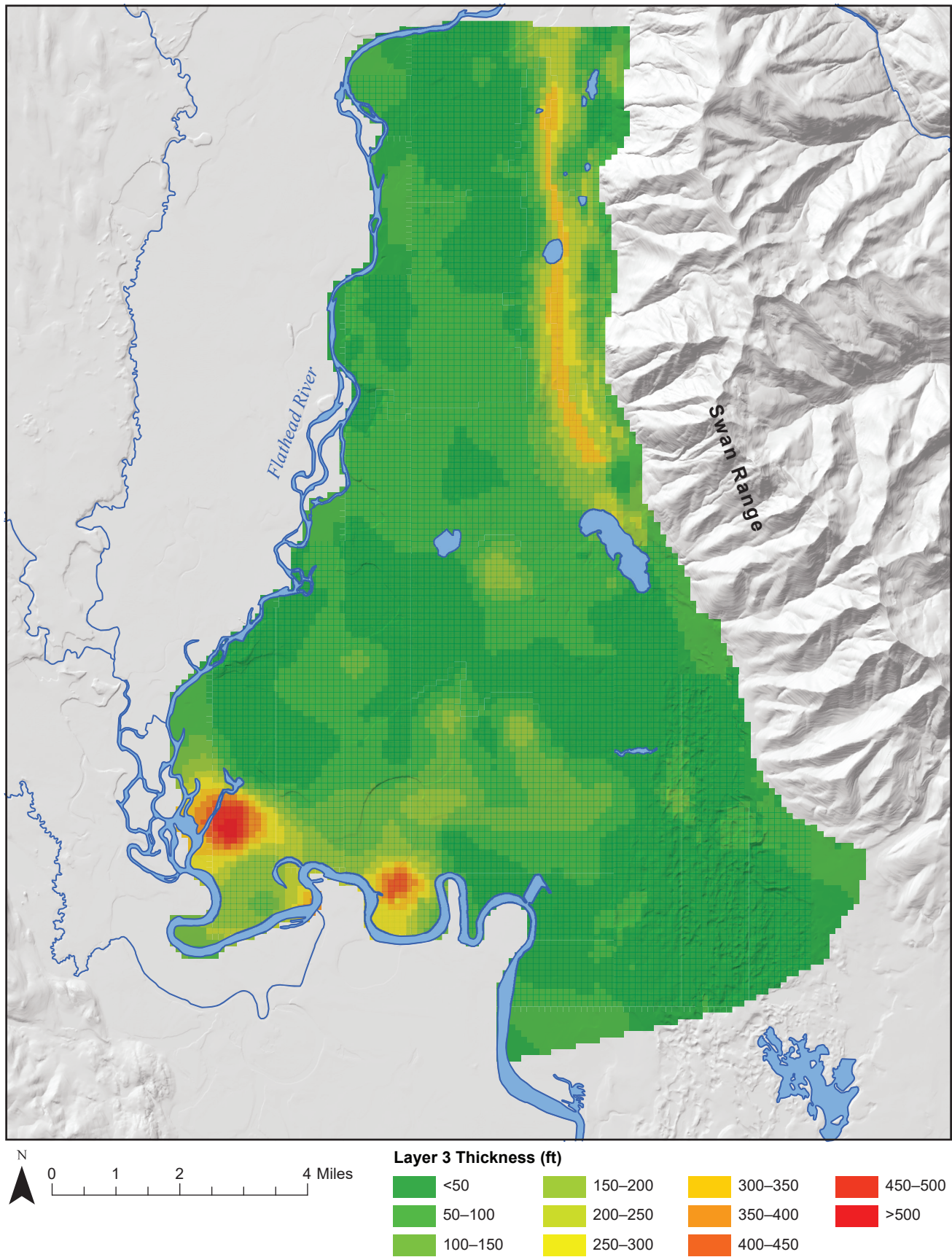
Figure F5. Model Layer 3 thickness (ft).

Layer 4 Thickness (ft)

<50	150–200	300–350	450–500
50–100	200–250	350–400	>500
100–150	250–300	400–450	
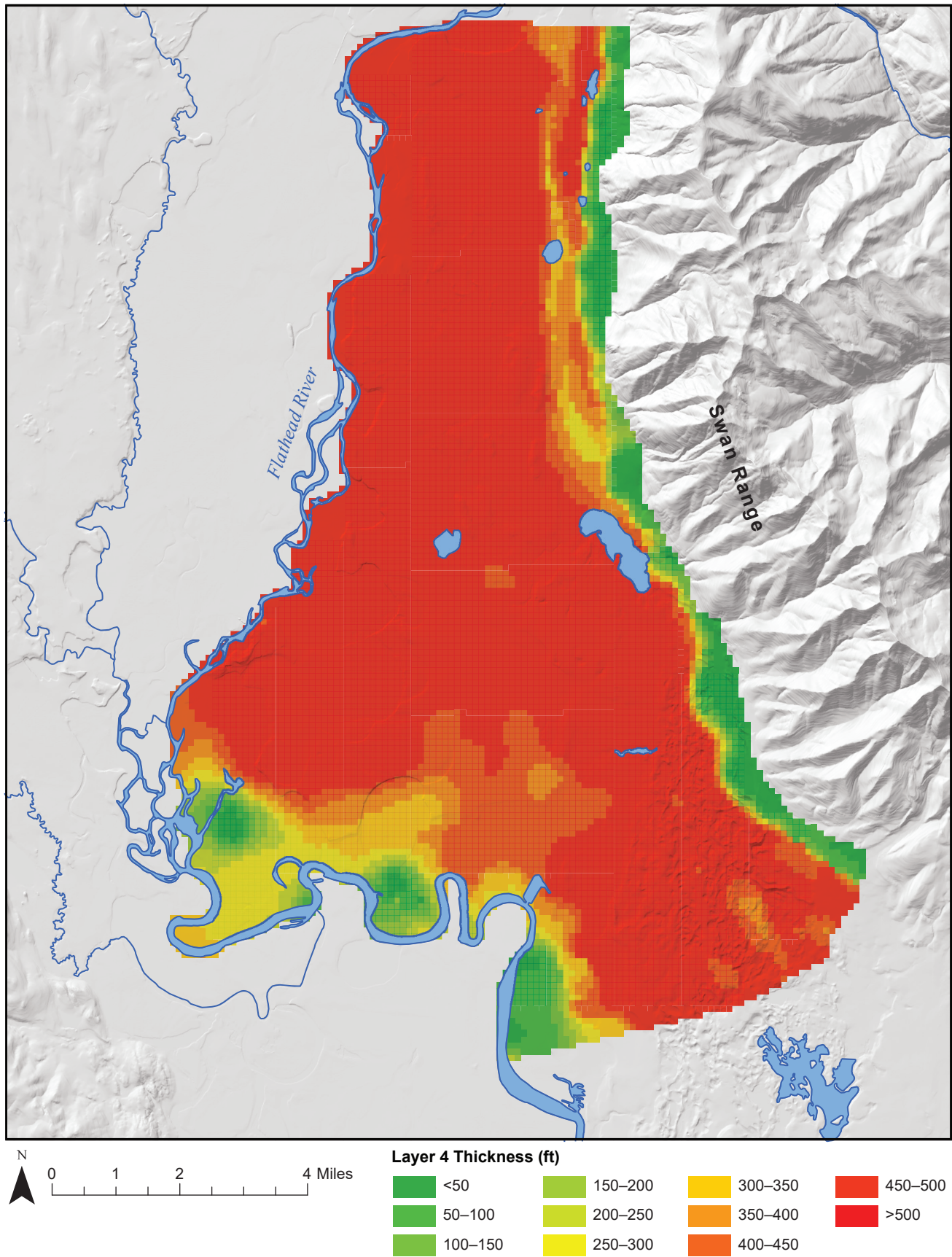
Figure F6. Model Layer 4 thickness (ft).
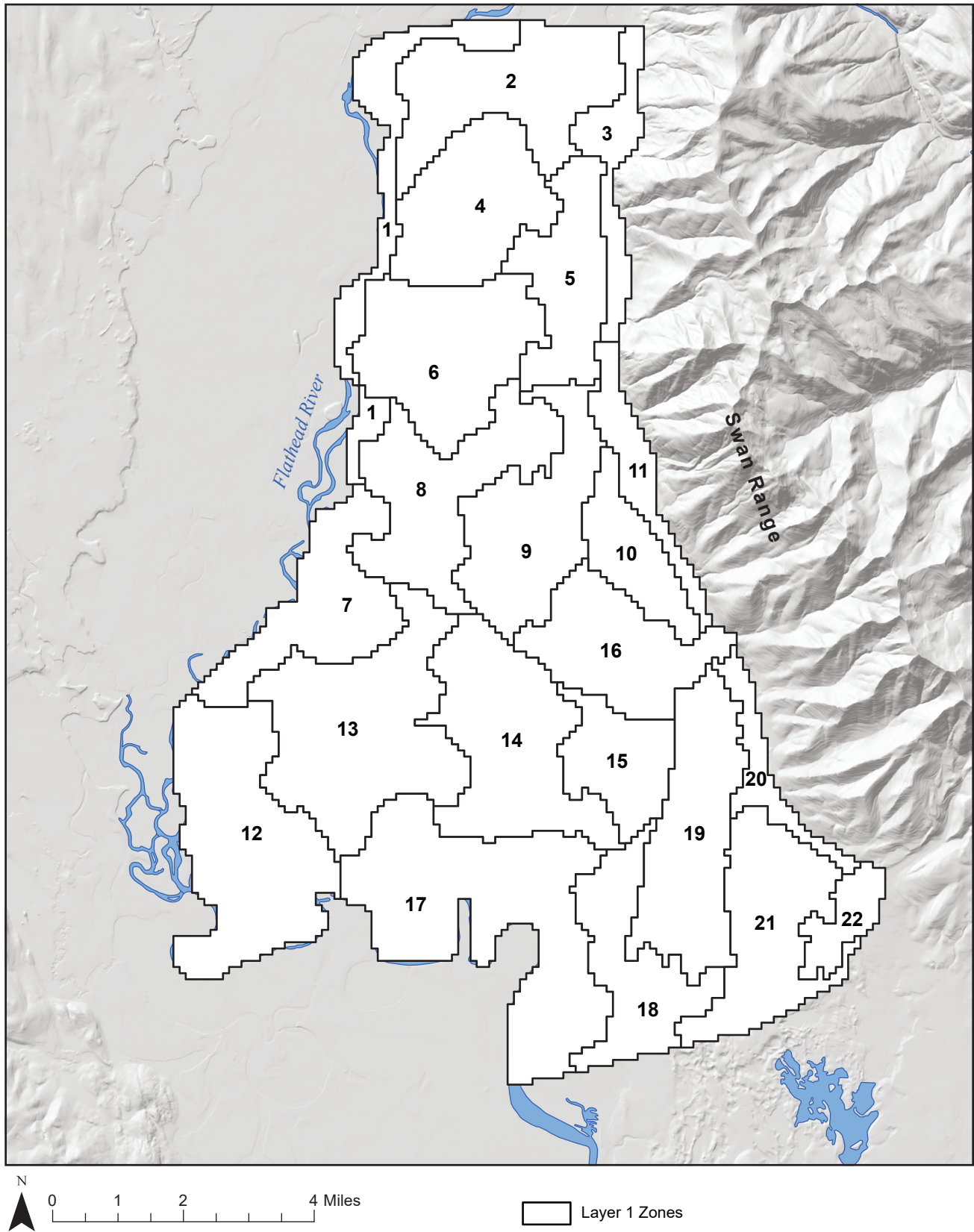
Figure F7. Zone IDs for Layer 1.
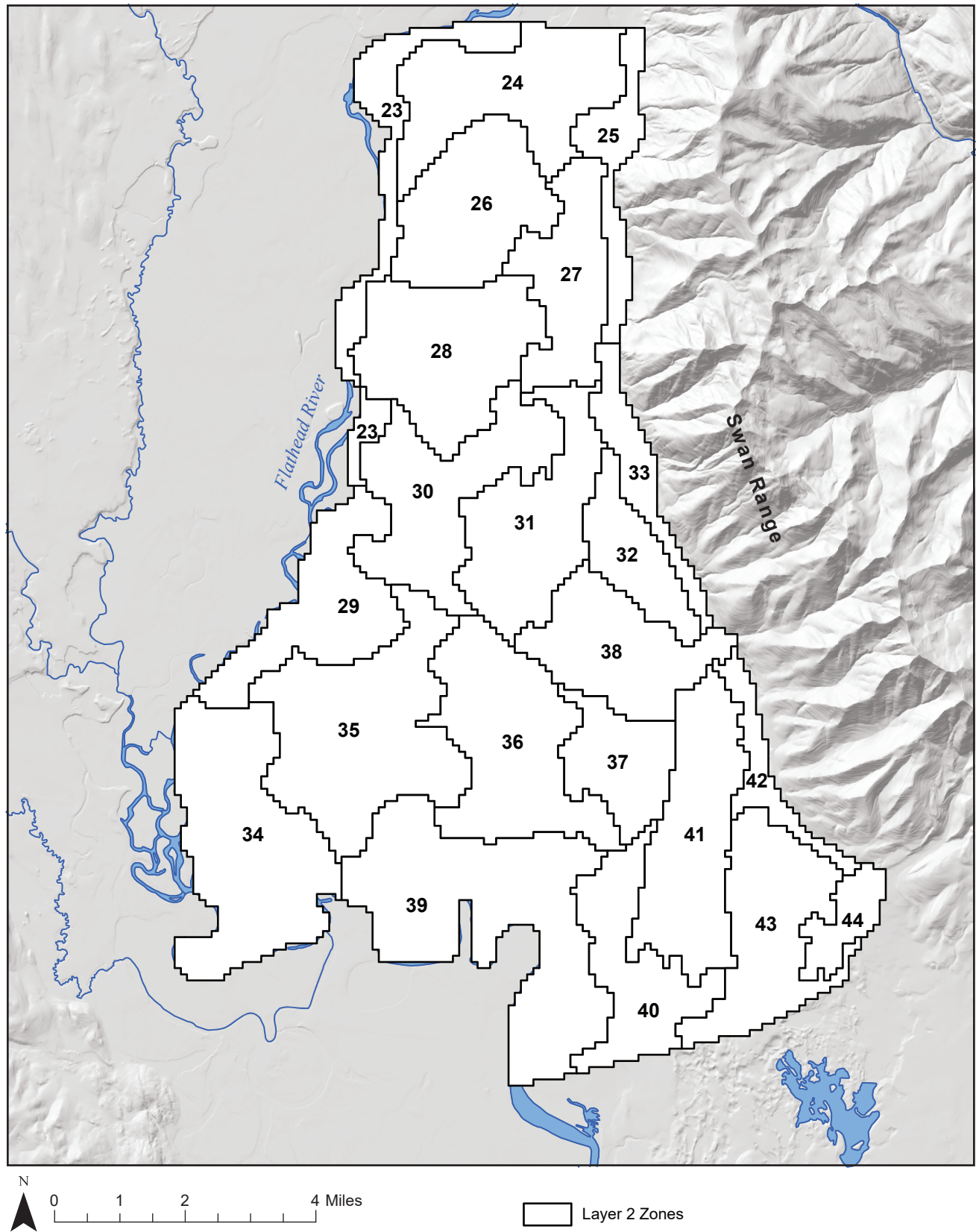
Figure F8. Zone IDs for Layer 2.
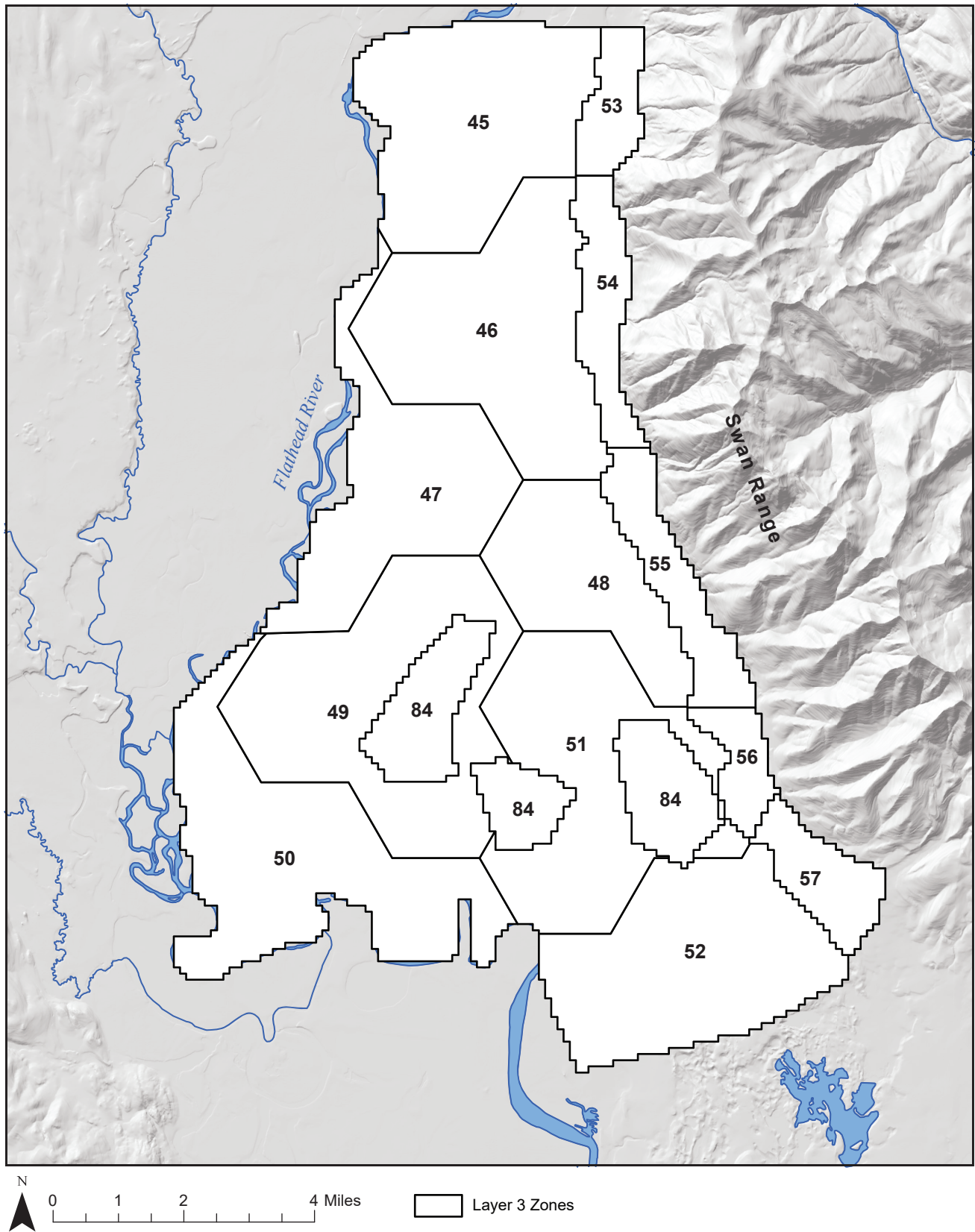
Figure F9. Zone IDs for Layer 3.
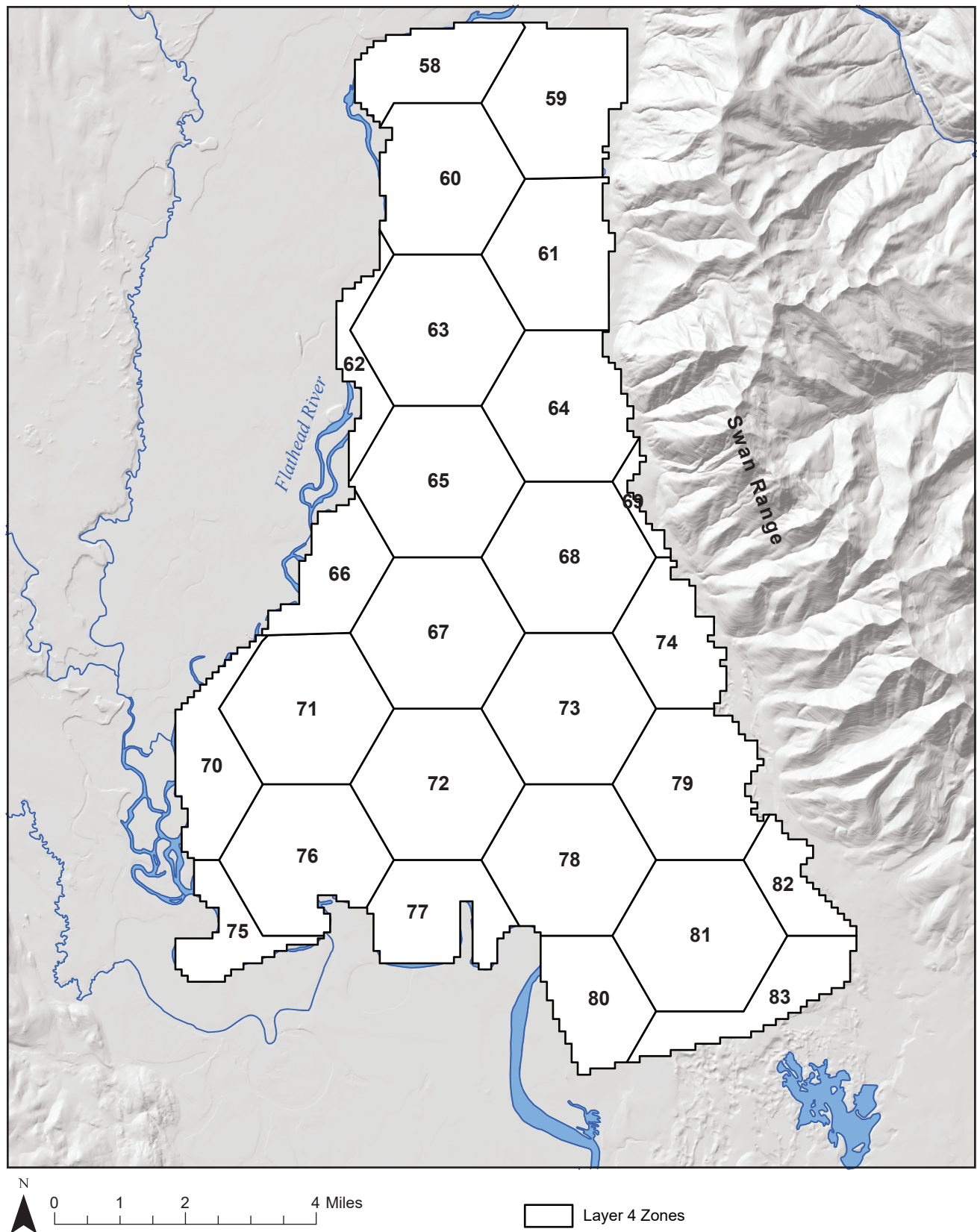
Figure F10. Zone IDs for Layer 4.
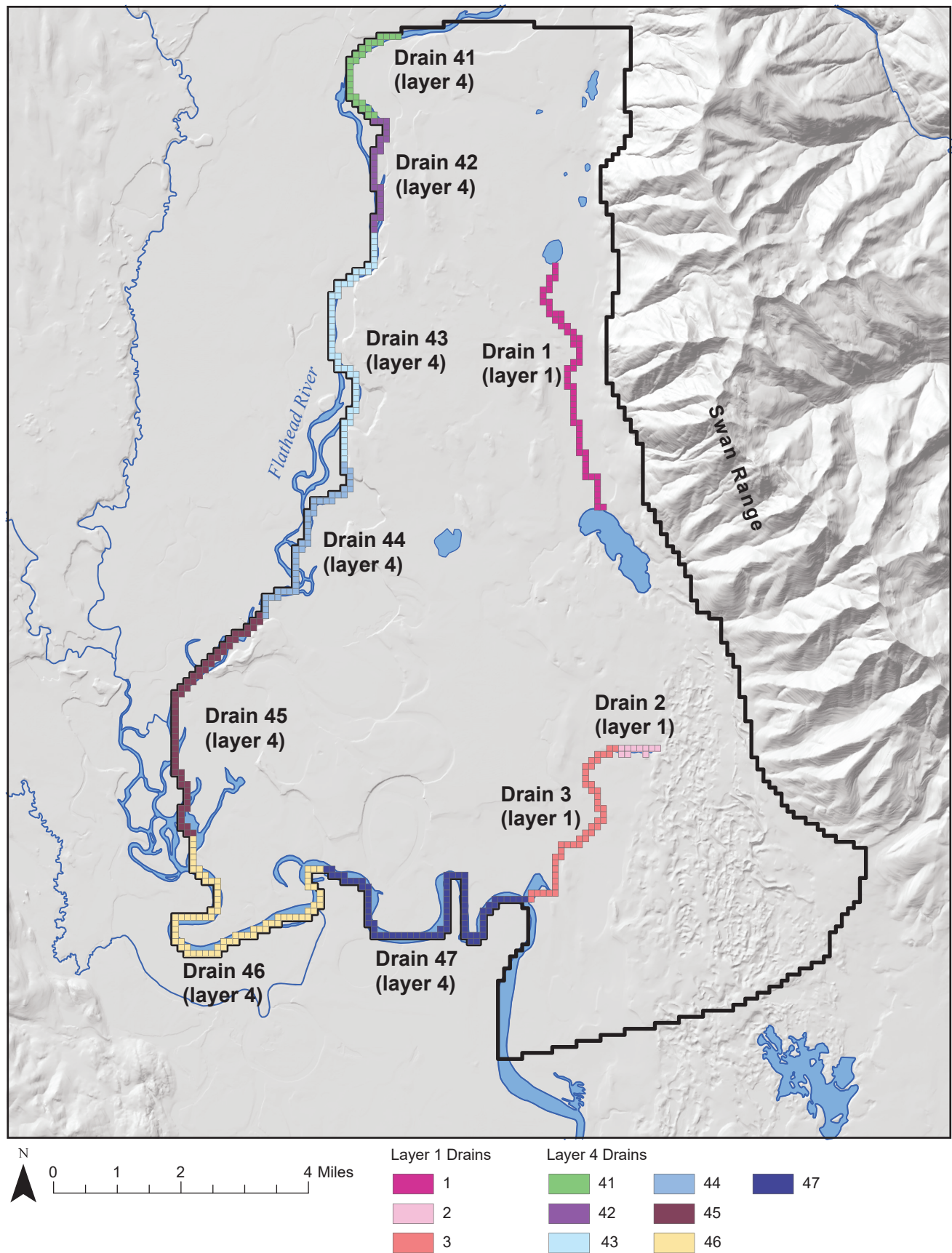
Figure F11. Drain reach numbering. See table F1 for conductance values.
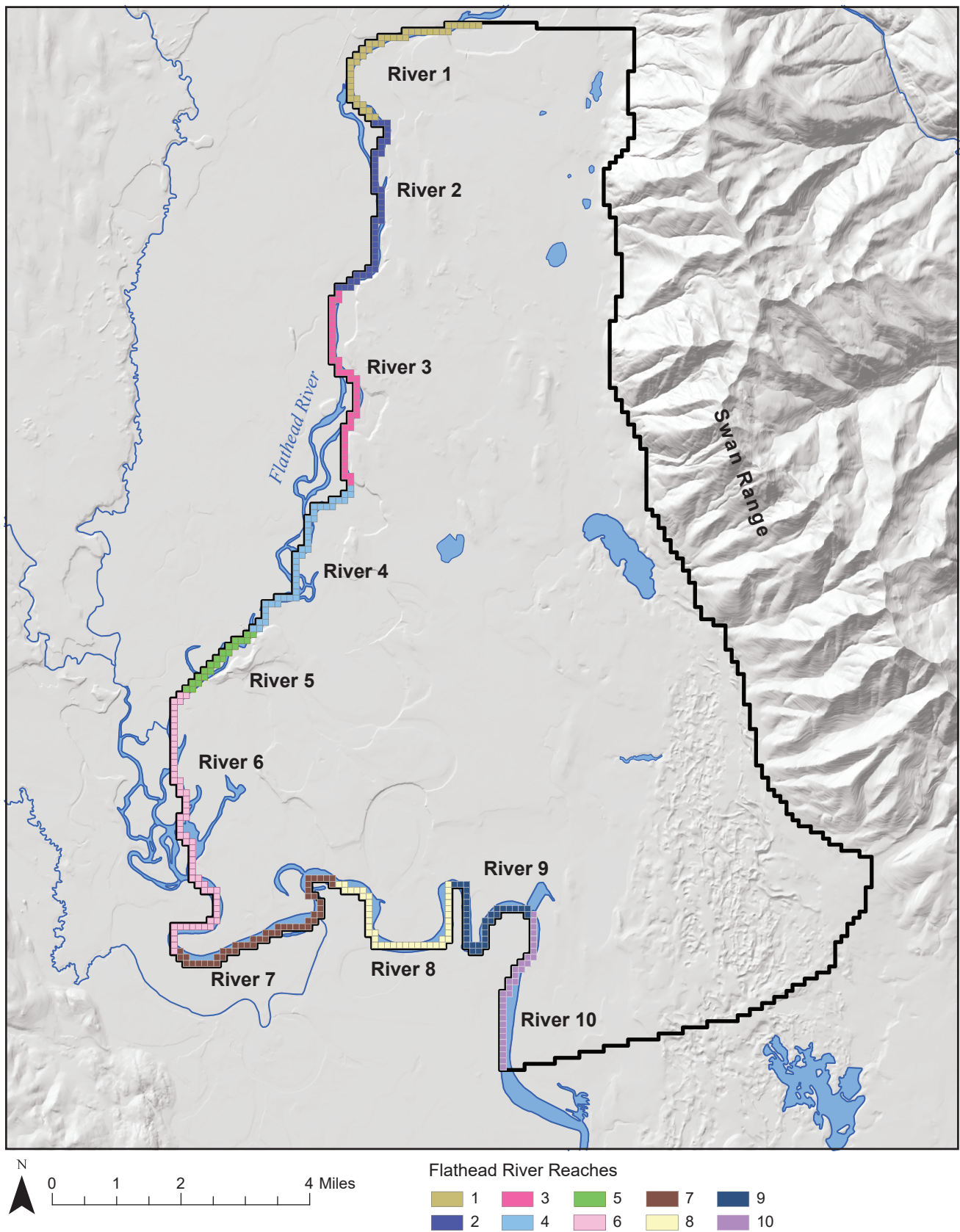
Figure F12. River reach numbering. See table F1 for conductance values.

APPENDIX G

STEADY-STATE MODEL CALIBRATION: RESIDUALS, POTENTIOMETRIC SURFACES, AND K DISTRIBUTIONS
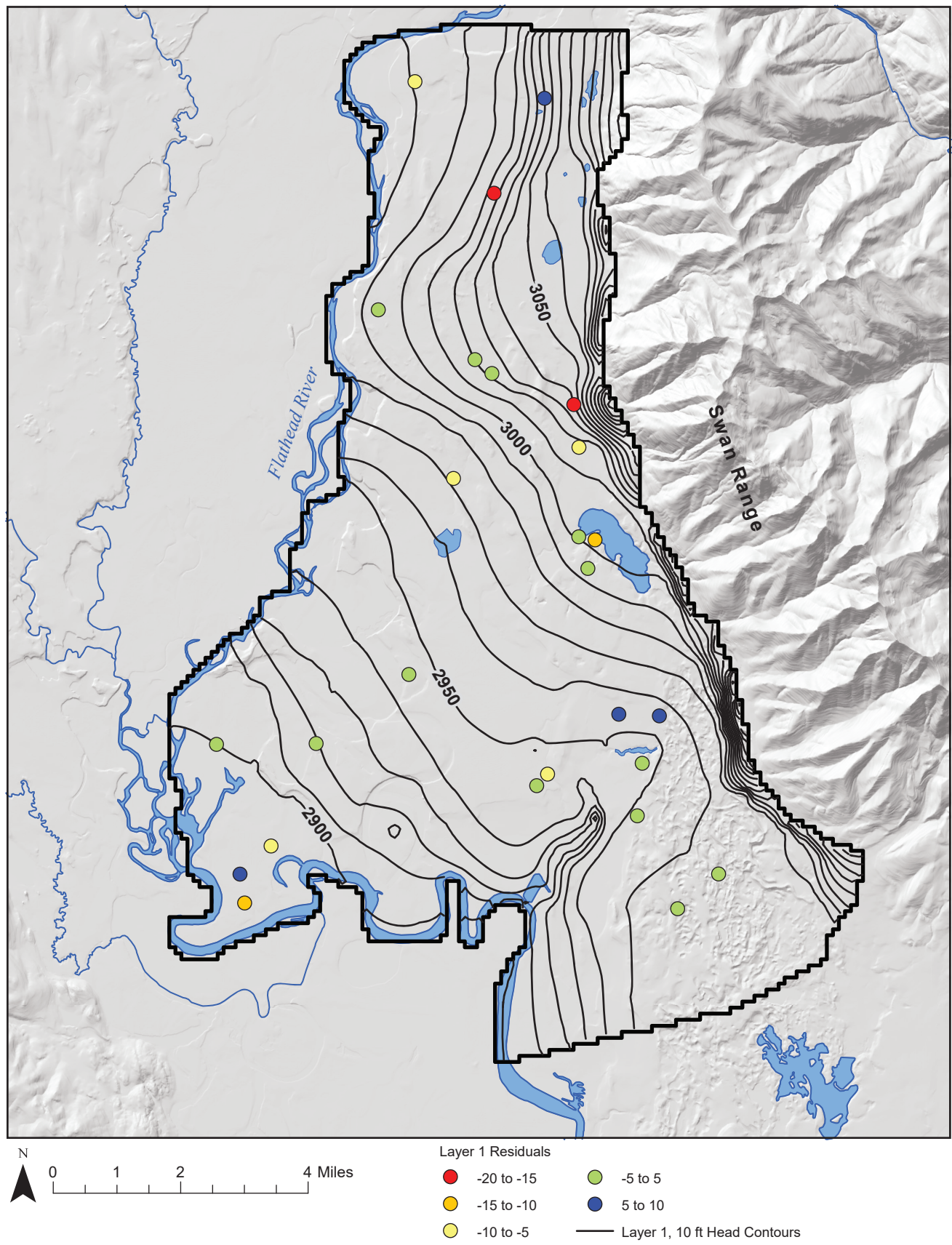
Figure G1. Modeled steady-state potentiometric surface (ft-amsl) for Layer 1 with head residuals (ft).
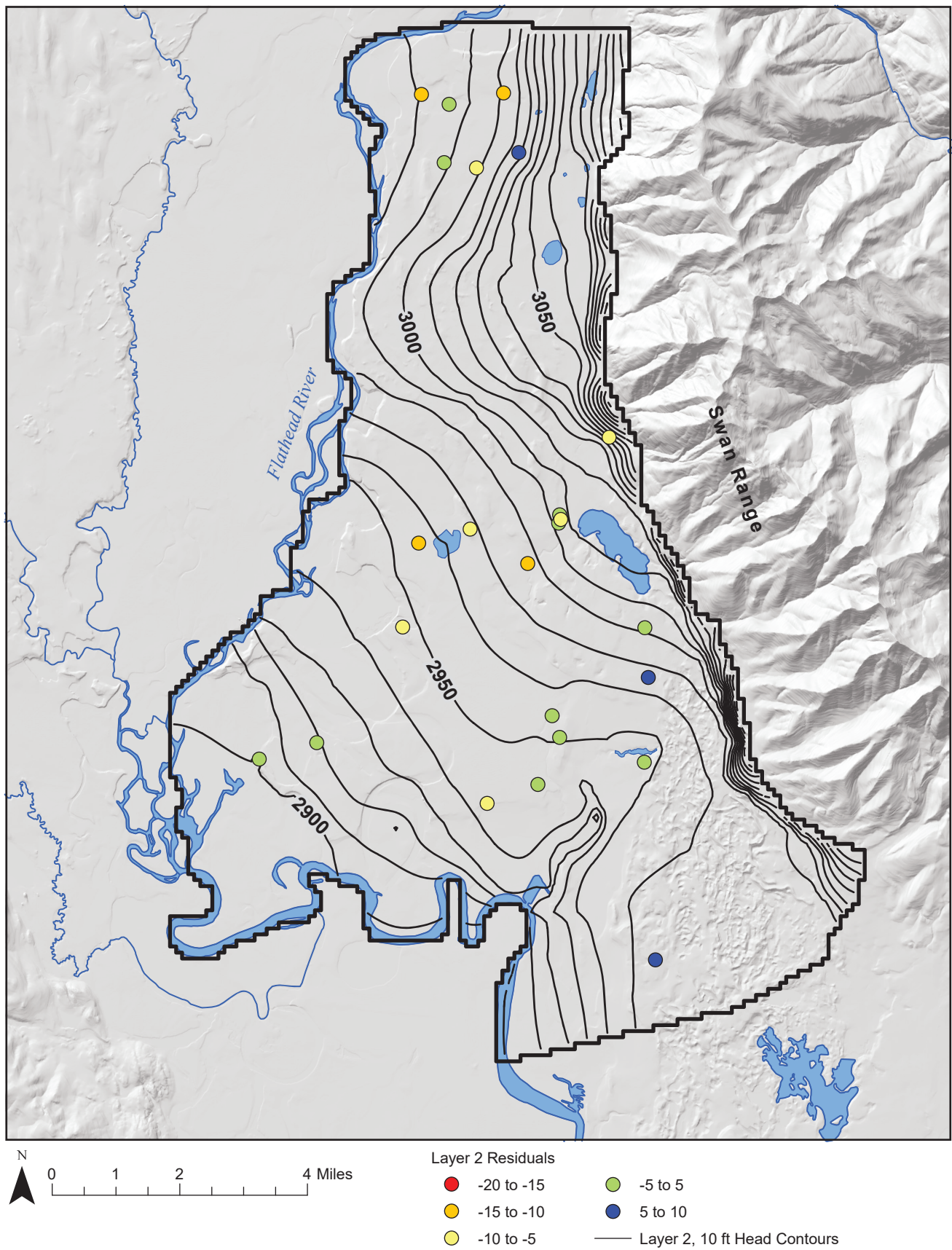
Figure G2. Modeled steady-state potentiometric surface (ft-amsl) for Layer 2 with head residuals (ft).
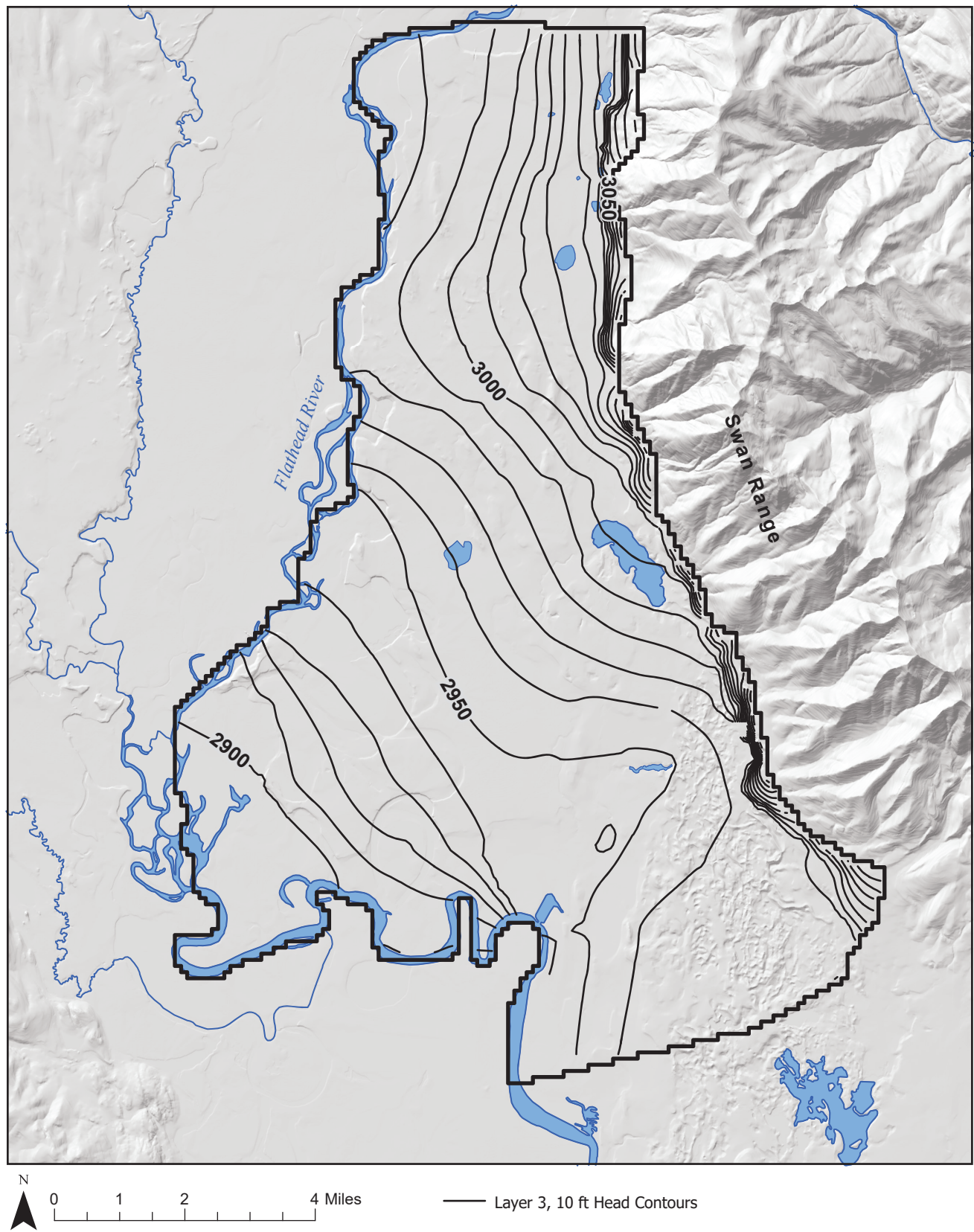
Figure G3. Modeled steady-state potentiometric surface (ft-amsl) for Layer 3. Note that no wells were monitored in this layer since it represents the confining layer.
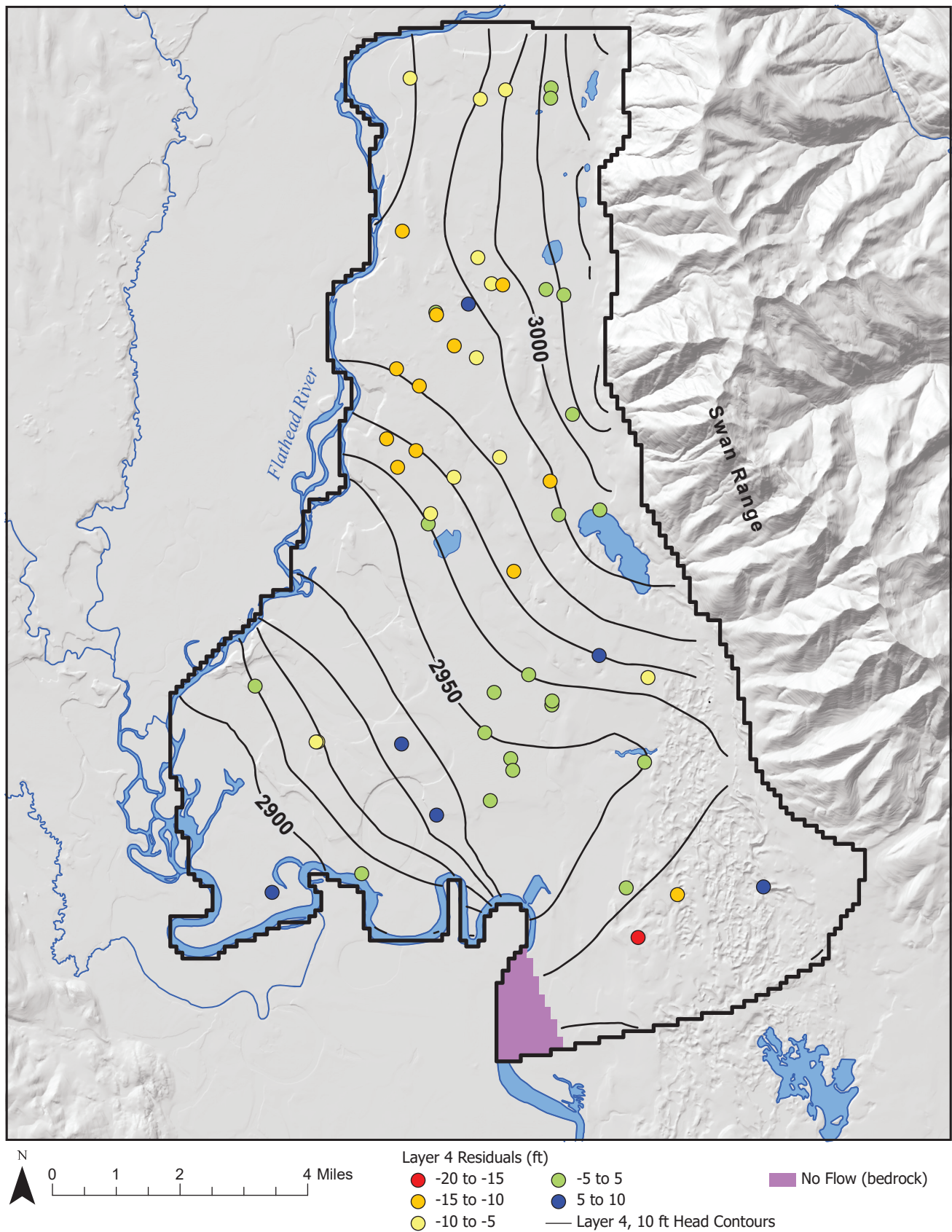
Figure G4. Modeled steady-state potentiometric surface (ft-amsl) for Layer 4 with head residuals (ft).
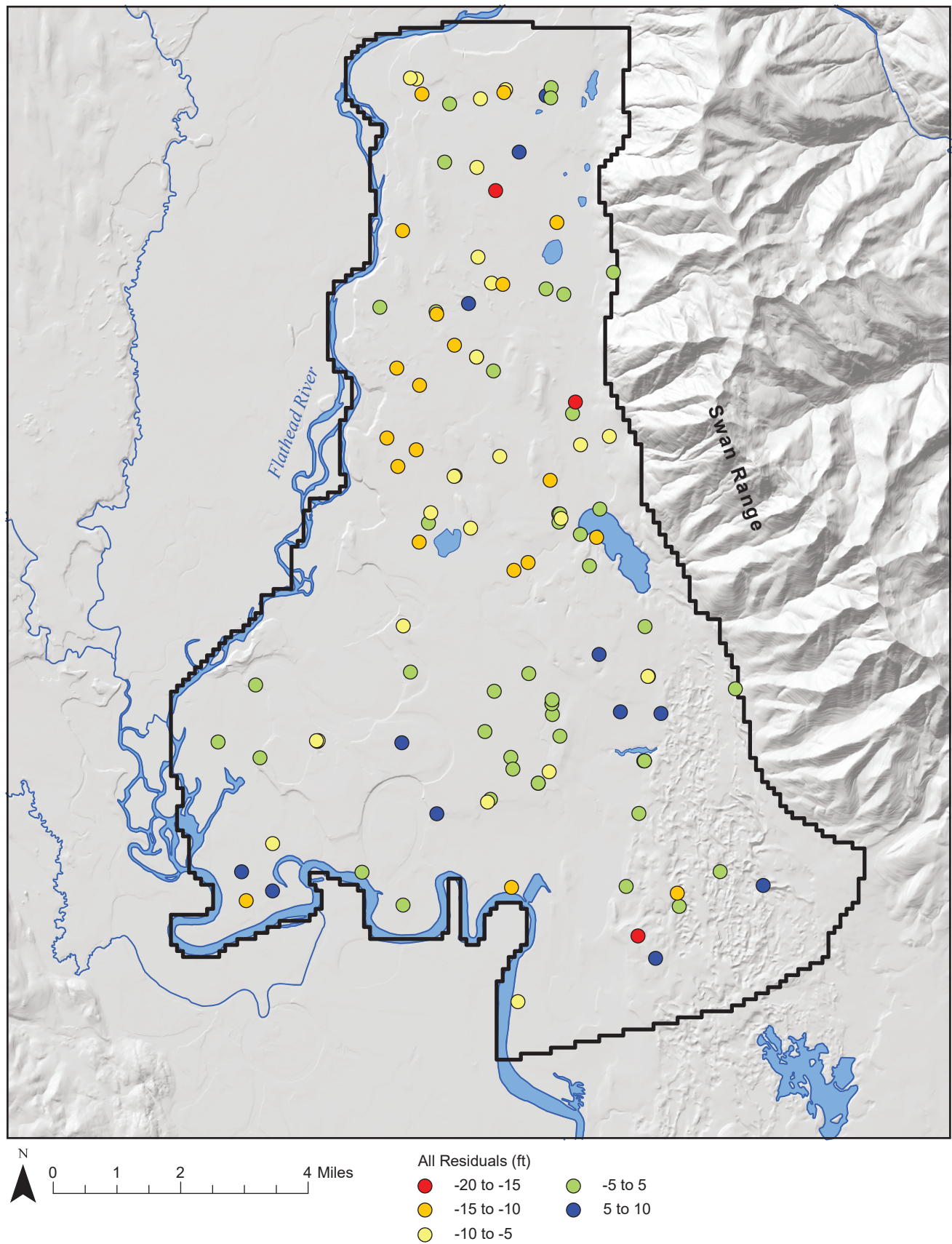
Figure G5. Modeled steady-state head residuals (ft) for all layers.
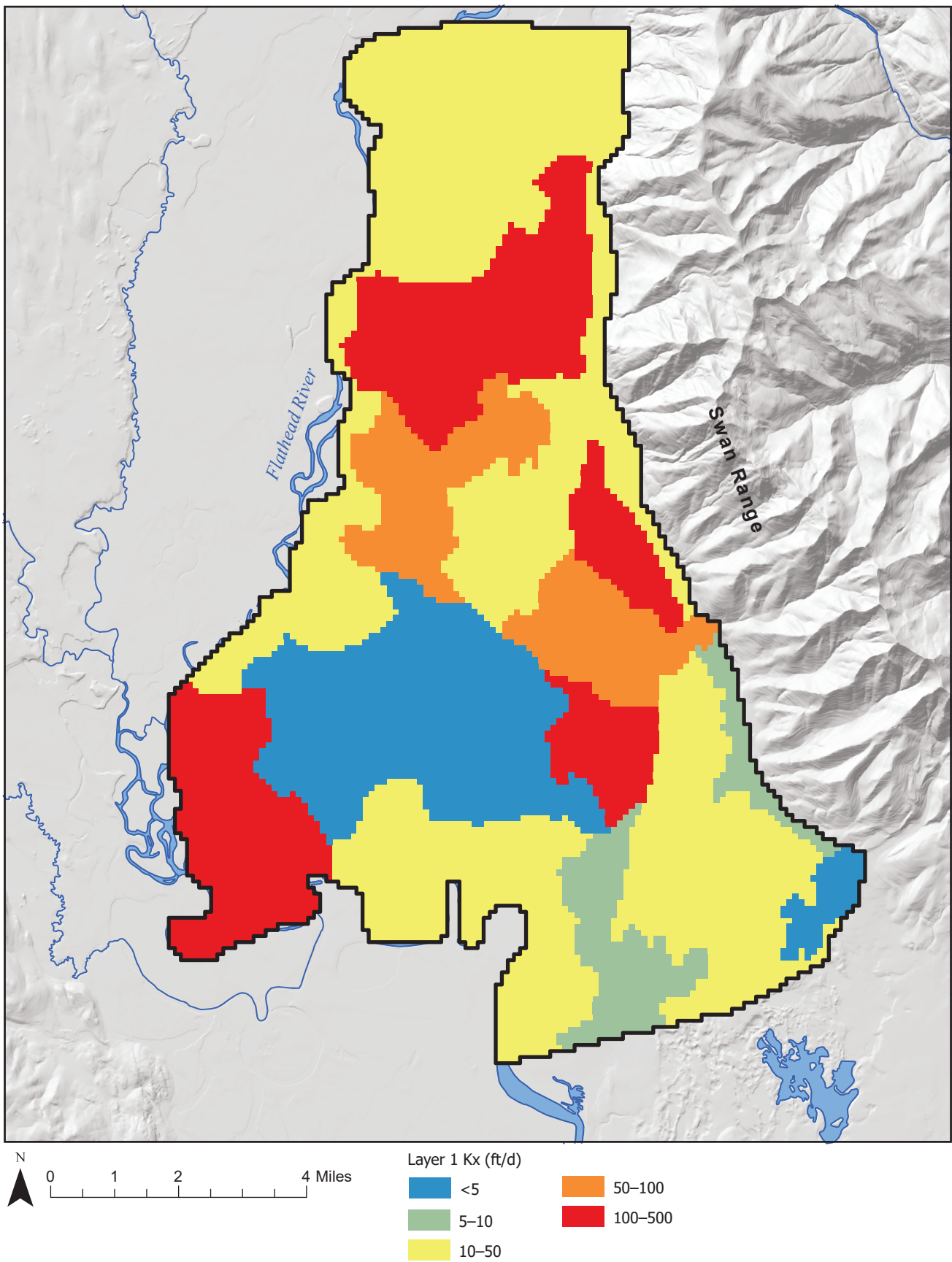
Figure G6. Horizontal K distribution in Layer 1 based on steady-state calibration.
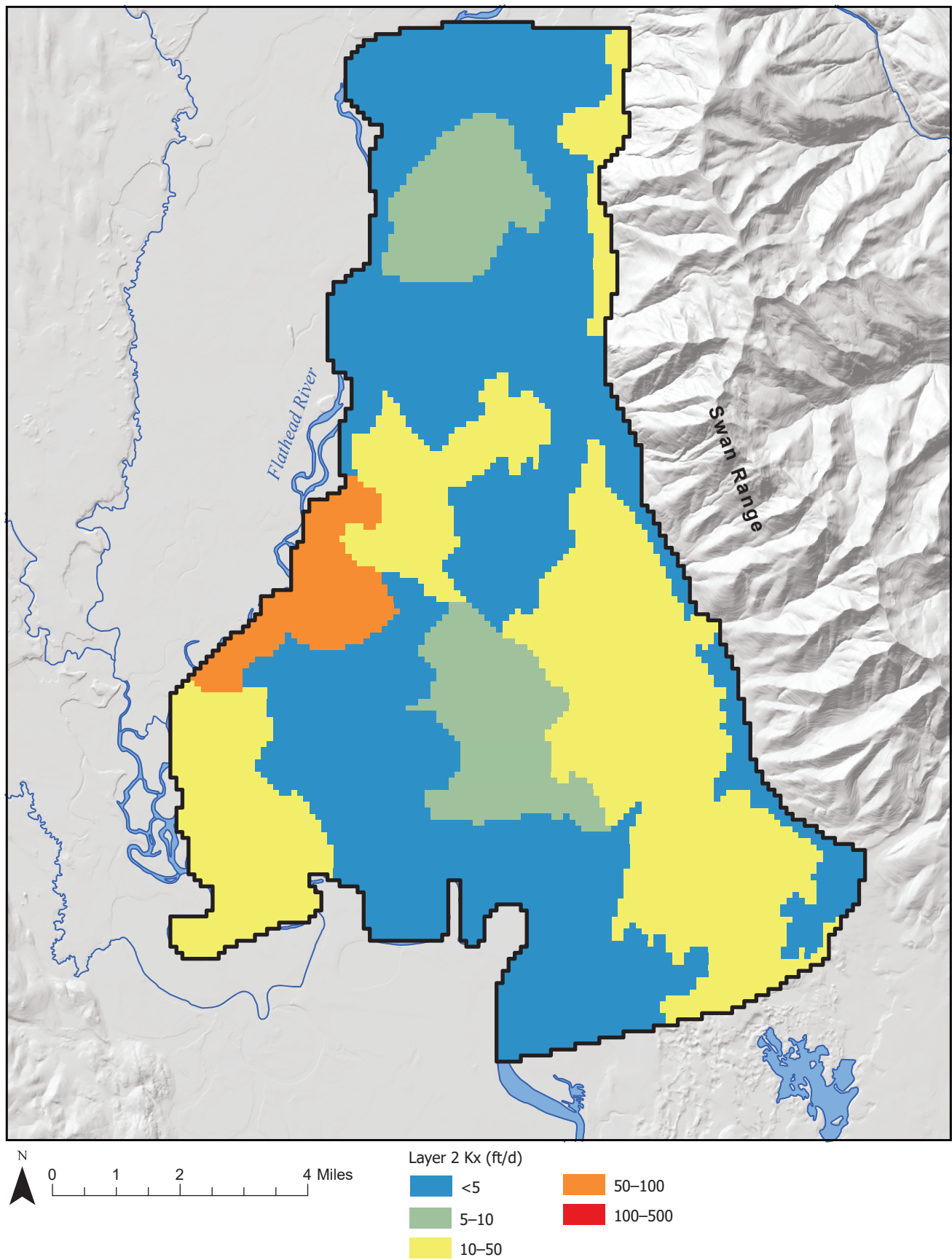
Figure G7. Horizontal K distribution in Layer 2 based on steady-state calibration.
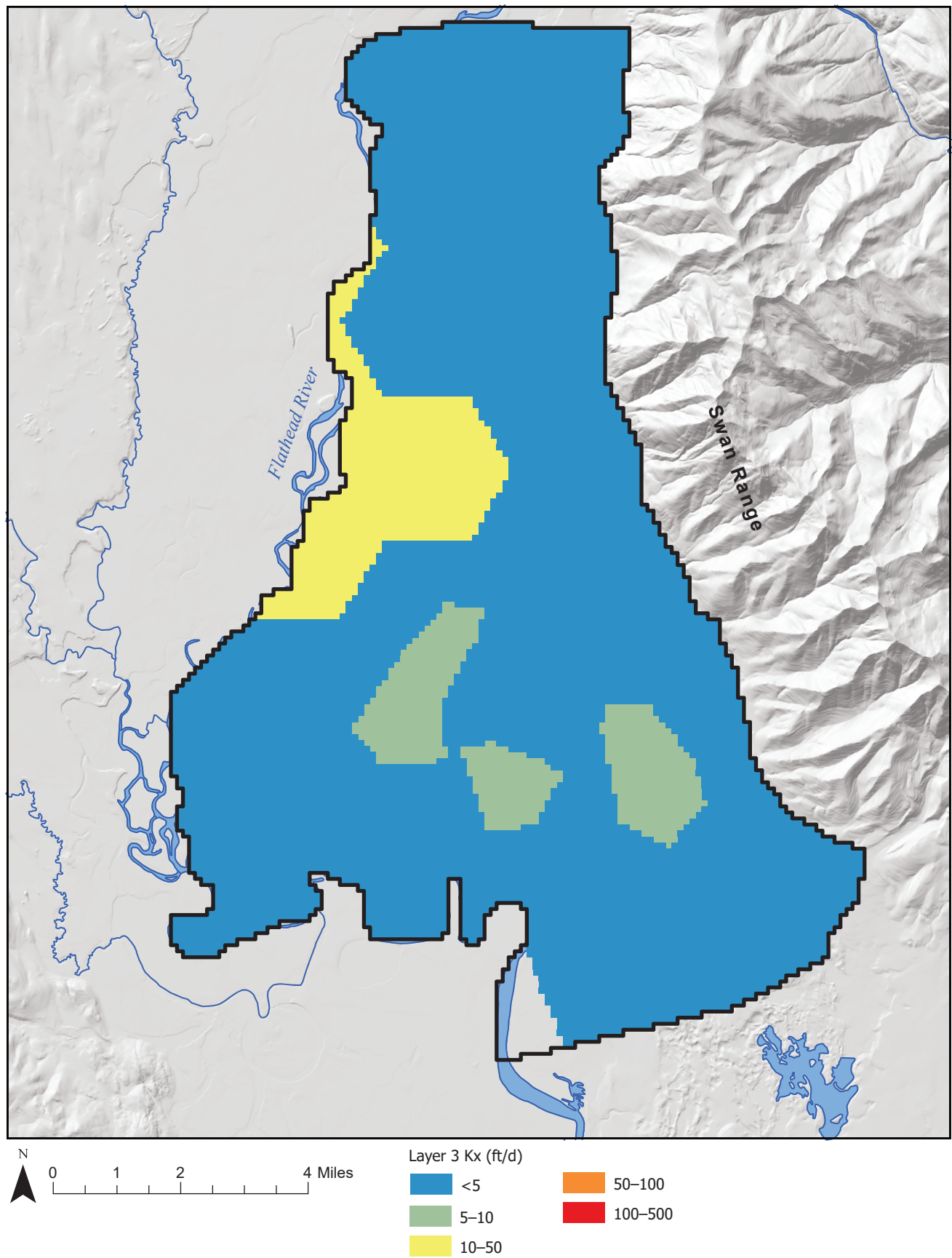
Figure G8. Horizontal K distribution in Layer 3 based on steady-state calibration.

Layer 3 Kx (ft/d)

- <5
- 5–10
- 10–50
- 50–100
- 100–500
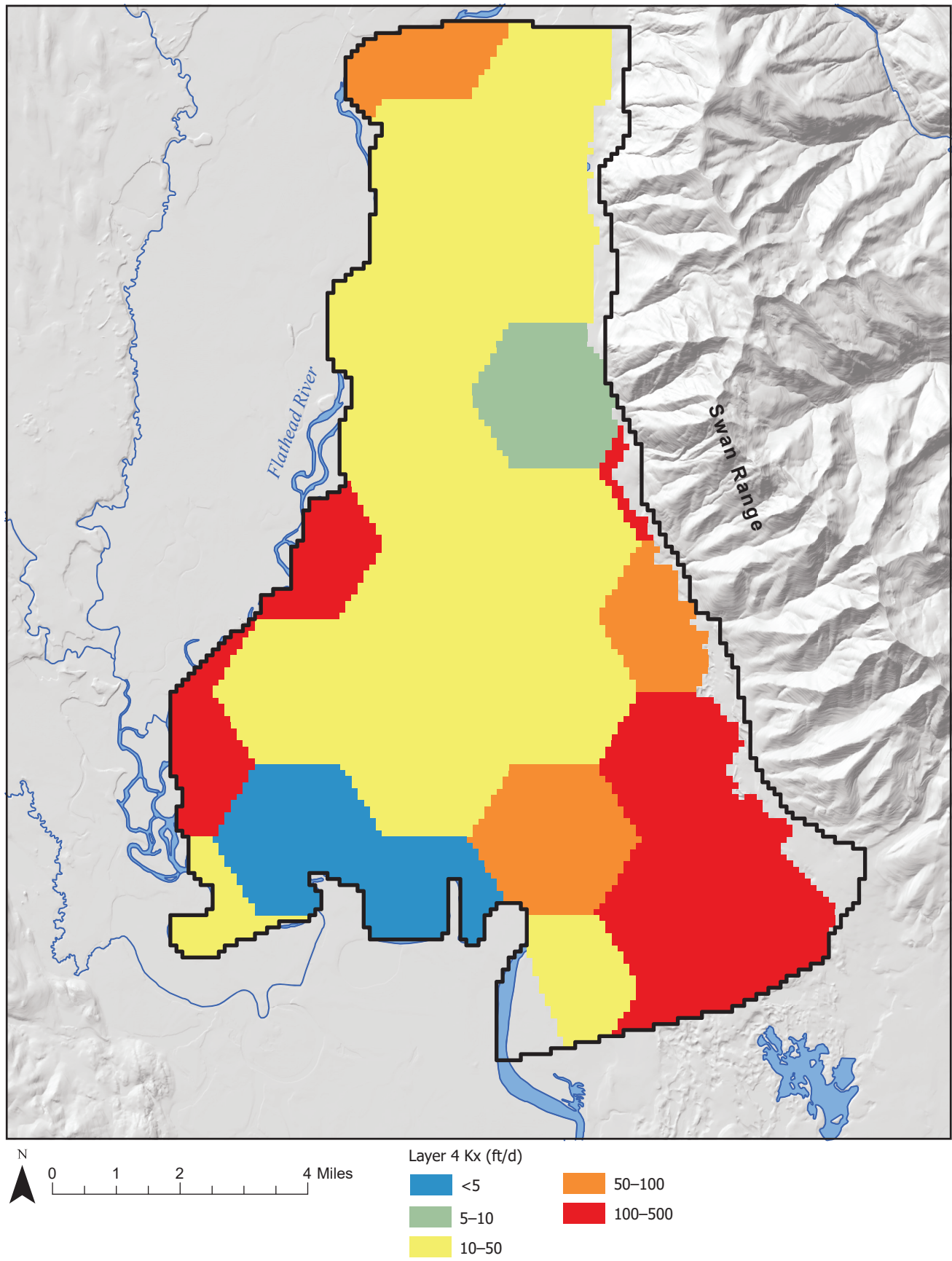
Figure G9. Horizontal K distribution in Layer 4 based on steady-state calibration.

APPENDIX H

TRANSIENT CALIBRATION INFORMATION

CALCULATING NASH–SUTCLIFFE COEFFICIENTS

For calibration of the transient model we adjusted the storage coefficients (S_y and S_s) in each zone to maximize the overall median Nash–Sutcliffe coefficient of efficiency (*NS*). This provided an objective summary statistic to guide the calibration process, where calculated *NS* values can range from negative infinity to 1, with NS values closest to 1 indicating a good fit. The change in head from January 2020 (drawdown; *dh*) was used as the target, rather than the absolute head elevation, since the absolute head had already been largely determined during the steady-state calibration of the *K* and conductance parameters. We used a simple Python code to efficiently calculate the *NS* for each model run.

NS is calculated for each well by (modified from Anderson and others, 2015):

$$NS = 1 - \frac{\sum_{i=1}^{n}|dh_m - dh_s|_i^2}{\sum_{i=1}^{n}|dh_m - \overline{dh_m}|_i^2}$$

where:

n is the number of drawdown observations;

dh_m is the observed drawdown;

dh_s is the simulated (modeled) drawdown; and

$\overline{dh_m}$ is the mean of observed drawdowns.

Example:

For well 84, the first three observations are shown on table H1. If this were the whole data set, NS would be calculated as:

$$NS = 1 - \frac{0.28}{1.13} = 0.75$$

Overall, 70% of the NS values were positive, the median NS was 0.27, and the range was from -12.43 to 0.90. One drawback of the NS approach is that hydrographs with low overall amplitude (low $|dh_m - \overline{dh_m}|$) are penalized as the ratio becomes large due to a small denominator, even when the difference between observed and modeled drawdown (i.e., error) is the same.

Table H1. Example NS calculation.

Date	Observed (dh_m)	Computed (dh_s)	dh_m-dh_s	$(dh_m$-$dh_s)^2$	dh_m-Avgdh$_m$	$(dh_m$-Avgdh$_m)^2$
1/9/20	0.50	0.21	0.29	0.09	-0.75	0.56
2/6/20	1.25	0.93	0.32	0.10	0.00	0.00
3/11/20	2.00	1.69	0.31	0.10	0.75	0.56
Average	1.25					
Sum				0.28		1.13
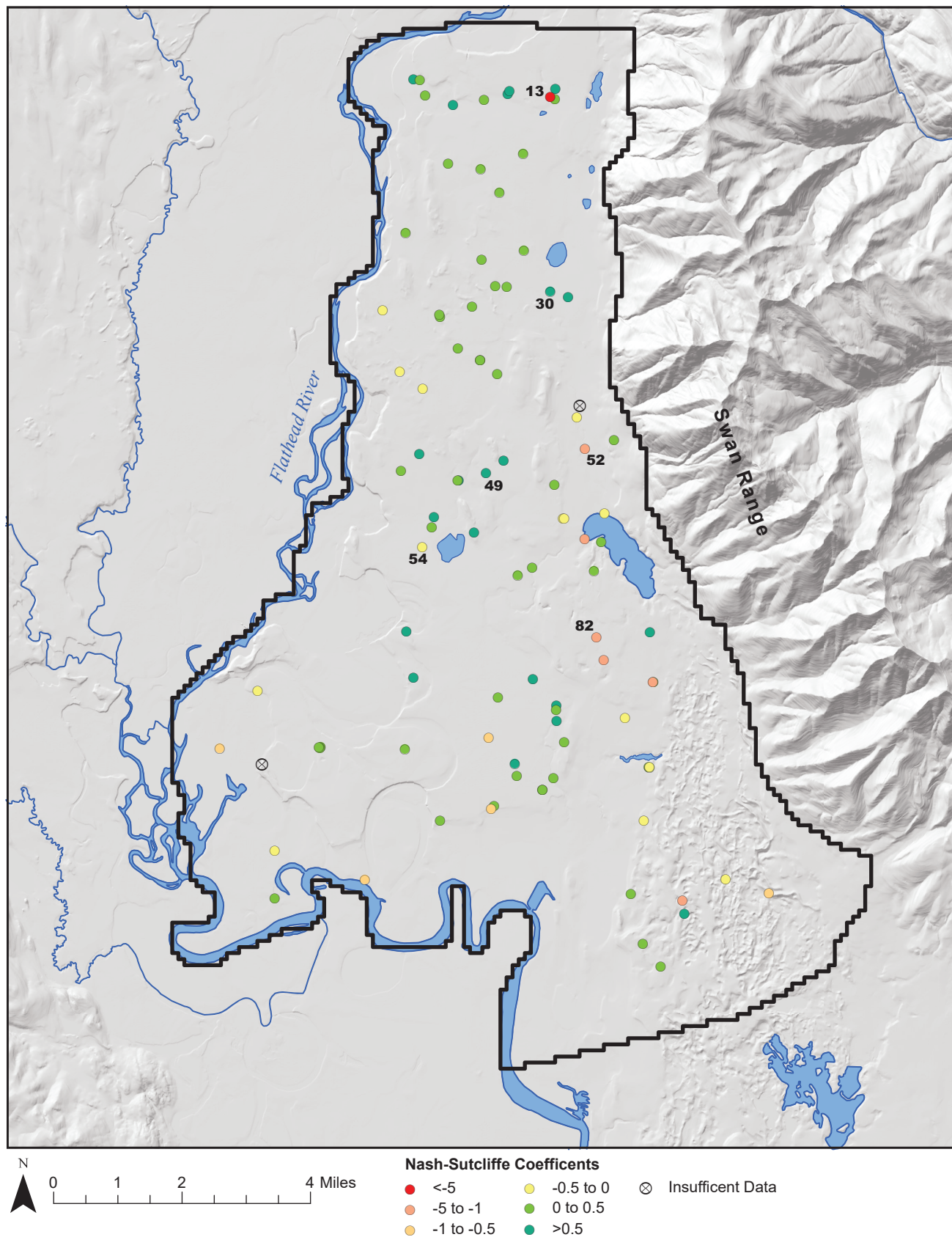
Figure H1. Nash–Sutcliffe efficiency coefficients were calculated for the observed and simulated transient drawdown data (relative to January 2020). There is no obvious geographic or stratigraphic pattern to the values. Low NS values occur within the same zone as high values, so further improvements would require changes in model construction (or zonation) rather than changes in model parameters. Hydrographs for labeled sites are shown in figures H3 and H4.

Drawdown *NS* values for Calibrated Transient Model (*n* = 98)
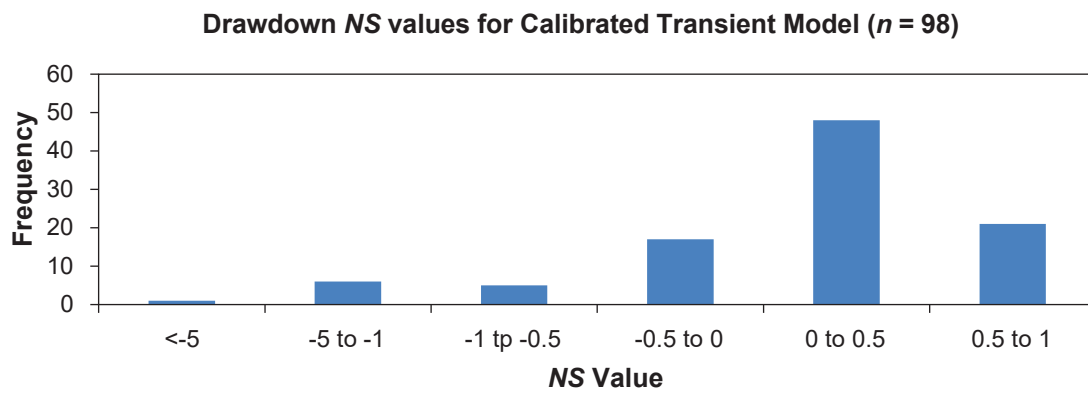
Figure H2. Nash–Sutcliffe efficiency coefficients were calculated for the observed and simulated transient drawdown data (relative to January 2020). The median value was 0.27, and 88% of values fell between -0.5 and 1.
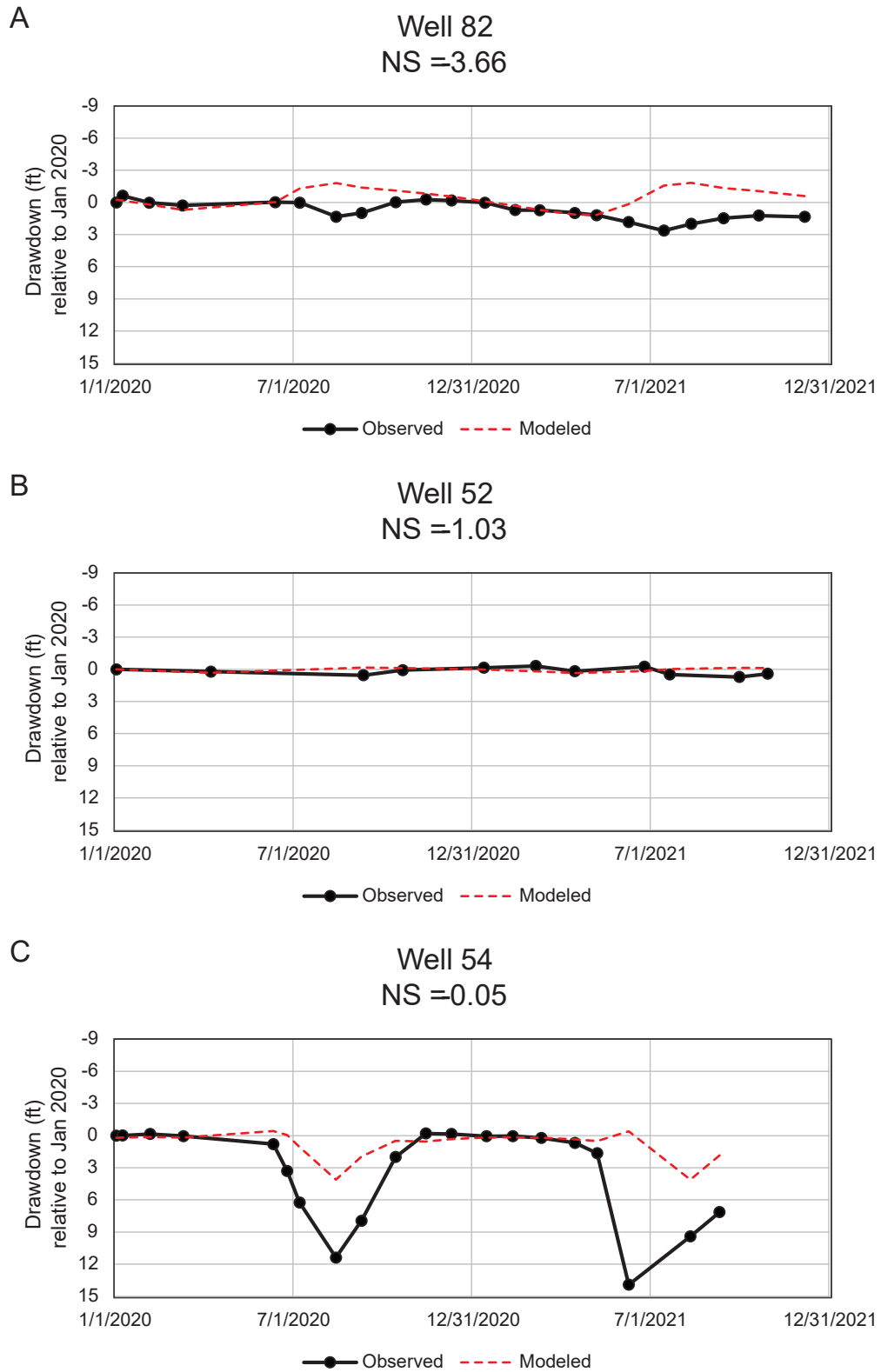
Figure H3. Example hydrographs comparing modeled to observed drawdowns (relative to January 2020), with Nash–Sutcliffe efficiency coefficients. See appendix A for well details. Locations are shown in figure H2.

A

Well 13
NS = 0.19

B

Well 30
NS = 0.51

C

Well 49
NS = 0.79
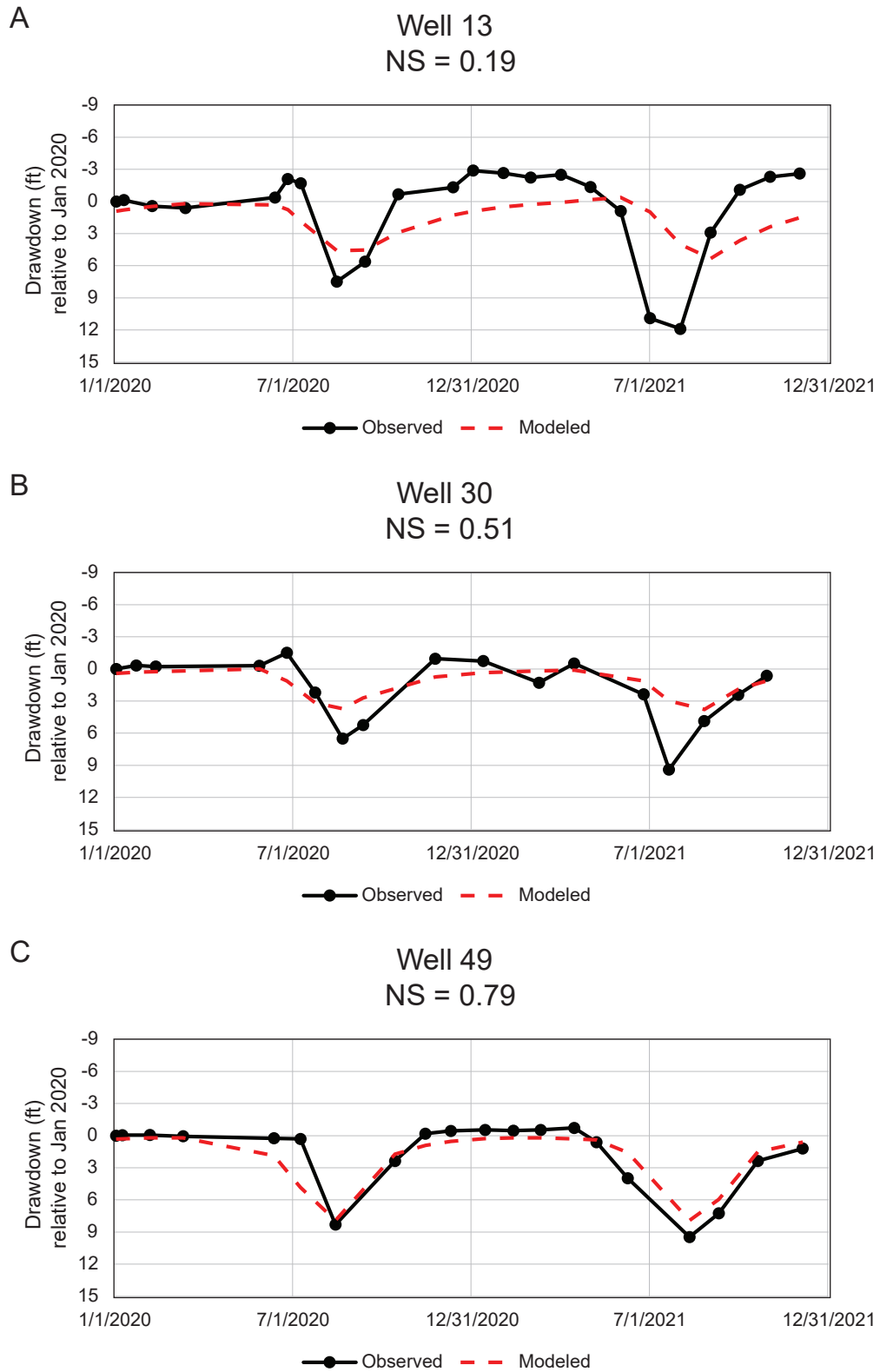
Figure H4. Example hydrographs comparing modeled to observed drawdowns (relative to January 2020), with Nash–Sutcliffe efficiency coefficients. See appendix A for well details. Locations are shown in figure H2.